Mondragon Unibertsitatea

DOCTORAL THESIS

CONTROL OF INTERLINKING CONVERTERS FOR HYBRID AC/DC POWER SYSTEMS

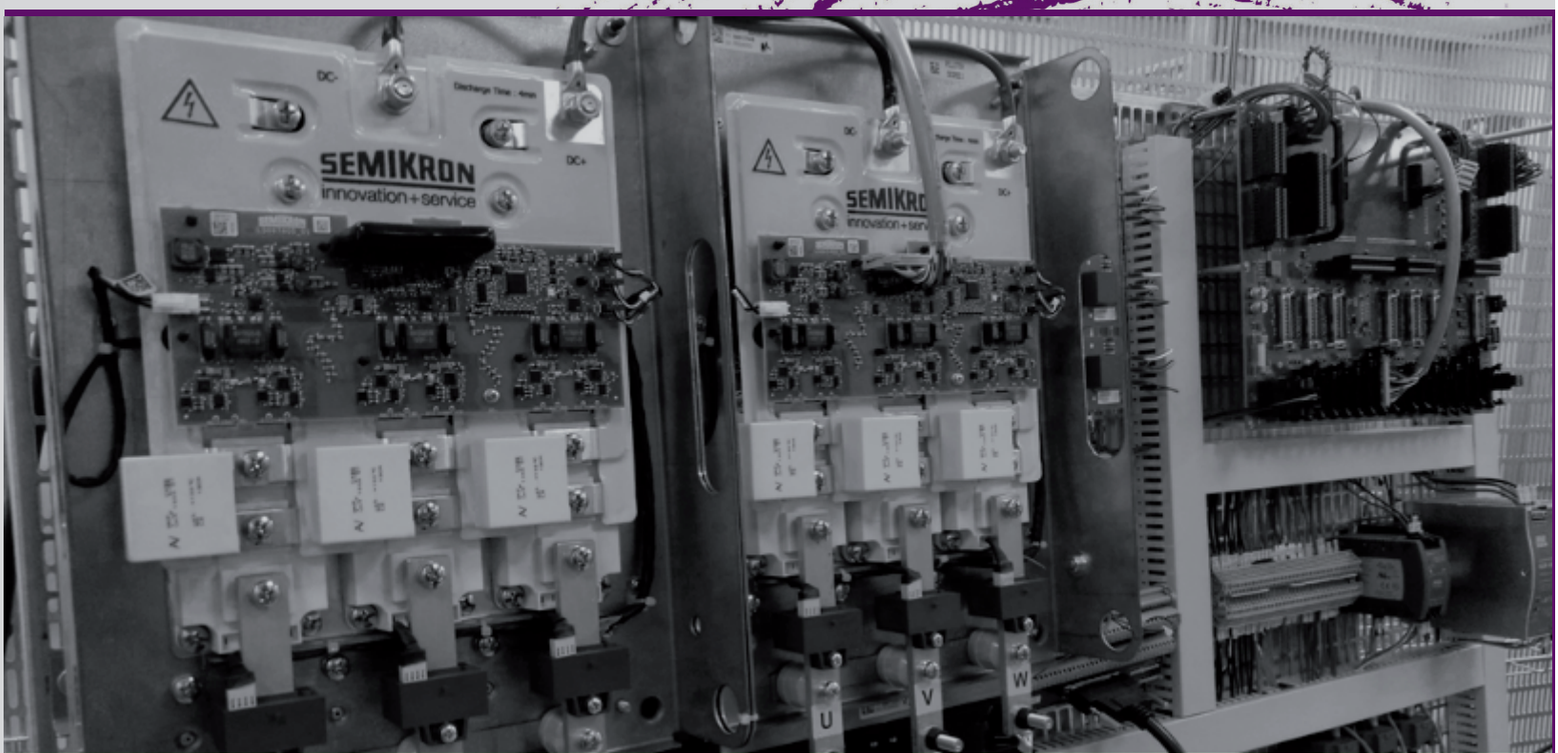

JULEN PANIAGUA AMILLANO | Arrasate-Mondragón, 2023

JULEN PANIAGUA AMILLANO | Control of Interlinking Converters for Hybrid AC/DC Power Systems

Mondragon Unibertsitatea

Goi Eskola Politeknikoa

Faculty of Engineering

Dissertation

Control of Interlinking Converters for Hybrid AC/DC Power Systems

Julen Paniagua Amillano

Mondragon Goi Eskola Politeknikoa
Electronics and Computing Department

Arrasate-Mondragón, 27 February 2023

Control of Interlinking Converters for Hybrid AC/DC Power Systems

Julen Paniagua Amillano

Supervisors:

Dr. Jon Andoni Barrena & Dr. Eneko Unamuno
Electronics and Computing Department
Mondragon Unibertsitatea

Submitted in partial fulfilment of the requirements
for the Degree of Doctor Philosophy under the program:
Applied Engineering

Thesis Committee:
President: Dr. Josep M. Guerrero (Aalborg University)
Vocal: Dr. Pablo García (Universidad de Oviedo)
Vocal: Dr. Daniel Serrano (Universidad Politécnica de Madrid)
Vocal: Dr. Markel Zubiaga (Ingeteam Power Technology)
Secretary: Dr. Ander Goikoetxea (Mondragon Unibertsitatea)

Arrasate-Mondragón, 27 February 2023

To my family

“Born to lose, live to win”
Lemmy

Abstract

Electrical power plays a very important role in today's society, but the necessity to reduce the greenhouse gas emissions requires to shift the classical fossil fuel-based power generation towards a renewable based model. In this transition, existing power systems need to embrace significant changes.

The operation of renewable-based power systems with a high presence of power converters becomes more challenging since these generators present a reduced inherent inertial response, reduced primary regulation capacity and the power generation is non-schedulable. At the same time, dc power systems are gaining popularity due to the advantages they offer for certain applications. Among the different changes that power systems might undergo in order to make them more controllable, reliable and with a better transient response, it is envisioned that power systems will adopt more modular topologies where different ac and dc subgrids will be combined, forming a grid of grids.

In this scenario, **interlinking converters (IC)**—which are power electronic converters to tie electric grids—will have a key role, since they can be employed to interconnect power systems of different natures and characteristics, and offer a high controllability over the flow of power among subgrids. The main purpose of this thesis is to **develop, analyse and validate control strategies for ICs that contribute to the transient response of interconnected ac and dc power systems**.

In order to achieve this objective, first we propose a power flow-based simulation tool, named *dynamic frequency power flow* (DFPF). This tool enables to study the dynamic behaviour of ac, dc and hybrid power system scenarios, and the contribution of ICs and their controls to the transient response of interconnected systems. Then, after carrying out a literature review, two IC controls are proposed in this document. The first technique is named as *dual inertia-emulation* (DIE) control, and it provides inertial response for both interconnected grids, contributing to improve both systems' inertial response. The second technique corresponds to a *virtual power line* (VPL) control, and makes the IC behave as a traditional power transmission line but it enables to tie power systems of different characteristics and natures. This technique unifies the interconnected power systems in terms of primary reserve and inertia, so the transient response is improved, and it facilitates the flow of power from generation to loading points in a natural way. Simulation results that validate the contribution of the proposed controls to the transient response of the grids under different test cases are provided throughout the document.

Laburpena

Energia elektrikoak gaur egungo gizartean garrantzi handia badu ere, berotegi efektua bultzatzen duten gasen isurketa gutxitzeko erregai fosilak alde batera utzi eta energia berriztagarriak erabiltzea ezinbestekoa izango da energia sorkuntza prozesuetan. Hau lortzeko, egungo sare elektrikoek hainbat aldaketa jasan beharko dituzte euren baitan.

Energia berriztagarrietan eta potentzia bihurgailuetan oinarritutako sare elektrikoen kudeaketa eta kontrola konplexuagoa da hainbat arrazoi direla medio. Besteak beste, erantzun inertzial urria, erreserba primario mugatua edo potentzia ekoizpenaren ez- programagarritasuna direla medio. Aldi berean, korronte zuzeneko sistemen erabilera areagotzen ari da eta horregatik, sare elektrikoak errazago kudeatu eta euren egonkortasun iragankorra hobetu ahal izateko, hauek egitura modularragoak hartuko dituztela aurreikusten da, non korronte zuzen eta alternoko sare desberdinak elkarren artean loturik egongo diren.

Lotura hauetan, ingelesezko *interlinking converter* (IC)-ek—sare elektriko ezberdinak lotzeko erabiltzen diren bihurgailuek hain zuzen ere—garrantzi handia izango dute. Horregatik, tesi honen helburu nagusia **IC bihurgailu bidez loturiko sare elektrikoen portaera iragankorra hobetuko duten kontrol estrategiak proposatu eta balioztatzea izango da**.

Helburu hau erdiesteko, lehenik eta behin korronte zuzen, alterno, zein sare hibridoen portaera dinamiko eta iragankorra aztertzea ahalbidetuko duen simulazio erreminta bat proposatu dugu. Baliabide honek IC-ek eta hauen kontrolak elkarrekin lotutako sareen erantzun iragankorrari eskaintzen dioten onura zenbatekoa den ebaluatzen lagunduko digu. Bestalde, literaturan topatu diren kontrol desberdinen gaineko azterketa egin ondoren, bi kontrol teknika proposatu ditugu. Lehenak erantzun inertziala eskaintzen die IC aren bi aldetan dauden sareei, honetarako potentzia sare batetik bestera maneiatuz. Bigarren proposamenak, elkarrekin zuzenean konektagarriak diren bi sare lotzen dituen transmisio linea bat bezala lan egitera bultzatuko du IC-a, baina zuzenean konektagarriak ez diren sistemak lotzea ahalbidetuz. Teknika honek bi sareak batu egingo ditu inertzia eta erreserba primarioari dagokionez, beraz sareen erantzun iragankorra hobetzeaz gain potentzia fluxua naturala izango da sorgailu eta karga ezberdinen artean. Proposaturiko kontrolen eraginkortasuna frogatu eta sareen portaera iragankorra hobetzen dutela egiaztatzeko simulazio proba ezberdinak egin dira, eta emaitzak eskuragarri daude dokumentuan zehar.

Resumen

La energía eléctrica juega un papel sumamente importante en la sociedad actual, pero la necesidad de reducir las emisiones de gases de efecto invernadero implica la sustitución de la generación basada en combustibles fósiles por generación renovable. Esta transición implica que los sistemas eléctricos actuales sufran cambios importantes, tal y como se detalla a continuación.

La operación y control de sistemas basados en fuentes renovables con una gran presencia de convertidores se presenta más compleja debido a la escasa respuesta inercial, capacidad reducida para llevar a cabo la regulación primaria y ajustar la generación a las necesidades del sistema. Al mismo tiempo, los sistemas de corriente continua son cada vez más populares en diferentes aplicaciones. Por lo tanto, con el fin de poder controlar y gestionar mejor con más facilidad los sistemas eléctricos modernos, se prevé que estos adopten topologías más modulares donde redes o subredes de diferentes características y naturalezas se combinen formando una red de redes.

En este escenario, los llamados *interlinking converters* (ICs) en inglés—ya que son convertidores de potencia empleados para enlazar redes eléctricas—adoptarán un papel muy importante, ofreciendo gran controlabilidad sobre el flujo de potencia entre subredes. Por lo tanto, el objetivo principal de esta tesis se centra en **el desarrollo de técnicas de control para ICs que mejoren la respuesta transitoria de las diferentes redes interconectadas ac y dc.**

Para conseguir este propósito, primeramente hemos propuesto una nueva herramienta de simulación que permite realizar simulaciones dinámicas de sistemas eléctricos, la cual está basada en flujos de potencia estáticos y permite simular sistemas ac, dc e híbridos. Además, permite la implementación del IC y su control en la misma, pudiendo así evaluar la contribución del IC a la respuesta transitoria de los sistemas interconectados. Después de haber realizado la revisión de la literatura, hemos propuesto dos estrategias de control. La primera estrategia proporciona respuesta inercial a ambas redes interconectadas, mientras que la segunda opera el convertidor IC del mismo modo en que una línea eléctrica conecta dos sistemas compatibles entre sí, pero extendiendo este comportamiento a uniones entre redes inicialmente no compatibles. Esta técnica unificara ambos sistemas en términos de inercia y reserva primaria, mejorando así la respuesta transitoria de las mismas. Durante el documento se presentan los resultados de simulación pertinentes que validan la contribución de los controles propuestos a la respuesta transitoria de las redes interconectadas.

Acknowledgement

Ezin dut eskerrak ematen hasi Eneko eta Jonan aipatu gabe, zuengatik ez balitz ibilbide hau ez litzateke posible izango eta. 2016ko maiatzeko egun hartan hamargarren eraikinean elkar ezagutu genuenetik ia zortzi urte igaro dira dagoeneko. Tartean ehundaka bilera, eztabaida, azalpen, txiste eta abar izan ditugu, eta atzera begiratzen dudan bakoitzean erakutsi eta eman didazuen guztia ikusten dut, ez soilik ingeniari, ikasle edo doktoregai bezala, baizik eta arlo pertsonalean ere bai. Horregatik, mila esker bihotz-bihotzez.

Bigarrenik, nire ikasle ibilbidean moduren batean zein bestean hor egon zaretenoi ere eskerrak helarazi nahi dizkizuet. Elektronikako graduan zein masterrean irakasle izan zinetenoi, nire grina eta interesa pizteagatik. Ikaskide eta lankideei, arrasaten bizi izan ditugun momentu guztiengatik. Modu berezian eskertu nahiko nituzke tesiko ibilbide honetan ondoan izan ditudanak bekadun eta doktoregaien gelan, asko izan zarete, tartean Laura, Ordoño, Imanol, Santiso, Udabe, Iosu, Beñat, Leire, Aritz, Atutxa, Antonio, Sagarna, Adrian, Haitz... eskerrak denoi atsedenaldi eta otorduak alaitu eta momentu zailetan eman didazuen laguntza eta babesagatik.

Aita, ama eta Kepari ere eskerrik beroenak eman nahi dizkizuet, beti hor egon zaretelako, laguntzeko prest eta oraindik ere gaur egun horrela jarraitzen duzuelako. Badakizue horrelakoak adierazten enaizela oso trebea, baina nire esker onik sakonenak zuentzako ditut gordeak. Osaba-izeba, amiña eta lehengusuei ere eskerrak eman nahi dizkizuet zuen etengabeko babes eta animoengatik. Zaudeten tokian zaudetela, faltan zaituztedanei besarkadarik sakonena bidaltzen dizuet, eredu izaten jarraitu, eta oraindik ere baloreak erakutsi eta adorea ematen baitidazue nire oroitzapenetara jotzen dudanean zuen bila.

Lagun guztiei eta niregatik kezkatu zaretenoi ere mila esker, denek ulertu eta onartu baituzue nire lan eta bizimoduarekin sarritan zaila egiten zaidala harremanei jarraikortasun bat ematea, eta hala ere beti hor egon baitzarete edozertan laguntzeko prest. Urdiaingo kuadrillari eskerrak, elkarrekin denbora gutxi igaro arren beti sentitzen baitut zuen gertutasuna, eta besoak zabalik hartzen nauzuelako zuekin egoten naizen aldioro. Altsasuko *Harrinton* taldeari ere eskerrik beroenak bidaltzen dizkizuet, zuen alaitasunak, adar-jotze eta aholkuek behar izan dudan oreka eman baitidate urte hauetan zehar. Modu berien, Dorrouko laguni de eskerrak ematen duzkuziet, asteburuero hor egondu zarieni, Txipi, Mayo, JonH, Beñat, Pintxo eta deni. *Errekondi* kuadrilleko laguni debei eskerrak, kazan basurdiei egurra ematen pasatu ttoun ordu guziengati, eta ez hori bakarrik, tartien akusi eta eman dezien guzieingati. Ezin dot esker oneko testubau akatu ne gerlari txikiyi eskerrak eman bai, Bat, Lagun eta Beltxa, egunerokotasunien ne rarokeiek aguantatziatis, eta halare dakazien hobeina ematiatis zuen alegrieiki, eta nola ez basurdien atzeti leixterkan.

Zuek denok, bakoitza bere modura, nire bizitzan oso garrantzitsuak zarete, non pauso bakoitza emanterakoak oinarri gisa, edo estropozu egitean helduleku izanez laguntzen nauzuen. Horregatik, zuek gabe tesi hau elitzateke inoiz idatzia izango, eta ez luke zentzurik izango. Urte askoan elkarrekin jarrai dezagun, aupa zuek!

Contents

1 Introduction **1**
- 1.1 Background . . . 2
  - 1.1.1 Classical Power Systems . . . 3
  - 1.1.2 Evolution of Power Systems . . . 4
  - 1.1.3 The Role of Interlinking Converters . . . 8
- 1.2 Key Challenges . . . 14
  - 1.2.1 Grid Interoperability . . . 14
  - 1.2.2 Power Reserve on Modern Power Systems . . . 14
  - 1.2.3 Inertial Response at Grids with High Penetration of Power Converters 15
  - 1.2.4 Grid-Forming and Black Start Operation Capability . . . 15
  - 1.2.5 Dynamic Simulations of Modern Power System Scenarios . . . 15
- 1.3 Goals of the Thesis . . . 16
- 1.4 List of Contributions . . . 16
  - 1.4.1 Journal Papers . . . 17
  - 1.4.2 Conference Papers . . . 17
  - 1.4.3 Magazine Papers . . . 17
- 1.5 Thesis Outline . . . 18

2 Dynamic Frequency-and-Voltage Power Flow-Based Simulations **21**
- 2.1 Introduction to Power System Simulation Methods . . . 22
- 2.2 Dynamic Frequency Power Flow Tool . . . 26
  - 2.2.1 Power Flow Solver . . . 26
  - 2.2.2 DFPF Tool based on Simulink Software . . . 31
- 2.3 Validation and Performance Comparison of the DFPF Tool . . . 35
  - 2.3.1 Simulation Considerations . . . 35
  - 2.3.2 Description of the Use Case . . . 36
  - 2.3.3 Simulation Results . . . 37
- 2.4 Simulation of a Hybrid AC/DC Power System in the DFPF tool . . . 43
  - 2.4.1 Description of the Hybrid AC/DC Scenario . . . 43
  - 2.4.2 Simulation Results . . . 45
- 2.5 Conclusion . . . 48

3 IC Control Techniques for the Provision of Transient support **49**
- 3.1 Technical Background . . . 50
  - 3.1.1 Hierarchical Control Layers on a Power System . . . 50
  - 3.1.2 Contribution of ICs to Hierarchical Power System Control . . . 53
  - 3.1.3 Classification of Grid-Connected Converter Controls . . . 55
  - 3.1.4 Analogy Between AC and DC Power Systems . . . 56

3.2 IC controls for the Provision of Virtual Inertia and Transient Support 62
3.2.1 Single Grid-Supporting Control Strategies 64
3.2.2 Dual Grid-Supporting Control Strategies 65
3.2.3 Single Grid-Forming Control Strategies 68
3.2.4 Dual Grid-Forming Controls 70
3.2.5 Single Grid-Forming and Dual Grid-Supporting Controls 70
3.3 Summary 70

4 Dual Inertia-Emulation Control Strategy for ICs 75
4.1 Introduction 76
4.2 Dual Inertia-Emulation Control 76
4.2.1 Operation Principle 76
4.2.2 Supporting the transient response of grids 79
4.3 DIE Control Validation 80
4.3.1 DIE Testing Scenario 80
4.3.2 DIE Operation Concept 82
4.3.3 DIE Test Cases 83
4.4 Conclusion 90

5 Virtual Power Line control for ICs 91
5.1 Introduction 92
5.2 Virtual Power Line Control 93
5.2.1 Power Line Tying Two AC Systems 93
5.2.2 Power Line Tying Two DC Systems 94
5.2.3 Virtual Power Line Control for ICs 94
5.2.4 Dual Grid-Supporting VPL Control (DGS-VPL) 95
5.2.5 Single Grid-Forming-VPL Control (SGF-VPL) 96
5.3 Performance of the VPL control 98
5.3.1 Test I: DGS-VPL on a Hybrid AC/DC Grid Link 98
5.3.2 Test II: DGS-VPL vs existing IC control strategies 101
5.3.3 Test III: SGF-VPL control operation 102
5.3.4 Test IV: SGF-VPL ICs Forming AC and DC grids 104
5.4 Conclusion 107

6 Conclusion and Outlook 109
6.1 Conclusions 110
6.2 Future Research Lines 112

List of Figures 115

List of Tables 118

List of References 119

Abbreviations

AS Ancillary Services

c-HIL Control-Hardware in the Loop

CC Current Controller

CCVSM Current-Controlled Virtual Synchronous Machine

CRC Current Reference Calculation

DD Dual-Droop

DFPF Dynamic Frequency Power Flow

DG Distributed Generation

DGS-VPL Dual Grid-Supporting VPL Control

DIE Dual Inertia-Emulation

EIA Energy Information Association

EMF Electromotive Force

EMT Electromagnetic Transient

ESS Energy Storage System

EV Electric Vehicle

GoG Grid of Grids

HIL Hardware in the Loop

HVDC High-Voltage DC

IC Interlinking Converter

LTDS Long Term Dynamic Simulation

MMC Modular Multilvel Converter

MPPT Maximum Power Point Tracking

MTDC Multi-Terminal DC

NR Newton-Raphson

p-HIL Power-Hardware in the Loop

PI Proportional-Integral

PLL Phase-Locked Loop

PV Photovoltaic

RES Renewable Energy Sources

RoCoF Rate of Change of Frequency

RoCoV Rate of Change of Voltage

SG Synchronous Generator

SGF-VPL Single Grid-Forming VPL Control

SME Synchronous Machine Emulation

SoC State of Charge

SRM Simplified Rotating Mass

SST Solid State Transformer

ST Smart Transformer

STATCOM Static Synchronous Compensator

V2G Vehicle to Grid

VC Virtual-Capacitor

VCVSM Voltage-Controlled Virtual Synchronous Machine

VDCM Virtual dc Machine

VPL Virtual Power Line

VSG Virtual Synchronous Generator

VSM Virtual Synchronous Machine

WP Wind Power

WSCC Western System Coordinating Council

Symbols

B_{ij} imaginary part of Y_{ij}

C capacitance

D $P-f$ droop coefficient

E EMF in volts

E_c electrostatic energy

E_k kinetic energy

G grid-connected generator

G_{ij} real part of Y_{ij}

H_C aggregated inertia of the Continental grid

H_N aggregated inertia of the Nordic grid

H_V virtual per-unit inertia

H_{WP} aggregated inertia of the WP system

I_{C_i} input capacitor current

I_{C_o} output capacitor current

I_i^* conjugate value of the current magnitude at node i

K constant that links the rotational speed and electromotive force in a dc generator

L_s inductance of a power system line

P_b base power of a dc system

P_e electrical active power

P_m mechanical power

P_{D_i} demanded active power at node i

P_{G_i} generated active power at node i

P_i active power delivery at node i

Q_{D_i} demanded reactive power at node i

Q_{G_i} generated reactive power at node i

Q_i reactive power delivery at node i

R resistance

S_{ij} apparent power exchange between nodes i and j

S_i apparent power delivery at node i

T_e electrical torque

T_m mechanical torque

T_D delay of the *transport delay* function block

T_s simulation step size

V_{GF} voltage of the grid-forming unit

V_{Node} voltage of the power system node

V_b base voltage

V_i voltage at node i

X impedance

X_s synchronous reactance of a SG

Y_{ij} admittance term between nodes i and j from the admittance matrix $\mathbf{Y}$

Z_{VPL} virtual impedance parameter of the VPL control in per-unit

δ angle difference between two voltage vectors

δ_{GF} angle difference between the grid-forming unit and the slack node of the power system in the NR algorithm

$|V_i|$ magnitude of the voltage vector at node i

$\mathbf{f}(\mathbf{x})$ set of power system equations in vector notation

$\mathbf{x}$ vector of the node variables in the NR algorithm

ω frequency

ω_{GF} frequency of a grid-forming unit

ω_{slack} frequency of the slack node in the NR algorithm

τ time constant of the first order filter that models the delay on the prime mover of the SG

θ_{ij} angle difference between nodes i and j

θ_i angle of the voltage vector at node i

ε error tolerance

f frequency in Hz

f_b base frequency

f_{max} maximum frequency

f_{meas} measured frequency

f_{min} minimum frequency

f_{pu} per-unit frequency

p_{gen} generated active power

p_{load} active power loading

p_{loss} active power losses

v voltage

v_{max} maximum voltage

v_{meas} measured voltage

v_{min} minimum voltage

v_{pu} per-unit voltage

x per-unit representation of frequency (for ac grids) and voltage (for dc ones)

y_{ij} admittance term between nodes i and j

z_{ij} impedance term between nodes i and j

H_{dc} per unit dc inertia

K_d damping factor

$\Delta\omega$ frequency difference

Δv voltage difference

J jacobian matrix

Y admittance matrix

H per unit mechanical inertia constant

J mechanical inertia

ω_b base frequency

S_b base power

V_b base voltage

Chapter 1

Introduction

Traditional power systems are undergoing several changes in the transition towards a cleaner and more sustainable model. This chapter identifies the most important issues that have arisen in the energy transition from the point of view of grid operation and stability. Besides, the background that motivates the presented work is explained, which at the same time is necessary to understand the presented problematic.

Once we have identified the most important challenges of the current scenario, we describe the main objectives of the presented work according to these challenges.

We conclude the chapter by summarising the main contributions made during the PhD, and describing the outline of the document.

1.1 Background

The great transformation that the civilisation has undergone in the last centuries would not be possible without the use of the different primary energy sources and the corresponding energy conversion, transport and storage systems. In this scenario, electrical energy plays a major role due to the numerous advantages it offers for its transmission, distribution and use in different areas of the modern society. A recent document by the U.S. Energy Information Association (EIA) about the international energy outlook[1], reports that the global energy demand will continue increasing in the coming decades as Figure 1.1 depicts. It further states that the use of fossil fuels will continue growing, and the use of electricity will also increase in all the areas, including the transport sector, where internal combustion vehicles are being gradually substituted by electric vehicles (EV)[2].

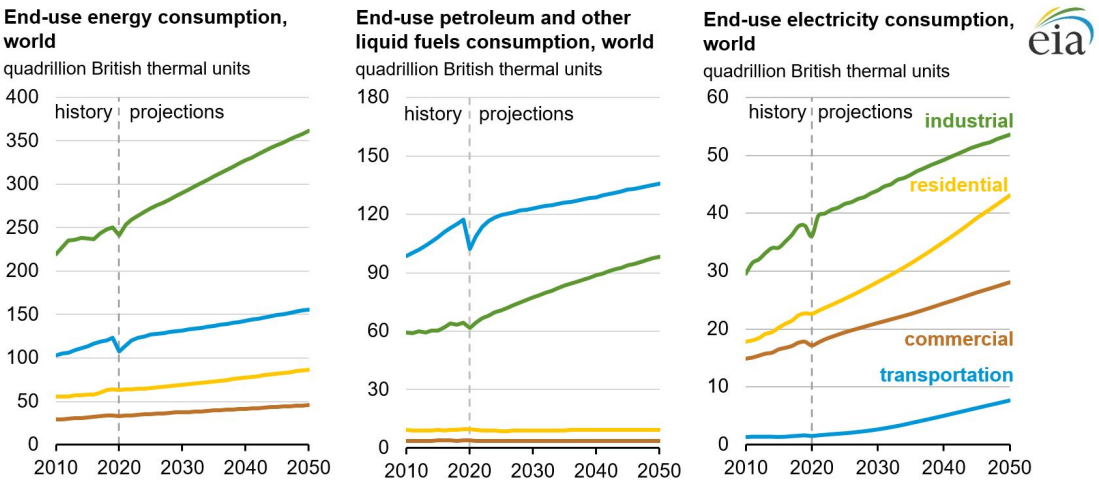

Figure 1.1: History and projection of the global end-use energy consumption according to EIA[1].

Additionally, the concern about climate change and global warming have led the nations all over the world to make a commitment to reduce the greenhouse gas emissions in the 2015 Paris Agreement[3]. This compromise entails the necessity to replace fossil-fuels with renewable-based power sources, and to gradually abandon traditional carbon-emitting generation technologies such as coal, oil or natural gas, as predicted by the EIA association[1] and depicted in Fig. 1.2.

In addition to the decarbonisation of the energy generation model, renewable energy sources (RES) are essential to achieve the freedom from imported primary energy sources in areas with scarce reserves of these fuels, as is the case in Europe, where most of the nat-

[1] EIA - International Energy Outlook 2021
[2] Electric Vehicle Market Projection
[3] Paris Agreement

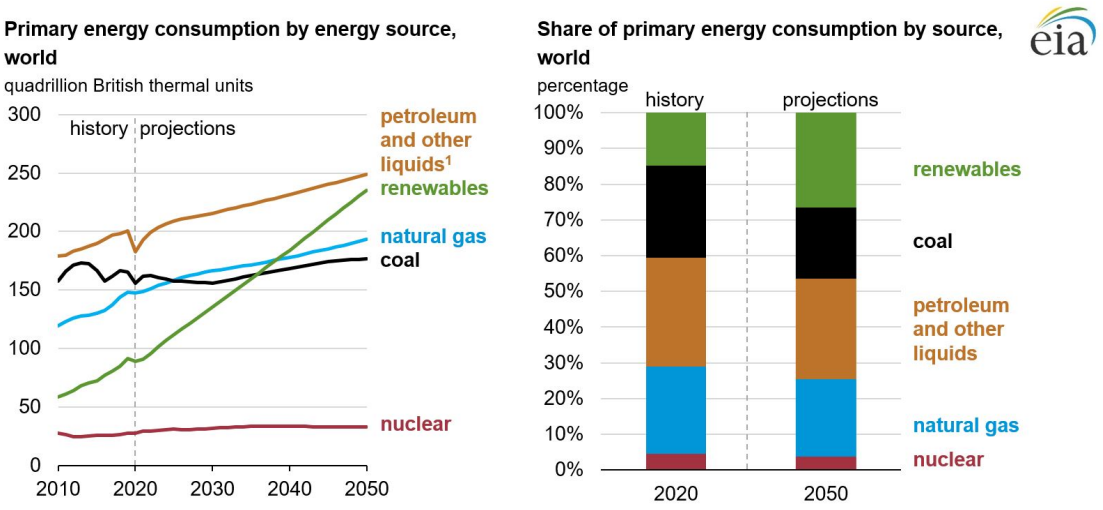

Figure 1.2: History and projection of the global primary energy consumption by source[1].

ural gas and crude oil is imported from non-EU countries[4]. Therefore, a renewable-based and self-sufficient energy market goes beyond the environmental aspects, with a high impact on the economy and well being of inhabitants.

In order to meet the established environmental guidelines and respond to the global electricity demand in the coming decades, electric power systems need to embrace severe transformations. With the aim of identifying the motivation and the key challenges of the presented thesis, the operation principles of classical power systems are first explained.

1.1.1 Classical Power Systems

At the beginning of the last century, ac was adopted as the best approach for the power transmission over long distances. Traditionally, power generation has been carried out by synchronous generators (SG) at big generation power plants where primary energy sources such as coal, gas, nuclear or hydro power have been used to drive the generators. The generated electricity is transported through power transformers and transmission lines, raising the voltage level for power transmission and reducing it for distribution and consumption. A simple example of a classical grid topology is shown in Figure 1.3, where the SGs in charge of the power generation are mainly concentrated in big generation plants and the power flows from these plants to multiple loads or users. Therefore, the topology of classical ac power grids is known as a top-down topology [1].

In SG-based power systems, the generators are directly connected to the grid and the electrical frequency is a reflection of the rotational speed of generators. These generators convert the prime mover's rotating mechanical power into electrical power to feed the system. When a power imbalance occurs between the mechanical and electrical power due to a load

[4] EU Energy Imports

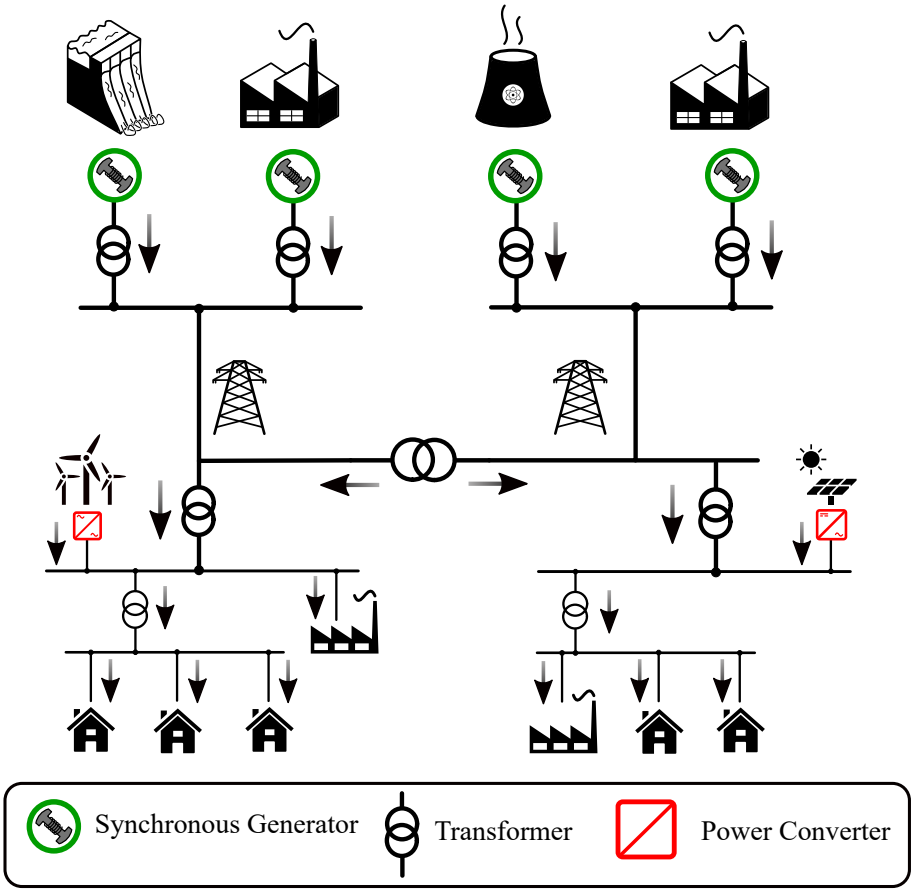

Figure 1.3: Illustration of classical grid top-down topology.

or generation variation, the generator (and hence the system frequency) tends to accelerate or decelerate. The magnitude of this acceleration depends on two factors: the amount of rotating inertia that the electromechanical conversion system has (composed by the SG rotor itself and the turbine attached to its shaft), and the magnitude of the power variation. For a given variation, the bigger the coupled inertia, the lower the acceleration magnitude and vice versa. Thus, we can say that the rotational inertia coupled to ac power systems acts as a kinetic energy buffer that releases or absorbs energy when a power imbalance occurs in the system. Classical SG-based grids are known to be very robust to sudden power variations because they present a very high amount of rotational inertia coupled to the grid.

1.1.2 Evolution of Power Systems

The integration of wind power (WP) and photovoltaic (PV) generators to power systems has been possible thanks to the advancements in power electronic converter technology. These sources are a key element in the decarbonisation of the energy generation model since they will replace traditional carbon emitting generators. Hence, they are playing a very important

role in the in the evolution of power systems, as it is explained hereafter.

The operation and control of power systems with a high penetration of RES and converter-interfaced generators is more challenging than in the traditional power systems for two reasons. On the one hand, the power generation of PV and WP plants cannot be scheduled since they rely on conditions such as the sun irradiation and the speed of the wind, and they operate with a very limited capacity to regulate their power in order to adjust to the demand (i.e. primary energy reserve capacity). On the other hand, these generators usually employ power converters in the energy conversion process, so the amount of rotating inertia (and hence the corresponding rotating kinetic energy storage) coupled to the grid is reduced. These aspects make it more difficult to keep the balance between the power generation and loading, and therefore to preserve the power system stability [2].

At the same time, the aforementioned aspects are related to the wholesale electricity market[5], which operates on an auction basis using a marginal price structure in Europe[6]. In other words, the different generators sell their power according to the consumption forecast that the system operator does for each hour of the day. In this market, the price of the energy for a certain hour is set by the price of the last unit of electricity that is purchased to cover the demand. Thus, lower-cost technologies such as nuclear, PV or WP technologies benefit from more expensive technologies that usually are employed to cover all the demand in the system. This market system causes a variable energy generation pool over time as it is shown in Figure 1.4, so producers aim to extract as much energy as possible from RES. Besides, the generation capacity may change its geographical location in the system [3], and hence the impedance between generation and load nodes.

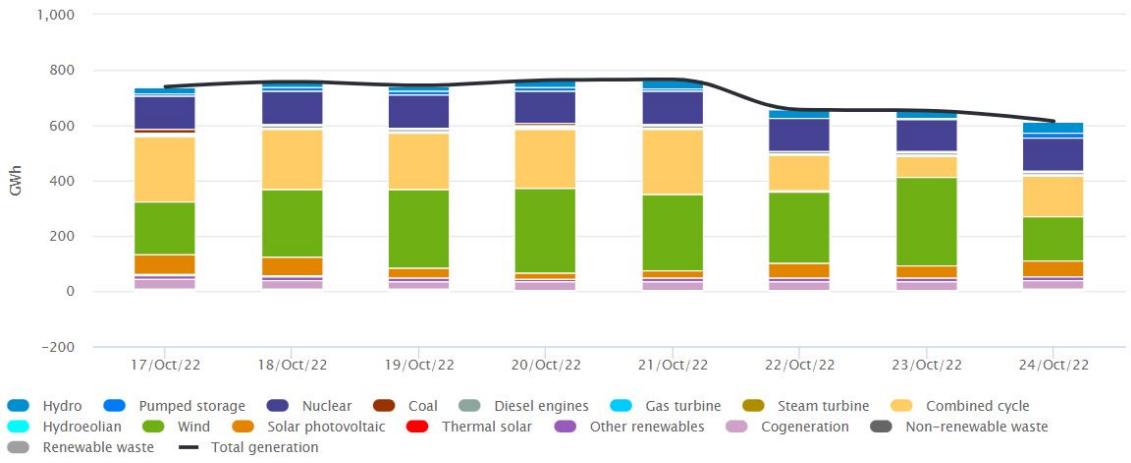

Figure 1.4: Energy generation pool data provided by the Spanish system operator Red Eléctrica[7].

[5] Iberian Electricity Market
[6] European Wholesale Energy Market

The variability in the employed generation technology might affect the system stability, for example, if the demand is mainly covered by WP and PV plants. These plants often are programmed to extract the maximum amount of available power and pour it to the grid, and hence they are not able to form the grid independently by themselves. This is related to the fact that they lack a primary energy reserve that can be employed to increase or decrease the power exchange with the grid. Furthermore, these sources usually employ power electronic converters instead of SGs in the energy conversion process, so if a sudden load increment occurs in the system (e.g. due to unexpected disconnection of a transmission line or power plant), their capacity to provide an inherent inertial response and to readjust the output power in order to cover the loading is very limited [4].

Therefore, the increasing penetration of RES requires additional changes in order to keep a reliable and stable power system. Grid-connected energy storage systems (ESS) can be employed to balance the difference between generation and load by providing primary reserve capacity to grids. Besides, ESSs use a power converter as interfacing element, so different Ancillary services (AS)s could be provided to power systems. In addition to the primary reserve and service provision, the available energy reserve on ESSs would make it possible for the converter to form the grid or provide islanding and black-start capabilities.

Beyond the aforementioned modifications in the generation technologies, power system loading is about to change as well. The electrification of road transport with the advent of EVs will increase the energy demand, and the power supply capacity of modern power systems must be enhanced. However, EVs can be at the same time part of the solution by balancing power generation and loading differences through the so-called vehicle to grid (V2G) concept[8]. The energy storage capacity of EVs combined with smart chargers could provide a great amount of power reserve to the grid, making it easier to cope with the variability of RES generation and paving the way towards a cleaner electric power system.

Taking into account the modifications that power systems need to undergo in this transition, their operation and management is posed as one of the main challenges for power system operators. Owing to the high number of generators and loads, and their variable power exchange with the grid, power systems need to evolve towards more controllable and smarter networks.

Existing ac power infrastructure might be, for instance, divided into different subgrids and new systems of different natures will be connected to it [5, 6]. This will lead to the concept known as grid of grids (GoG), and the newly formed subgrids or microgrids will be created according to the necessities of each case. In this context, dc systems are gaining popularity thanks to the advantages they provide over ac in certain applications. For example, many of the renewable-based generators have a dc stage on their power conversion process, so the combination with ESS—that in most cases are based on dc voltage—could be easier and more

[8] Vehicle to Grid, how does it work?

efficient within a dc microgrid system. This aspect can be also observed in the transportation of energy, where dc systems such as multi-terminal dc (MTDC) grids or high-voltage dc (HVDC) links are becoming a cheaper and more interesting technical solution compared to links based on ac current. Among the advantages, there is a lack of reactive power, lack of synchronisation units, absence of leakage capacitive currents on underground transmission lines or the reduction of conversion stages in converter-based applications [7]. The vast majority of household loads are based on dc or make use of a dc stage on their power conversion process, so dc networks will also become popular at the distribution level. Taking into account the aspects mentioned above, the power systems of the future will be a combination of ac and dc grids, forming a hybrid interlinked system [8, 9].

Although the most efficient way to manage the available resources of each system is by operating them independently, the interconnection and coordination of the different subgrids will improve the entire system's robustness, reliability and utilisation of resources. Figure 1.5 provides an illustrative simplified example of a modern power system scenario, where ac and dc subgrids host generators, loads and ESSs. When power systems of the same nature and characteristics need to be tied, power transformers (for synchronised ac grids) or tie lines (for synchronised and same voltage ac and same voltage dc systems) can be employed (these elements have not been illustrated in the single-line representation from Figure 1.5). However, when grids of different characteristics need to be linked, the use of power electronic converters becomes essential.

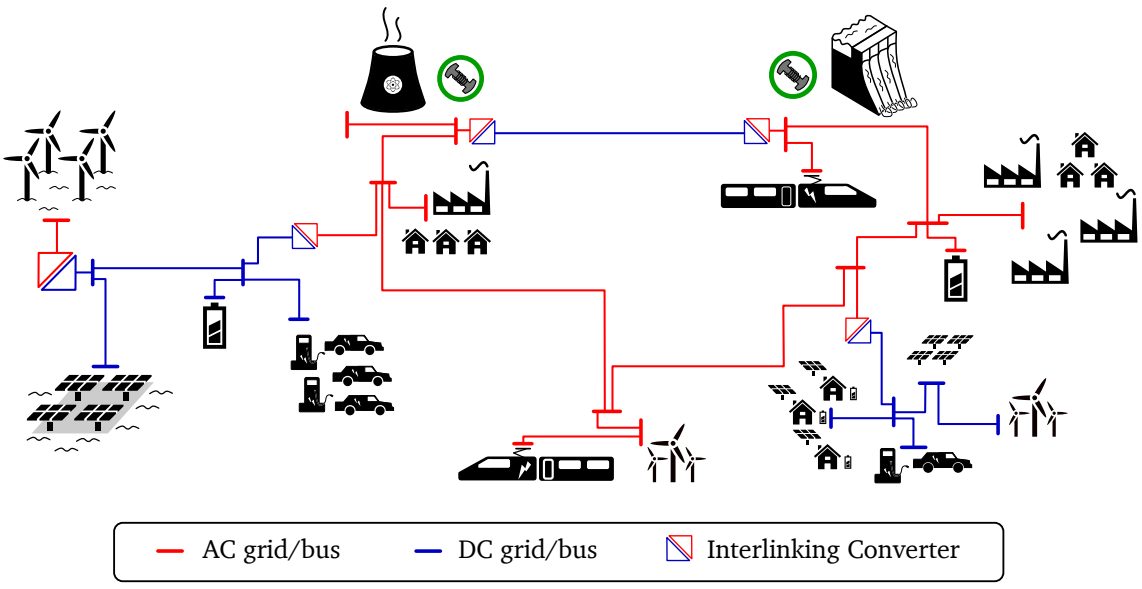

Figure 1.5: Illustration of a modern power system scenario, a hybrid GoG.

1.1.3 The Role of Interlinking Converters

Power transformers and tie lines are widely employed to link different power systems and they offer a higher robustness, lifetime and reliability compared to converter-based solutions. However, their deployment in modern power systems is limited due to electric compatibility issues. In Figure 1.6 a), b) and c), compatible ac and dc grids are connected by using a tie line or a power transformer. In such cases, the power flow through the interconnection cannot be directly controlled since tie lines and transformers are passive elements and the power transmission depends on factors like voltage/angle difference and impedance. However in cases depicted in Figure 1.6 d), e) and f), power electronic converters are required to interconnect the power systems due to the different voltage and frequency levels. These converters are known as **interlinking converters (ICs)** [10], and in addition to controlling the flow of power between subgrids, they can offer a wide variety of services to improve the performance of interconnected systems and therefore, they will play an important role in modern power systems.

In general terms, we refer to ICs as controllable converter-based units that are able to exchange power between two interconnected grids. For the sake of clarity, more detailed insights about the IC concept are provided thereupon.

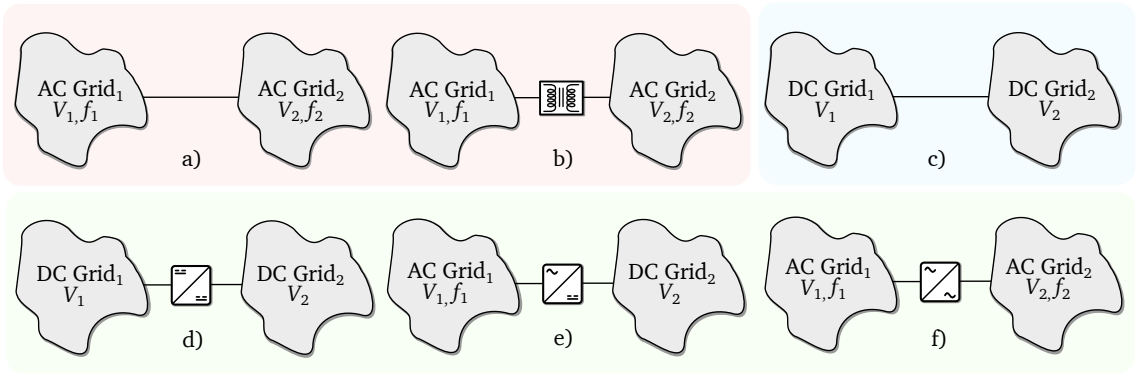

Figure 1.6: Interconnection of: a) synchronised ac grids with same voltage and frequency, b) synchronised ac grids with different voltage and same frequency, c) dc grids with same voltage levels, d) dc grids with different voltage levels using an IC, e) an ac and dc grid using an IC and f) two ac systems using an IC.

The most relevant features of ICs compared to traditional, passive tying methods are:

- **Connectivity regardless of grids' nature:** ICs enable to interconnect asynchronous ac grids as well as ac and dc systems with different voltage levels.
- **Grid decoupling:** since ICs are actively controlled, they can be employed to prevent the propagation of voltage sags, current harmonics of even system blackouts due to contingencies.

- **Power flow and voltage control:** active and reactive power flows can be actively controlled in a IC, and they can be also used as a voltage source for one of the interconnected systems.
- **Contribution to ASs:** as other converter-based solutions, ICs can be employed to provide ASs to the interconnected systems, such as reactive power control, inertia-emulation or harmonic current compensation.

The main difference between a power converter interfacing an ESS and an IC resides on the fact that in the case of the IC, both sides of the converter will be variable. Although in the first case the state of charge (SoC) and the voltage of the ESS will vary over time, from the converter control viewpoint the supply can be considered to be constant. However, when two grids are tied by an IC, frequency and/or voltage values (either ac or dc) might vary dynamically and thus they cannot be considered to be constant any more. Besides, both interconnected grids may require to be supported under sudden power variations.

The IC concept encompasses any type of converter-based grid interconnection such as tying microgrids, distribution networks, linking different energy transport systems or a combination of the above. For instance, a converter interconnecting an ac and dc microgrid is considered a IC, and a converter that links a high-voltage MTDC grid with a large ac system can be considered a IC as well. Thus, the employed IC topology and components will depend on the characteristics of the interconnection, i.e. on the nature of interconnected grids, voltage level difference, required maximum power transfer and so on. For some particular interconnections, these elements are often referred in the literature as solid state transformers (SSTs) or smart transformers (STs), usually referring to ac-ac interconnections. In general, ICs can be classified according to the voltage nature of the interconnected grids [11], or according to the number of stages they employ in the power conversion process [12–14].

When the latter classification is employed, some authors state that the intermediate bus of each conversion stage can be considered as another grid, and hence each stage as an independent IC [11]. As an example, Figure 1.7 shows how an ac-ac interconnection can be coceptually carried out by employing different IC configurations.

However, if Figure 1.7 b) is taken as an example, at first glance it can be seen as a back to back converter configuration in which both stages are part of the same device and they share the same control unit and purpose. At the same time, this illustration can correspond to two converters that are part of a dc link where the converters are physically separated, have their own control units, or there might exist more elements connected to the dc link making use of it. Thus, **regardless of the number of power conversion stages, we will consider a single IC unit the device with a given purpose and a unique controller that rules the different power conversion stages according to its aim**.

Following the above mentioned example of the two-stage ac-ac interconnection and our

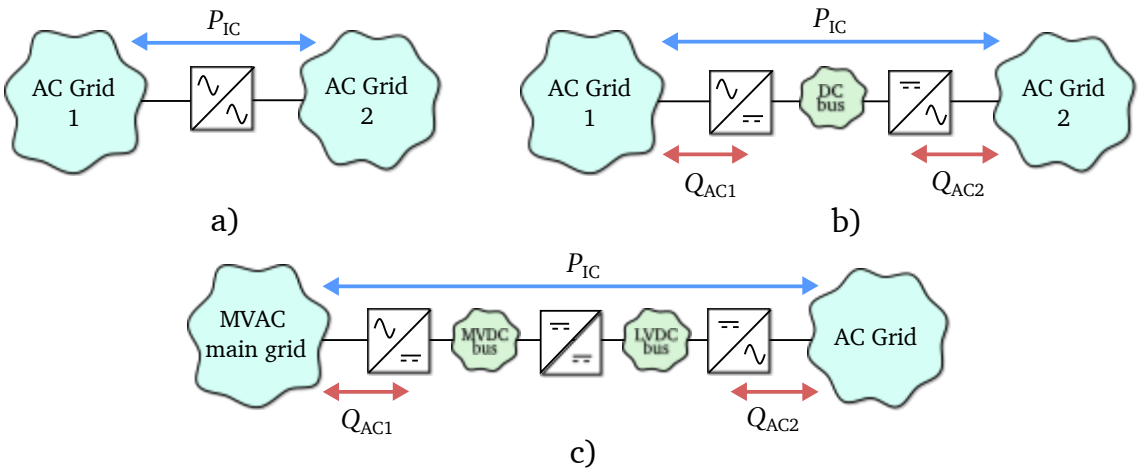

Figure 1.7: a) single-stage, b) two-stage with an intermediate dc grid and c) three-stage and two intermediate dc grid ac-ac interconnection illustrations from [11].

criteria to classify ICs, Figure 1.8 a) shows a two-stage IC with a unique controller, while Figure 1.8 b) depicts two ICs connected to a dc system (they can be the ones that form it or not), where additional units can be connected to intermediate dc system. In the latter case, each IC has its independent control and it might respond to different necessities.

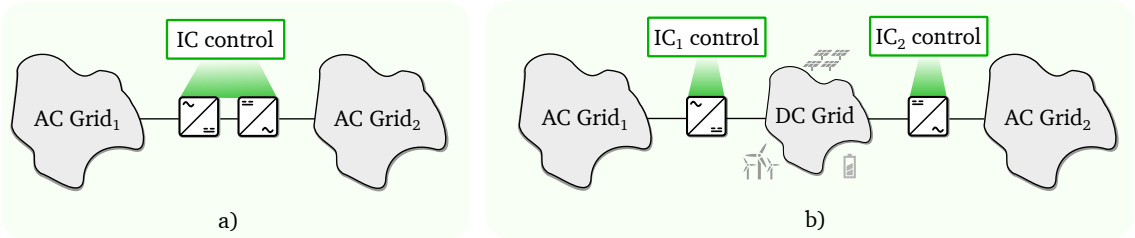

Figure 1.8: a) Two-stage IC, b) two single-stage ICs.

Thus, we can consider a multiple stage converter as an IC unit if it has a unique control unit, and all the stages work according to the same purpose. We would like to clarify that under our criteria, ESS—beyond dc link capacitors or possible inductances—will not be considered part of a IC unit. In other words, the IC itself will not be able to provide any power or energy reserve, and the steady-state or average power circulation among interconnected grids must be equal (leaving aside the differences derived from converter losses). This results from the idea that an IC can take advantage of the energy reserve of interconnected grids, so if there exists an additional energy reserve inside a power conversion stage, it must be considered as an additional subgrid, and it will provide an additional degree of freedom in the operation of adjacent stages. Besides, since traditional tying methods cannot provide any energy reserve by themselves, the comparison with storage-based ICs would not be possible or even fair.

When a IC interconnects two different systems, the reserves of both systems can be in-

creased by adequately controlling the transferred power [15]. At the same time, the reliability and robustness of the interconnected systems can be enhanced, helping to reduce the load shedding as well. As it is further studied in Chapter 3, ICs can provide ASs to the interconnected grids by taking the contrary grid as source.

Some of the already operating and ongoing projects that employ ICs in real grid interconnections are presented below.

HVDC between Spain and France

International grid interconnections allow energy exchange between neighbouring countries, which is essential in the way towards decarbonisation, implementation of RES, and it brings a variety of technical and economical advantages for the connected countries[9]. Besides, the European Union Member states must achieve at least a 15% interconnection Ratio by 2030, and the interconnection ratio of Spain at the present time is less than 5%[9]. In this path, the Spanish transmission system operator has foreseen new international grid links in the transmission system development planning by 2026[10].

The first converter-based interconnection between Spain and France was launched in 2015 by the Spanish-French company INELFE[11] and it linked Santa Llogaia in Spain with Baixas town in France[12]. The interconnection takes place over the Pyrenees, using two 1 GW HVDC links of ±320 kV, and it enabled to increase the power exchange capacity with France up to 2.8 GW.

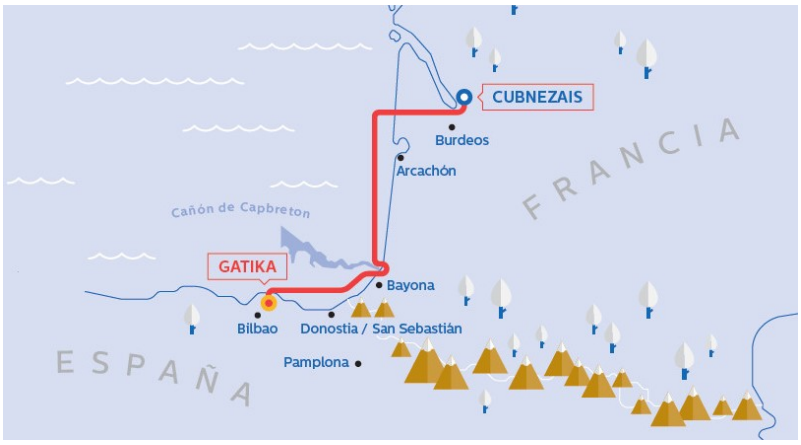

Figure 1.9: Foreseen HVDC undersea interconnection between Spain and France by INELFE[13]

Additionally, with the aim of increasing the power exchange capacity with France up to 5 GW, INELFE is working on a second HVDC link (see Figure 1.9), in which the converter stations

[9] Redeia, Strengthening Interconnections
[10] Development Plan of Spanish Transmission System 2021-2026
[11] INELFE
[12] HVDC link, Baixas - Santa Llogaia

are located in Gatika (gulf of Biscay) and Cubnezais (Aquitaine). This interconnection consists of four undersea cables, where two links of 1 GW are being installed, and are scheduled to be operational by 2027[13].

These converter-based links are considered ICs under our criteria, and depending on the employed control approach, each converter station could be considered as a single IC.

Combined Grid Solution

The German and Danish transmission network operators inaugurated the Combined Grid Solution[14] project in 2020, where a IC and power transformers are combined to link the *Krieges Flak* (DK) offshore WP park with the *Baltic Sea 2* (D) park (see Figure 1.10). This interconnection enables the energy exchange between two grids by means of two sea cables with a transmission capacity of 400 MW, taking advantage of the existing and recently built infrastructures for offshore wind farms.

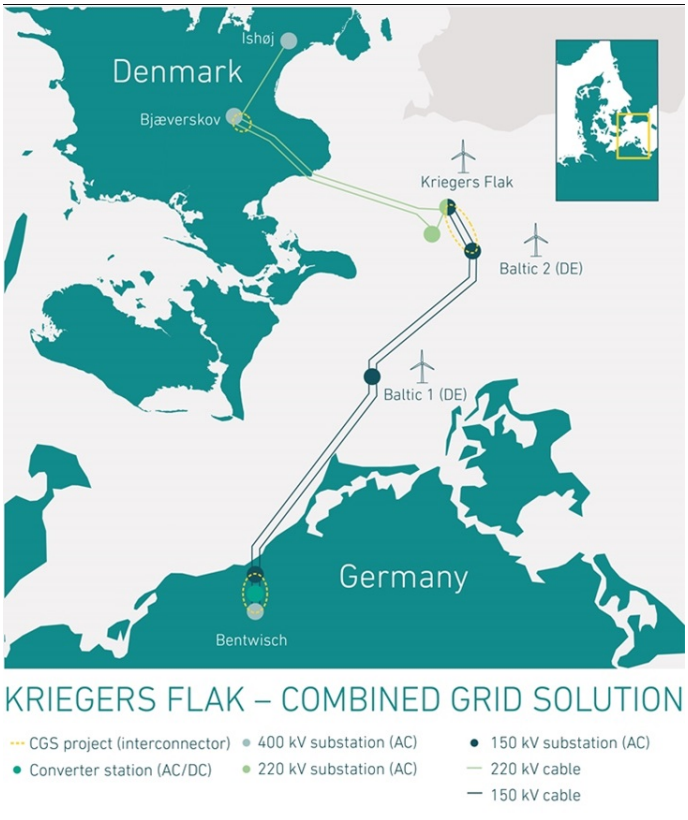

Figure 1.10: Illustration of *Combined Grid Solution* project[14]

Although the Danish and German transmission power networks have the same rated frequency of 50 Hz, they are not synchronised and the energy transport systems' voltage to off-

[13] HVDC link, Gatika - Cubnezais
[14] Combined Grid Solution

shore farms is different (220 kV and 150 kV for the Danish and German systems, respectively). Therefore, this project has two main parts. First, both systems are linked using a power transformer at *Kriegers Flak* offshore wind farm and then, the phase difference issue is solved using a back-to-back IC at *Bentwisch*, Germany as illustrated at Figure 1.10.

Network Equilibrium

This IC application case belongs to the power distribution network of the south-west part of the UK, as Figure 1.11 depicts. The power network infrastructure was initially designed for passive power distribution requirements, and the problem arose when two distribution networks of 33 kV from Somerset and Devon could not be tied directly due to a number of issues, such as circulating currents, protection grading and fault event constrains. On the other hand, the integration of new RES units would cause grid management and thermal issues if no action was taken by operating the system actively. The *Network Equilibrium*[15] project integrates the so-called *Flexible Power Link*, which consists of an IC with a back-to-back topology in charge of the power transfer and support across two different 33 kV ac distribution networks.

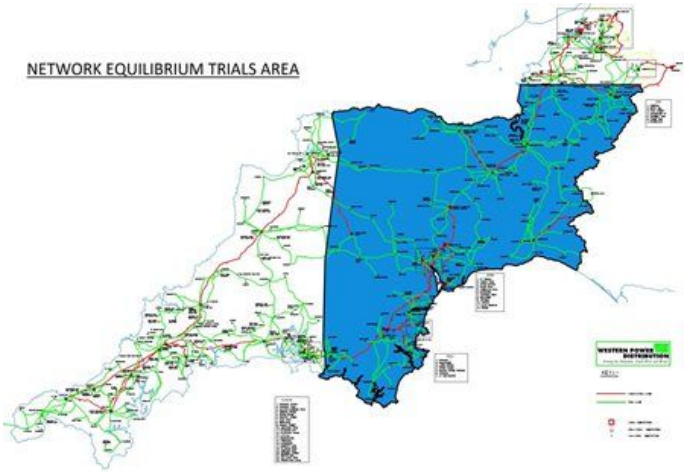

Figure 1.11: Illustration of *Network Equilibrium* project area[15].

The power converter is provided by ABB company[16] and it has a rated power of 20 MVA (Figure 1.12). With this project the resilience of the electricity network is improved and it allows the system operator to control the active and reactive power flow between two power systems through the IC.

[15] Network Equilibrium
[16] ABB, Flexible Power Link UK

Figure 1.12: ABB's Flexible Power Link (IC) installed at the Network Equilibrium project[16].

1.2 Key Challenges

Considering the insights we have presented about the operation and evolution of power systems and the role of ICs, in this section we give the most relevant **key challenges** which have set the course of the research of the presented PhD thesis.

1.2.1 Grid Interoperability

In a GoG scenario, the different subgrids might be of different current natures and characteristics and hence, traditional tying methods might not be adequate to carry out such interconnections. ICs are able to tie these grids and exchange power among them, and if they are controlled properly they can be employed to provide a wide amount of services to interconnected grids as well. Thus, we have identified as a challenge the necessity to develop and propose new control strategies to make grids of different characteristics and natures compatible, while the operation of such grids is improved by taking full advantage of ICs.

1.2.2 Power Reserve on Modern Power Systems

Keeping the balance between the generated and consumed power is essential to ensure the stability of electric grids. While traditional SG-based grids have the capacity to regulate their power according to the demand, this capacity is notably reduced in renewable based modern power systems. The reason is that they are not dispatchable, so the capacity to balance the system loading and generation is very limited, and the most significant decision that can be taken is power curtailing of RES generators. Thus, we have identified the availability of sufficient power & energy reserve to be of vital importance for keeping the modern power systems' stability, and ensure the power supply of the system. In this task, ESS will have a very important role handling the stochastic character of renewable energies and responding to the power demand of the users without compromising the resilience of the grid. Besides, ICs and their corresponding controllers will help to increase the available reserve capacity of the

interconnected grids, by taking advantage of existing generators and ESS of interconnected grids.

1.2.3 Inertial Response at Grids with High Penetration of Power Converters

When power electronic converters are used for power conversion on grid-connected applications, they do not present an inherent inertial response under active power variations. Furthermore, if there is any rotating inertial element that could provide some sort of response, they would decouple its response from the grid. Therefore, the improvement of the inertial (or transient) response is one of the main challenges to overcome in the transition towards cleaner renewable-based modern power systems. We have seen that ICs can contribute to improve this response by utilising the opposite grid as an energy source to synthesise the inertial response, so the challenge resides on proposing, testing and validating new control strategies that will contribute to the transient response of interconnected systems.

1.2.4 Grid-Forming and Black Start Operation Capability

Renewable-based generation units usually aim to extract the maximum amount of available power and deliver it to the grid. In order to achieve so, the grid must be set by other devices such as SGs or power converters controlled as voltage sources. However, with the gradual replacement of SG-based generation plants by renewable ones, the number of devices that are able to "form" the grid (known as grid-forming devices) is being drastically reduced [16].

In other words, there is a need for grid-connected converters to participate in the voltage and frequency regulation of the grid to compensate for the disconnection of classical grid-forming devices. Besides, if a power system fails and suffers a blackout, grid-forming units can be employed to restart the system, provide reference and power supply to energise the rest of the devices. In this sense, ICs can be very suitable to restart a grid since the power and energy capacity that one subgrid might offer will probably be higher than the one provided by distributed ESS units. Thus, the development of grid-forming controllers for ICs will help to make modern power systems more reliable, and will be essential for black start operation in case of system blackout.

1.2.5 Dynamic Simulations of Modern Power System Scenarios

Until recently, the time domain response of power systems has been represented assuming that the frequency and voltage would evolve according to the dynamic behaviour of classical SGs. However, with the massive penetration of power converters this premise is no longer valid due to the fact that the fast dynamics of converters and their controllers entail different implications on the power system's response, as it as been pointed out in the previous challenges. Thus, the classical methods and tools used to simulate modern power system scenarios

might not be the most suitable ones to carry out some types of analyses. For instance, we have seen that there is a need to reduce the computational burden of power systems' dynamic simulations, in order to perform simulations of longer time ranges. Besides, we consider that a user-friendly environment is an essential feature for a simulation tool, since it will enable to implement and test new power system scenarios and the corresponding controllers of the grid-connected devices.

1.3 Goals of the Thesis

Inspired by the identified challenges, the main goal of this thesis is to **develop, analyse and validate control strategies for ICs that contribute to the transient response of interconnected ac and dc power systems.**

In order to achieve the main objective of the thesis, we have set the following specific goals:

[O1] Development of a dynamic simulation tool for modern power systems to assess the contribution of ICs and grid-connected converter control strategies to the transient response of grids.

[O2] Review and classification of existing low-level IC control strategies for the provision of virtual inertia and transient response at the interconnected ac and dc systems.

[O3] Development and evaluation of IC control techniques for the provision of virtual inertia and transient support in modern power system scenarios.

1.4 List of Contributions

The most relevant technical contributions of this thesis can be summarised as follows:

- A **Matlab/Simulink® based simulation tool** that combines static power flows with simplified dynamic models of grid-connected elements **for the representation of the transient response related to electromechanical oscillations and converter controller dynamics of ac, dc and hybrid ac/dc power systems**.
- The **establishment of a unified framework for developing IC control strategies regardless of the nature** of the interconnected grids.
- A detailed **review** of **IC control strategies** that contribute to the transient response of interconnected power systems.
- The **proposal** of a novel ***dual inertia-emulation*** **IC control technique** to improve the transient response of interconnected power systems regardless of their nature.

- The **proposal** of a novel ***virtual power line*** **IC control technique** that unifies transient and steady state responses of interconnected power systems regardless of their nature.

The contributions made in the form of **publications** during the realisation of the thesis are summarised as follows:

1.4.1 Journal Papers

[J1] J.Paniagua, E. Unamuno and J. A. Barrena, "Dual Inertia-Emulation Control for Interlinking Converters in Grid-Tying Applications," *IEEE Transactions on Smart Grid.*, 2021. DOI:10.1109/TSG.2021.3078839

[J2] J.Paniagua, E. Unamuno, J. A. Barrena, D. Serrano-Jiménez and Ander Goikoetxea, "A Dynamic Frequency Power Flow Simulation Tool for AC Power Systems based on Simulink," *Electric Power Systems Research EPSR.*, 2023. → **Under Review**

[J3] J.Paniagua, E. Unamuno and J. A. Barrena, "Virtual Power Line Control for Interlinking Converters on AC, DC and Hybrid Grid Links," *IEEE Transactions on Smart Grid.*, 2023. → **Under Review**

[J4] A. Ordono, E. Unamuno, J. A. Barrena, J.Paniagua, "Interlinking Converters and their Contribution to the Primary Regulation: A Review," *International Journal of Electric Power and Energy Systems IJEPES.*, 2019.
DOI: 10.1016/j.ijepes.2019.03.057

1.4.2 Conference Papers

[C1] J.Paniagua, H. Gezala, E. Unamuno, M. Zubiaga and J. A. Barrena, "A Dynamic Frequency-and-Voltage Power Flow Simulation Tool for Hybrid AC/DC Power Systems based on Simulink," *IECON 2022 – 48th Annual Conference of the IEEE Industrial Electronics Society.*, 2022.
DOI:10.1109/IECON49645.2022.9968708

1.4.3 Magazine Papers

[M1] E. Unamuno, J.Paniagua J.A. Barrena, "Unified Virtual Inertia for ac and dc Microgrids: and the Role of Interlinking Converters," *IEEE Electrification Magazine.*, 2019.
DOI: 10.1109/MELE.2019.2943978

1.5 Thesis Outline

In Figure 1.13 we show the structure of the presented thesis, and how each chapter is related to specified objectives on the project and realised publications through it.

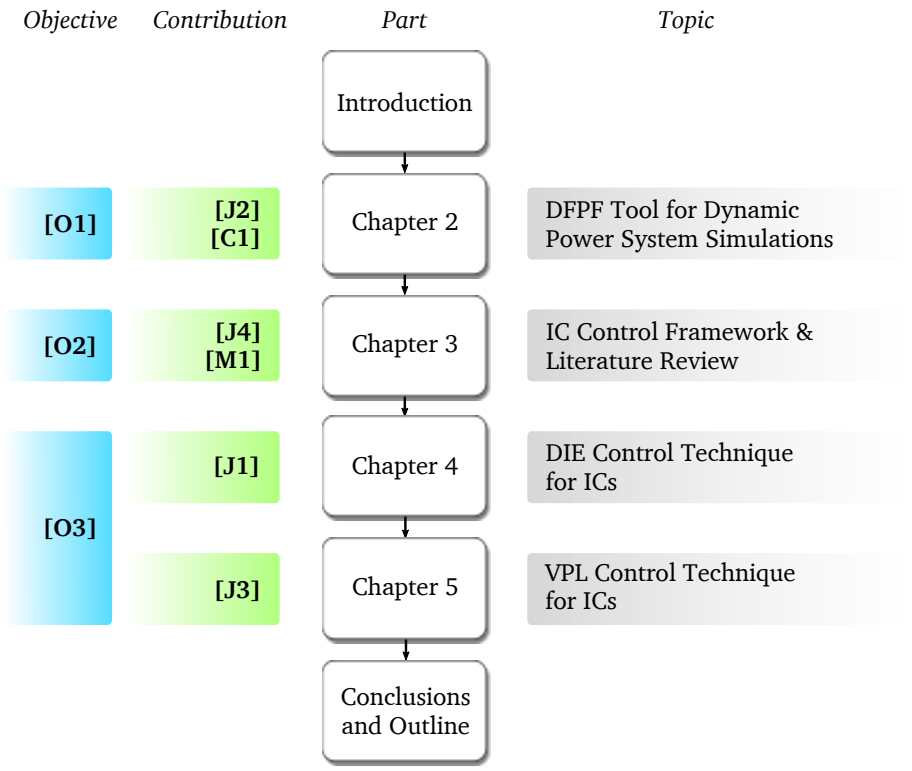

Figure 1.13: Structure of the thesis and its relation with specified objectives, contributions and topic of each chapter.

Once we have explained the background, the main challenges and objectives of the thesis in the current **Chapter 1**, in **Chapter 2** we explain the principles of the proposed dynamic simulation tool for ac, dc and hybrid power systems. This tool, named dynamic frequency power flow (DFPF), is compared and validated against electromagnetic transient (EMT) and Phasor simulation methods using the Matlab Simulink® environment and it has been employed during this PhD thesis to validate and test the newly proposed IC control strategies for the provision of transient support in modern power systems (i.e., the ones explained in Chapters 4 and 5).

In **Chapter 3** we first provide a technical background related to the control of power systems, grid-connected converters and the analogy between ac and dc systems. These concepts are analysed from a IC perspective, and are essential to lay the foundations to set a unified framework for developing IC controls as well as to understand the approaches in the literature. Then, a review of the existing IC control strategies that contribute to the transient support of interconnected grids is provided.

One of the most important contributions of the performed work is presented in **Chapter 4**, where we propose a dual inertia-emulation (DIE) control for ICs. This strategy can be implemented to support different types of grids due to the fact that it uses the normalised values of frequency and voltage derivatives of ac and dc grids respectively.

In **Chapter 5**, we present the virtual power line (VPL) control for ICs. This control enables to tie different power systems in the way a power line would do tying two compatible power systems. We have seen that the proposed control unifies the inertial and primary responses of interconnected systems effectively. The VPL control is proposed with two variants, contributing to form and make the interconnected power systems more reliable.

In **Chapter 6**, the most important conclusions we have obtained during the realisation of the presented research work are summarised. Last but not least, we conclude the presented work with the most interesting research lines that would follow the work done throughout this thesis.

Chapter 2

Dynamic Frequency-and-Voltage Power Flow-Based Simulations of AC, DC and Hybrid AC/DC Power Systems

A more renewable energy generation model entails more susceptible power systems in terms of frequency and voltage oscillations under sudden power perturbations. In addition, dc-based power systems are becoming very popular thanks to the advantages they offer compared to classical ac systems for certain applications. This entails the necessity to develop new time-domain simulation tools to represent the dynamic behaviour of converter-dominated, hybrid ac/dc power systems.

This chapter presents a dynamic frequency power flow (DFPF) tool that combines classical power flow algorithms with simplified generator and grid-connected device models in the Simulink® environment to study oscillations associated to the electromechanical phenomena of rotating generators and the most representative control dynamics of grid-connected converters. Thus, the dynamic performance of ac, dc and hybrid power system scenarios can be studied, including the integration of renewable energy sources and dynamically varying loads. Among the advantages of the proposed tool, the low computational burden of the employed method and the Simulink interface simplify the simplifies the definition of new test scenarios and permits to carry out dynamic power system scenarios very time efficiently.

2.1 Introduction to Power System Simulation Methods

Until recently, most power system studies have been focused only on ac systems and have considered the grid frequency to be constant, but since the properties of modernised and newly created systems are different from the classical ones, this is no longer a valid assumption. Thus, the development of new tools and algorithms capable of representing and studying the dynamic evolution of the frequency and voltage of ac, dc and hybrid ac/dc power systems is gaining importance. Among the existing simulation methods to assess the frequency and/or voltage stability of power systems, EMT simulations can be found. These simulations can represent the power system with a high level of detail and provide accurate results of the dynamics associated to electromagnetic as well as electromechanical phenomena. However, they become very time consuming as the system complexity and simulation time increases. Usually, setting up an EMT simulation to study the frequency or voltage stability for time spans in the order of several minutes to hours becomes unfeasible, so they are usually employed to study fast electromagnetic transients of power system scenarios.

To accelerate the study of power systems, the electrical part of the system is usually simplified and based on the algebraic equations that describe the power flow through the system lines. The premise is that the (electromechanical) dynamics of power systems are slow compared to electromagnetic transients. Depending on the level of detail that is required in the simulation, the methods where the electrical part of the system is described with power flow equations can be classified as follows:

1. Active elements represented with algebraic equations.

2. Active elements aggregated in a dynamic equivalent model.

3. Individual dynamic models for each active element.

Figure 2.1 illustrates the capabilities of each method to represent dynamic phenomena in power systems.

In the first group, classical load flow or power flow analyses can be found [17–20]. These studies are focused on ac power systems and compute the steady-state operating points of classical power systems, providing the bus voltage magnitudes and phase angles and the power flowing through the lines depending on the loading of the system. Static load flow studies can be also employed to study slow voltage variations for different loading conditions. These steady-state analyses help to detect overloading conditions, system losses as well as weakened voltage nodes across the system. As mentioned before, one of the main assumptions is that the frequency of the system is constant, meaning that the use of static power-flows is not valid to represent dynamic frequency transients under power perturbations. In the case of dc systems there is no reactive power circulation and hence, static load flow studies are simpler and study

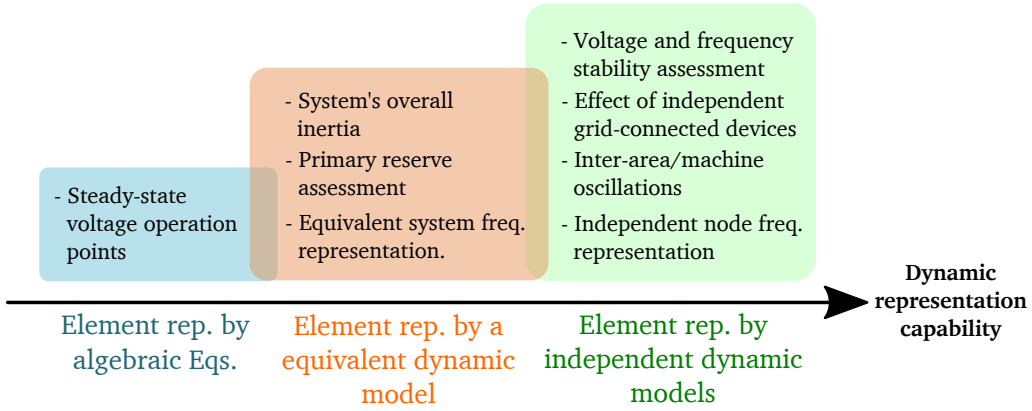

Figure 2.1: Power flow equation-based power system simulation methods classified according to the capability to represent the system dynamics.

the dependence between the active power and system's voltage, as authors propose in [8] and [21].

In the second group the study of the system's frequency is carried out globally by aggregating the dynamic response of the devices that carry out the system frequency regulation. Instead of representing the frequency at each node of the system, a single frequency is assumed for the entire system. The so-called long-term dynamic simulation (LTDS) is an example of this approach, which was proposed by the electric power research institute (EPRI) in 1974 [22]. The method consists on solving a static load flow problem with a 1 s time step and the obtained results are combined iteratively with an equivalent generator and prime mover model, obtaining an aggregated dynamic frequency and voltage response. Recently, Haines employed the LTDS method to develop a Python-based tool to track the frequency in large power systems [23]. In [24], Fan *et al.* propose a dynamic power flow simulation model, which is intended for the analysis of the post-contingency flow of power. The authors consider a nonlinear generator dynamic model for the slack node of the ac power system. The slack node's inertia is determined by the center of inertia of the grid. This equation is integrated in the power flow algorithm, and then the system is solved iteratively to obtain the frequency variations at the slack node. All the aforementioned methods usually employ a simulation step around 1 second, so very long simulations can be carried out. However, it is not possible to consider oscillations between different generators or system areas, or the influence of a specific device in the node where it is connected.

In the third group, power flow algorithms are combined with the individual models of grid-connected devices. The dynamic models usually represent the electromechanical phenomena associated to SG or other grid-connected elements. Compared to the methods in the second group, they can represent the system frequency at any node of the system. This means that the oscillations between different devices or system areas can be also studied. Several methods have been proposed in the last decade to carry out this type of simulations. Dynamic power

system studies for dc or hybrid ac/dc systems that employ load flow algorithms are not common in the literature and therefore, the following literature review covers the load flow-based ac dynamic power system studies.

In [25], Pawellek *et al.* compare two dynamic power-flow simulation approaches in an eleven node system with three SGs. The first approach corresponds to the simplified rotating mass (SRM) method, that represents all the rotating masses in a single dynamic model. The second approach is called distributed rotating mass (DRM), and it considers a differential equation system per generator. In both approaches, the load flow problem is solved employing a newton-raphson (NR) numerical method.

In [26] Li *et al.* propose a power flow method to study the power-frequency dynamics on power systems. The proposed method is named direct current load-flow based frequency response model (DFR), and the ac network is modeled employing dc equations. In this method generator and grid voltage dynamics are neglected to reduce the computational burden. This method employs the modified Euler's method to solve the load flow problem, and it is developed using C++ code.

Last but not least, Abdulrahman *et al.* propose an analytical tool based on MATLAB in [27] to carry out different studies such as time-domain simulations, modal analysis or frequency response analysis. According to the authors, the available software for power system analysis does not consider the full advantages of MATLAB solvers. The proposed tool models synchronous generators, excitation systems and the turbine system by means of differential equations. Stator and power line impedances are represented with algebraic equations, and are solved in a power flow algorithm with Euler's method. In spite of the wide range of possibilities offered by the tool, all equations must be written down in MATLAB, meaning that it does offer the advantages of a graphical interface and nonlinear functions such as saturations or rate limiters cannot be easily implemented.

With similar functionalities, Abdulrahman *et al.* propose a tool based on MATLAB/Simulink for the dynamic analysis of power systems in [28]. In this case, the Simulink graphical interface is only employed to implement the differential equations of the SG model, while the algebraic equations from the SGs' stator are implemented in a *MATLAB function*. The implementation of multiple SGs in the system under study is achieved by providing model parameters in Simulink as arrays, so the results are obtained as arrays as well. Moreover, only a sixth order SG model can be employed as the generator model. Additional MATLAB files are employed to declare bus, machine, excitation and turbine data, as well as bus loading, and the power flow algorithm is solved via MATPOWER. In short, the tool proposed in [28] does not take full advantage of the graphical interface of Simulink, since it is only used to integrate the SG differential equations and the rest are defined in MATLAB code. Thus, it is not straightforward to implement dynamic load or generation profiles in the system nodes, or to integrate other types of grid-connected devices that do not correspond to the predefined SG model.

Table 2.1 summarises the most relevant features of the tools capable of representing frequency variations identified in groups two and three above.

Table 2.1: Classification of different simulation methods for ac power systems that employ power flow algorithms and represent frequency dynamics

Method	f transient	f distributed	V transient	Graphical interface	PF method	Language
[22]	✓	✗	✓	✗	NR	LOTDYS
[23]	✓	✗	✓	✗	Several*	Python
[24]	✓	✗	✓	✗	NR	Not specified
[25]	✓	✓	✓	✗	NR	MATLAB
[26]	✓	✓	✗	✗	Euler	C++
[27]	✓	✓	✓	✗	Euler	MATLAB
[28]	✓	✓	✓	✗	Euler	MATLAB/Simulink + MATPOWER

*Euler, Adams-Bashforth and Runge-Kutta.

Other approaches that do not make use of power flow equations but are capable of representing dynamic frequency variations include the so-called Phasor or RMS simulations. In this case, the electrical part of the grid is represented algebraically and solved with current and voltage phasor equations [29]. These simulations are usually aimed at representing electromechanical phenomena by studying the fundamental frequency of positive sequence voltages and currents. In addition to classical power systems, they have been also employed to study the transient, voltage or frequency stability and other dynamic phenomena of grid-connected, converter-interfaced generation systems [30]. As an example, Simulink offers the possibility to carry out Phasor simulations taking advantage of its graphical interface.

The aim of this section is to propose a load flow-based simulation tool capable of representing frequency and voltage dynamics of ac and dc power systems, taking full advantage of Simulink® capabilities to graphically implement and interconnect different power systems and their grid-connected device models. The tool, named dynamic frequency power flow (DFPF), is comprised by a power flow algorithm that solves the electrical part of the grid on the one hand, and the dynamic models of grid-connected elements–built with classical Simulink blocks–on the other one. By solving the power flow on each simulation time step and combining the results with the dynamic models, the DFPF tool offers significantly faster simulations compared to available EMT or Phasor simulation methods. This allows to represent the frequency and voltage transients of power systems during larger time spans, which is necessary e.g. to study the implementation of RES or ESSs providing some kind of frequency or voltage regulation to improve the system's stability under power perturbations. In such cases, the frequency transients need to be considered because 1) they are an indicator of the system's performance, 2) they will influence the energy balance of the system and 3), because they have an impact on the lifespan of the device. Similarly, parametric simulations to analyse the influence of

control or physical parameter variations in long-term simulations can be carried out. It must be highlighted that employing the DFPF tool, multiple ac and dc power systems can be interconnected and simulated, obtaining the frequency and voltage dynamics of each node as it is further demonstrated during this document.

In view of the above-mentioned features, the DFPF tool is ideal for industry, research and academic purposes where the electromechanical oscillation-derived frequency transients need to be studied in time spans beyond hours. In the upcoming section 2.2, the principles of operation of the DFPF tool are explained in detail.

2.2 Dynamic Frequency Power Flow Tool

The aim of the DFPF tool is to represent frequency and voltage variations of modern ac, dc and hybrid power systems. These dynamics can be associated to the electromechanical behaviour of generators, or to the dynamics of employed grid-connected converters and their controllers. Thus, we consider essential to be able to study the interactions between classical generators and electronic power converters that contribute in the frequency/voltage regulation of the grid (named grid-forming and grid-supporting devices, as it is further explained in 3.1.3).

The DFPF tool solves the electrical part of the power system by means of power flow equations of ac and dc systems employing the well-known NR numerical method [17, 18, 20]. The power flow is solved iteratively at each time step of the dynamic simulation and it is combined with the transient response of the devices connected to the grid. The DFPF tool is implemented in MATLAB® Simulink® to take advantage of MATLAB functions and the graphical interface offered by Simulink to integrate the grid-connected device models. As it will be explained hereafter, other numerical methods could be also employed to solve the system of power equations.

Figure 2.2 shows the operation principle of the proposed DFPF algorithm for a four node ac power system. The NR algorithm to solve the power flow is implemented in a *MATLAB function* from Simulink. On the other hand, the dynamic models of grid-connected devices are implemented with Simulink classical blocks. The power flow equations are solved for the inputs at the current iteration, and the obtained node voltages and powers are fed back to the element models to obtain a new point of operation. The following subsections describe the main parts of the DFPF tool in detail.

2.2.1 Power Flow Solver

At classical static power flow studies of ac power systems, the aim is to determine the steady-state operating point for given generation and loading conditions. These studies usually employ four independent variables to solve the system: voltage magnitude, voltage angle,

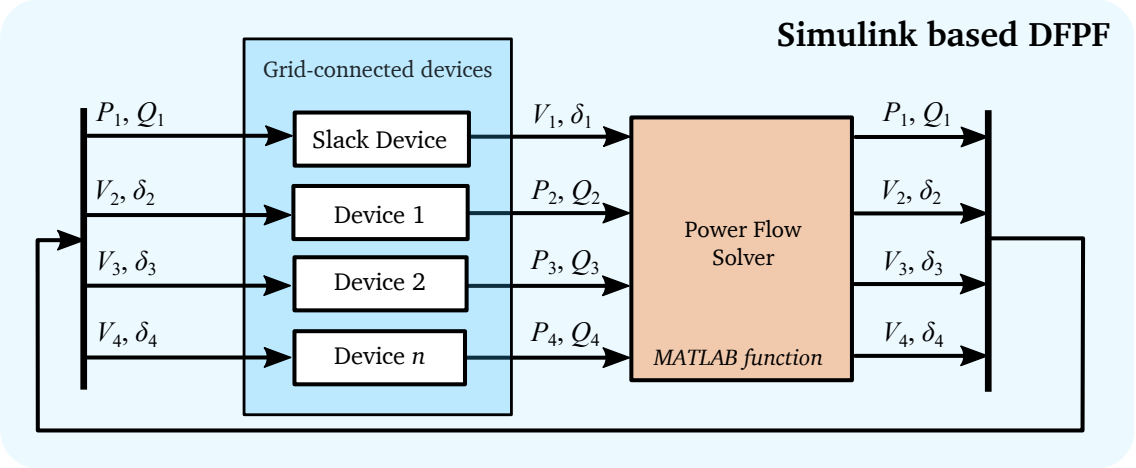

Figure 2.2: Description of the DFPF algorithm for an ac power system.

active power (P) and reactive power (Q). Table 2.2 shows the different types of nodes that are usually distinguished, including the variables that are already defined and the ones that need to be solved by the power flow algorithm. The **slack bus** (also referred as slack node or swing node) is the one that presents a fixed voltage magnitude and angle and it is considered as the system reference. The device connected to the slack node is required to provide the mismatch power between the active and reactive power balance of the overall system. At **PQ nodes** the active and reactive power is defined, so they are used to integrate load or generation devices. The magnitude and phase of these buses is calculated according to the total power balance and lines' admittance in the power flow algorithm. Other type of buses such as **PV nodes** where the active power and the voltage amplitude are defined can be also considered in power flow algorithms. However, the most common devices can be connected to slack or PQ nodes, so PV nodes are not considered in the following sections.

Table 2.2: Different node types on an ac static load flow problem

Node Type	Defined Variables	Unknown variables
Slack	$\theta, \lvert V \rvert$	P, Q
PQ	P, Q	$\theta, \lvert V \rvert$
PV	$P, \lvert V \rvert$	θ, Q

In the case of dc power systems, the node types can be defined following the same procedure. The slack node only sets the system's voltage reference and the rest of the nodes can be defined as simple P nodes, as Table 2.3 suggests.

The algebraic equations that define the flow of power through the lines of an ac power system are well known and have been widely covered in the literature. However, the method followed to obtain them is repeated here for convenience, since they are some of the key

Table 2.3: Different node types on a dc static load flow problem

Node Type	Defined Variables	Unknown variables
Slack	$\|V\|$	P
P	P	$\|V\|$

functions of the DFPF tool. The process begins with the following apparent power equation:

$$S_i = V_i I_i^* = V_i \left(\sum_{j=1}^{n} Y_{ij} V_j \right)^* = V_i \sum_{j=1}^{n} Y_{ij}^* V_j^* \tag{2.1}$$

where S_i is the power that one node exchanges with the system, calculated as the sum of the power exchanged with other nodes (S_{ij}).

In the DFPF tool, the p.u. frequency of the system is considered to be very close to 1 and thus, line impedances are calculated with this nominal value, assuming that the error caused by frequency deviations will be very small. The admittance of an *RL* line between nodes i and j is named y_{ij} and is the inverse of the impedance z_{ij}:

$$y_{ij} = \frac{1}{z_{ij}} \tag{2.2}$$

It must be noted that the terms y_{ij} do not correspond to the admittance terms Y_{ij} in Eq. (2.1). The latter are elements extracted from the so-called admittance matrix **Y**. The non-diagonal terms of this admittance matrix are the negative value of the admittance between two nodes, while the diagonal terms represent the total node admittance, calculated as the sum of the admittance of all the lines that are connected to a node:

$$Y_{ii} = \sum_{j \neq i \, j=1}^{n} y_{ij} \quad Y_{ij} = Y_{ji} = -y_{ij} \tag{2.3}$$

For the sake of simplicity, the real and imaginary parts of the admittance matrix (Eq. 2.1) are separated as:

$$Y_{ij} \triangleq G_{ij} + jB_{ij} \tag{2.4}$$

and voltage magnitude and phases are expressed as:

$$V_i \triangleq |V_i| \, e^{j\theta_i} = |V_i| \angle \theta_i \tag{2.5}$$

$$\theta_{ij} \triangleq \theta_i - \theta_j \tag{2.6}$$

Taking into account that $e^{j\theta}$ can be expressed according to Euler's formula as $e^{j\theta} = \cos\theta + j\sin\theta$, from Eq. (2.1) the equations of the active and reactive power of the i^{th} node can be expressed as:

$$P_i = \sum_{j=1}^{n} |V_i| \left|V_j\right| (G_{ij}\cos\theta_{ij} + B_{ij}\sin\theta_{ij}) = P_{G_i} - P_{D_i} \tag{2.7}$$

$$Q_i = \sum_{j=1}^{n} |V_i| \left|V_j\right| (G_{ij}\sin\theta_{ij} - B_{ij}\cos\theta_{ij}) = Q_{G_i} - Q_{D_i} \tag{2.8}$$

where P_i and Q_i represent the active and reactive power of a node, described as the balance between the generated (P_{G_i}, Q_{G_i}) and demanded (P_{D_i}, Q_{D_i}) power.

In the case of dc power systems, the active power flow delivered by a node to the rest of the nodes is defined as:

$$P_i = \sum_{j=1}^{n} V_i \left(\left(V_j - V_i\right) Y_{ij}\right) = P_{G_i} - P_{D_i} \tag{2.9}$$

where V_i and V_j are the voltages of nodes i and j respectively, and Y_{ij} is the admittance between these two nodes. The total power (P_i) is equal to the balance between the generated (P_{G_i}) and demanded power (P_{D_i}) in that node. It is important to mention that unlike in ac systems, the admittance matrix $\mathbf{Y}$ for dc power flows is defined only by considering the resistive values of power lines. Inductive values of power transmission lines are not contemplated because in steady-state they do not influence the power or current transmitted through the dc lines.

Due to the nonlinear nature of Eqs. (2.7), (2.8) and (2.9), they are usually solved by means of numerical methods. Among these methods, the already mentioned NR [17], the Gauss-Seidel [31] or the Fast Decoupled Load Flow [32] are the most widely used methods and could be employed in the DFPF tool as power flow solvers. A detailed review and explanation of the aforementioned methods can be found in [19,33]. In the DFPF tool the NR method has been chosen for solving power flow equations, thanks to its good compromise between simplicity and convergence to the solution. The implementation and evaluation of other numerical methods, which might be necessary to simulate certain power system topologies is not covered in this document and is left as a possible research activity.

The NR method consists of iteratively solving a system of equations as pointed in [17]:

$$\mathbf{f}(\mathbf{x}^{(\nu+1)}) \approx \mathbf{f}(\mathbf{x}^{(\nu)}) + \mathbf{J}(\mathbf{x}^{(\nu)})\Delta\mathbf{x}^{(\nu)} = 0 \tag{2.10}$$

where $\mathbf{f}(\mathbf{x})$ represents the system of equations in vector notation. In the DFPF tool, $\mathbf{f}(\mathbf{x})$ corresponds to the power expressions in Eqs. (2.7) and (2.8) for ac systems, and Eq. (2.9) for dc

systems. The vector **x** in this case represents the node variables $(\theta, |V|)$. The value of **x** is updated iteratively and the estimation is considered sufficiently good when the absolute error is smaller than a predefined tolerance (ε), i.e. when $|\mathbf{f}(x)| < \varepsilon$ is fulfilled. The reader is referred to [17] for more details about the basics of the NR numerical method and the assumptions made to obtain Eq. (2.10). As a remark, it is worth mentioning that special care must be taken with the initialisation of variables to ensure a good convergence to the final result. Figure 2.3 shows the structure of the algorithm employed to solve the system power flow equations at each Simulink time instant.

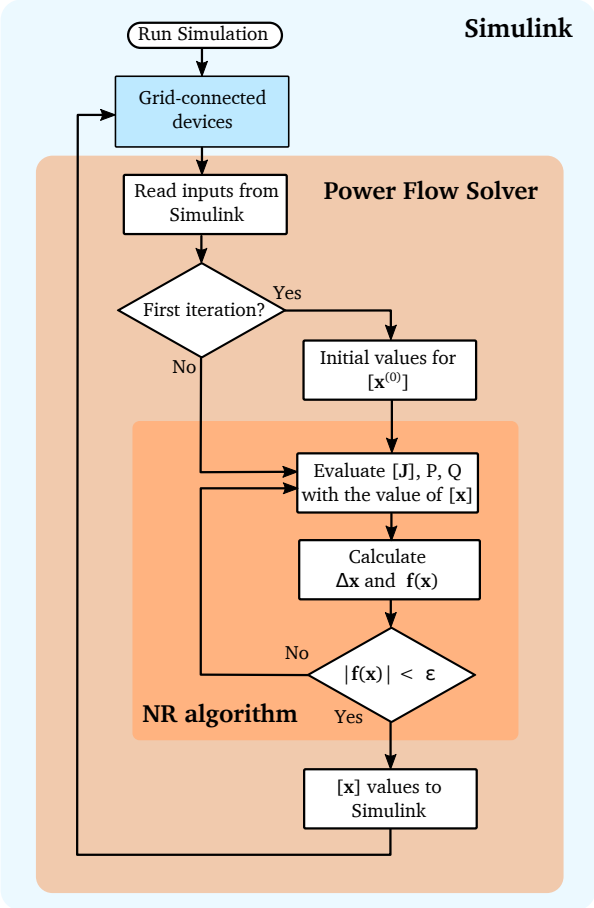

Figure 2.3: Flow chart of the power flow solver with the NR algorithm.

The developed *MATLAB function* includes the necessary information to solve the system of equations with the NR algorithm, i.e. the admittance matrix **Y**, the jacobian matrix **J**, and the power Eqs. (2.7), (2.8) and (2.9). Taking as an example the resolution of an ac power system, the first step of the function is to read the node variables from the Simulink environment. Then, if the current iteration of the main program is the first one, voltage and phase values of PQ nodes are initialised to $1\angle 0°$ (employing a per-unit notation). In the next Simulink time step, the input variables are read from Simulink (voltage of the slack node and active and reactive

powers of PQ nodes), and the NR is solved iteratively by evaluating the jacobian matrix and power equations and by obtaining the new value of the variables. When the error goes below the predefined tolerance, the last values of the variables are sent back to the Simulink model. The results consist of P and Q powers for the Slack node and voltage amplitudes and angles for PQ nodes. Since at this stage the node powers and voltages are known, line and node currents can be also obtained.

2.2.2 DFPF Tool based on Simulink Software

As it has been mentioned before, different ac and dc power systems can be interconnected and simulated in parallel in the DFPF tool. Besides, the different power systems can be interconnected by ICs, developed using the Simulink environment as well. The following Figure 2.4 shows the conceptual implementation of a hybrid ac/dc interconnection in the DFPF tool.

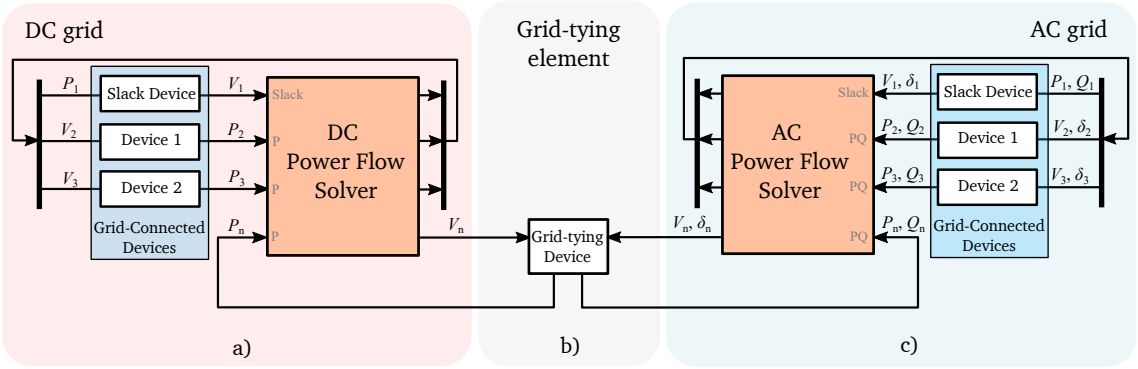

Figure 2.4: Conceptual interconnection diagram of a hybrid ac/dc link in the DFPF tool: a) dc system, b) IC and c) ac system.

As Figures 2.4 a) and c) depict, the inputs for the ac and dc load flow solvers are the voltage values of the slack nodes and the power values of PQ and P nodes. Since the employed power flow solver (explained in the previous Section 2.2.1) is based on a static load flow algorithm, electromagnetic transients of power systems cannot be represented in DFPF simulations. Therefore, the dynamic models employed for grid-connected elements do not need to include inner voltage or current control loops. For example, when a SG is implemented in an ac grid model, a second order model (similar to the one proposed in [1]) can be used to represent the electromechanical behaviour of the machine, instead of using higher order models that also consider electromagnetic variables and hence require a higher computational cost to be solved. Regarding the governor and the excitation system of the machine, any model can be easily implemented using the Simulink interface of the DFPF tool, e.g. the ones that appear in Chapters 8 and 9 of [1]. Nonlinear control functions such as saturations or discontinuities can be also considered in the model. Similarly, when converter-based units are implemented in the DFPF tool (which are very common in modern renewable-based systems),

only their outer loop controllers need to be considered (power regulation, inertia-emulation algorithms, etc.) inasmuch as inner voltage and current control loop dynamics are at the spectrum of the electromagnetic dynamics and they are not contemplated in the DFPF. In such a way, the DFPF tool simulations are capable of representing the transient behaviour of the system frequency and voltage while maintaining a good compromise between accuracy and simulation time.

Unlike other analytical tools in the literature, one of the most important advantages of implementing the grid-connected element models in Simulink is that it is possible to model a wide range of non-linear functions in the controllers. For instance, saturation blocks and rate limiters can be implemented to test the system performance under abnormal operation conditions. Moreover, rule-based control algorithms can be easily implemented to study the performance of discontinuous management strategies. The following subsections provide a detailed description of the most common Simulink elements that can be connected to the nodes of ac and dc power flow algorithms.

Slack Node

In classical ac static power flow problems, the slack node establishes a constant voltage amplitude and reference angle ($|V|$,θ), and is in charge of providing the required power to ensure the power balance of the system. When an ac system is implemented using the DFPF tool, the slack node determines not only the voltage amplitude, but also the frequency reference from which all angle deviations are calculated. Therefore, the grid-connected element on the slack node of the ac system needs to be a grid-forming device, i.e. capable of setting the voltage and angle at its terminals as shown in Figure 2.5 a). This means that the slack node can be either a classical SG or an electronic power converter controlled as a grid-forming system (e.g. emulating the behaviour of a SG).

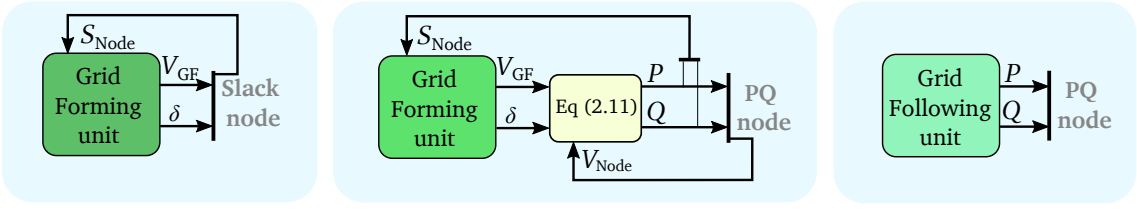

a) b) c)

Figure 2.5: Different ac grid-connected device configuration schemes at the DFPF tool.

Since the angle reference is obtained from integrating the frequency of the device connected to the slack node, it means that the angle will have a new value at every Simulink iteration. When more than one SG or grid-forming generators are considered in the simulation, the constant variation of the the reference angle might lead to inaccurate results. The reason is that the power transfer depends on the angle difference (δ) between the device terminals and the

point of connection, the voltage amplitudes, and on the impedance (X) between both points. For instance, for a SG connected to the i^{th} node, the power transfer can be calculated as:

$$P_i = \frac{|V_{\text{GF}}||V_{\text{Node}}|}{X}\sin\delta \quad Q_i = \frac{|V_{\text{GF}}||V_{\text{Node}}|}{X}\cos\delta - \frac{|V_{\text{Node}}|^2}{X} \tag{2.11}$$

The inaccuracy might arise from the simulation step delay contained in the voltage of the node, as it is obtained from the power flow algorithm. Moreover, constantly varying angle values might complicate the convergence of the NR algorithm, since the operation point might vary abruptly between two Simulink iterations. To overcome these issues, the DFPF tool employs angle *differences* rather than constantly varying angles. This is done by decoupling the slack node frequency and reference angle. The angle difference of the slack node is set to zero, making it the reference angle. Then, the frequency of the slack node is fed to the rest of the devices with grid-forming capabilities to calculate the relative angle deviation of these devices (δ). These angle deviations will be then used by the Simulink solver to obtain the power values of PQ nodes according to Eq. (2.11), and by the NR algorithm to calculate the power through lines according to Eqs. (2.7) and (2.8).

In the case of dc systems, this fact is more simple since there does not exist a continuously changing angle, and only dc voltage amplitude variations need to be considered. Figure 2.6 a) and b) show how a dc grid-forming unit is connected to the slack or a common P node, while Figure 2.6 c) depicts the connection of a grid-following unit in a P node of the dc power system.

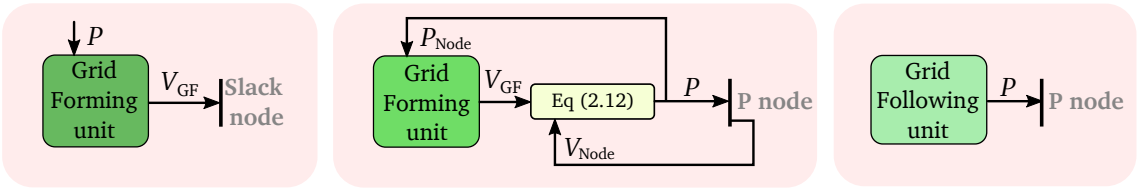

Figure 2.6: Different dc grid-connected device configuration schemes at the DFPF tool.

The equation that determines the active power transfer between a grid-forming unit connected to the i^{th} P node in a dc power system is

$$P_i = \frac{V_{\text{GF}} - V_{\text{Node}}}{X} \tag{2.12}$$

where $V_{\text{GF}} - V_{\text{Node}}$ is the voltage difference between the terminals of the grid-forming and the system noe, and X is the resistive interconnection impedance (see Figure 2.6 b)).

PQ Grid-forming Nodes

Any grid-forming device can be directly connected to the slack node of the power flow solver of the corresponding ac or dc system. However, there usually is more than one device of this type participating in the regulation of a power system. There are two possibilities to integrate more grid-forming devices within the same power system in the DFPF tool. On the one hand, the number of nodes of the system can be increased to consider the terminals of the grid-forming device as an additional node, declaring such node as an additional slack node whose voltage vector is defined. This would mean incorporating the series impedance of the device into the admittance matrix, and adding a new active and reactive power equation. In that case, the voltage amplitude and angle difference would be set by the new grid-forming device, and the additional equations would be used to calculate the power exchanged with the grid. The second approach is presented more simple and it is shown in Figures 2.5 b) and 2.6 b) for ac and dc systems respectively; it basically consists of keeping the original admittance matrix and integrating the additional grid-forming devices as PQ or P nodes. The equations to calculate the power (i.e., Eq. (2.11) and (2.12)) are outside the NR algorithm, in the Simulink environment. This method is equivalent to the first one, since the equations to calculate the power exchange are the same in both cases.

It must be also noticed that, as mentioned in the previous section, the angle deviation of grid-forming PQ nodes in ac systems is obtained by considering the slack node frequency as the reference:

$$\delta_{\mathrm{GF}} = \int \omega_{\mathrm{GF}} - \omega_{\mathrm{slack}} \tag{2.13}$$

where ω_{GF} is the frequency of the grid-forming device, ω_{slack} is the reference frequency, and δ_{GF} is the angle deviation used to calculate the power transmitted by the grid-forming device according to Eq. (2.11).

PQ Loads and Grid-following Generation Nodes

The implementation of grid-following generation devices and loads in the DFPF tool consists of setting a power value for each time instant (Figure 2.5 c) and Figure 2.6 c)). These devices can be easily implemented using Simulink library blocks, and the most simple approaches correspond to repeating sequences or lookup tables.

2.3 Validation and Performance Comparison of the DFPF Tool on a 9 Node ac Power System

The aim of this section is to provide use case examples to demonstrate the accuracy and test the performance of the DFPF tool against EMT and Phasor simulation methods. In the following subsections, the simulation considerations to validate the DFPF tool are explained first, the use case scenario is described then and the results for three different simulation tests are provided in last place.

2.3.1 Simulation Considerations

To carry out a fair comparison between the three different simulation methods, the employed generator and load models are equal in all cases, and the power system parameters are the same as well. Simulations have been carried out using MATLAB® and Simulink® software. In all the cases, the synchronous generators and their prime movers are modeled in Simulink by a second order nonlinear differential equation—i.e. the well known *swing equation*, [1]–. This is combined with a droop controller as illustrated in Figure 2.8. Between the droop control and the *swing equation*, the delay of the prime mover and the governor is modeled with a *transport delay* and a first order low-pass filter. The time constants of the delay are modified depending on the performed test (specified in the upcoming sections). Last but not least, the reactive power control along with a PI controller regulates the excitation system and thus the voltage at the terminals of the machine. When SGs are employed in the three simulation methods, the difference resides in how the electrical part of the power system is modeled, and in the way in which devices are connected to it.

In EMT and Phasor simulations, the representation of transmission lines and power transformers is done using *SimPowerSystems*™ toolbox library models. In the case of power transformers, apart from the winding impedance, the magnetisation resistance and inductance are included in the models. In the DFPF tool, the electrical part of the power system is represented with the admittance matrix, where lines as well as transformers are represented as *RL* impedances. All the elements and the system have been implemented employing a per-unit representation. The reason for modelling transmission lines as simplified *RL* impedances is that they are adequate to determine the voltage angle aperture on each node of the system. This means that they provide sufficient accuracy to represent frequency dynamics associated to the electromechanical behaviour of generators and loads. More complex line models are often used to represent electromagnetic transients of power systems and hence, they are not contemplated in the presented tool. In any case, it must be noted that the susceptance of equivalent π transmission line models could be included in the DFPF tool, e.g. to evaluate their reactive power consumption. This might be done by directly including the susceptance in the

admittance matrices or by adding the corresponding reactive power load at each node in the DFPF Simulink file.

Regarding generation devices, in the EMT simulation *abc* instantaneous voltages are obtained and set with controllable voltage sources connected to the three-phase power system circuit. In the Phasor simulation, *abc* voltages are fed as magnitudes and angles to the controllable voltage sources. Finally, in the DFPF, one of the SGs is connected to the power system as the slack node, and the rest ones are implemented as PQ nodes as explained in Sections 2.2.2 and 2.2.2.

With respect to loads, time-varying power profiles are employed to test the dynamic performance of the three simulation methods. In the EMT simulation, SimPowerSystem load elements are used, to which the instantaneous power values must be provided as reference. In the case of the Phasor simulation, a custom constant power load has been developed to absorb the predefined amount of power. Finally, in the DFPF tool loads are simply implemented as time-varying active and reactive power references directly connected to the PQ nodes of the NR algorithm, meaning that no specific library elements are required.

2.3.2 Description of the Use Case

The western system coordinating council (WSCC) is chosen as the benchmark system for the validation of the DFPF tool [34]. As shown in Figure 2.7, this grid is comprised by nine buses and three synchronous generators, which are connected to the grid by means of power transformers.

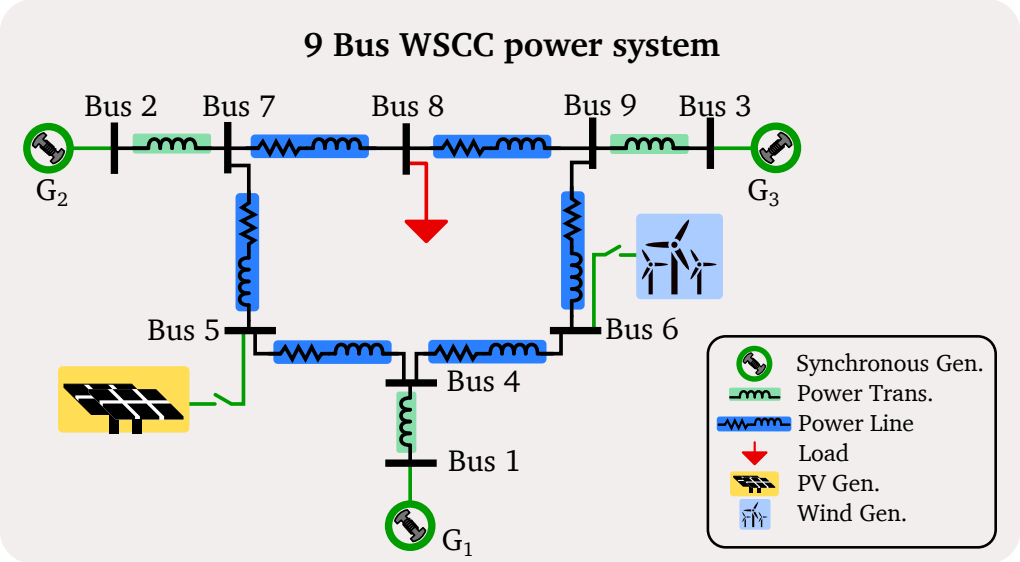

Figure 2.7: WSCC 9 node system benchmark illustration.

The first generator is connected to the slack node, so its voltage amplitude and angle will

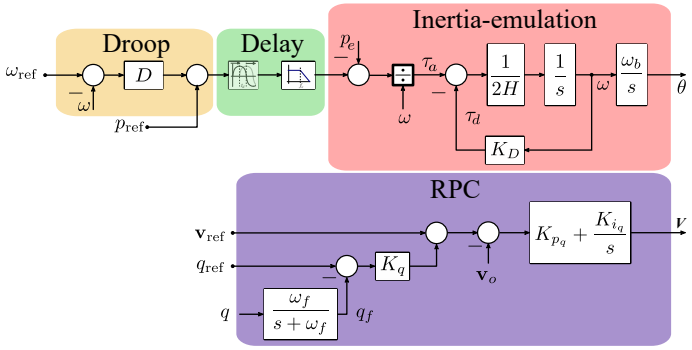

Figure 2.8: SG model of the Slack node implemented in Simulink.

be directly fed to the power flow algorithm. The second and third SGs have the same structure as the first one, but are integrated as PQ nodes. The power of these generators is calculated as explained in Section 2.2.2.

The power system and generator data is taken from [34], and can be found in Table 2.4. The parameters are represented employing a per-unit notation with a base power of 100 MVA. H corresponds to generator inertia, D corresponds to the $P-f$ droop coefficient and τ refers to the time constant of the first order filter that models the delay on the prime mover of the SG. The transport delay shown in Figure 2.8 is only considered in Test C, so its parameters are provided in that section.

Table 2.4: Generator parameters for the WSCC 9 node system from [34]

Device	Parameter	Value [p.u.]
	H_1, H_2, H_3	$23.64, 6.4, 3.01$
G_1, G_2, G_3	D_1, D_2, D_3	$20, 30, 25$
	τ_1, τ_2, τ_2	$0.1, 0.1, 0.1$

PV and WP generation plants and loads are also depicted in Figure 2.7 since these elements are part of different tests in the upcoming sections.

The employed computer is running a *Windows 10 Pro* OS, with an *Intel(R) Core(TM) i5-7200U CPU @ 2.50GHz - 2.71 GHz*. The comparative evaluation of simulation methods is carried out in the same conditions and only running the simulation files on the computer.

2.3.3 Simulation Results

In the following subsections the results obtained for three different tests are shown, which are carried out in the 9 bus use case described in Section 2.3.2.

Test A – Active Power Load Step

The aim is to corroborate the validity of the proposed DFPF tool for a simple power perturbation. For that purpose, results are compared with the ones obtained with Phasor and EMT simulations in Simulink. A 1 p.u. active load is introduced in bus 8 at the instant $t = 1$s, and this load is disconnected at $t = 5.5$s as illustrated in Figure 2.9 a). The results for the frequency of the first, second and third SG are shown in Figure 2.9 b), c) and d), respectively.

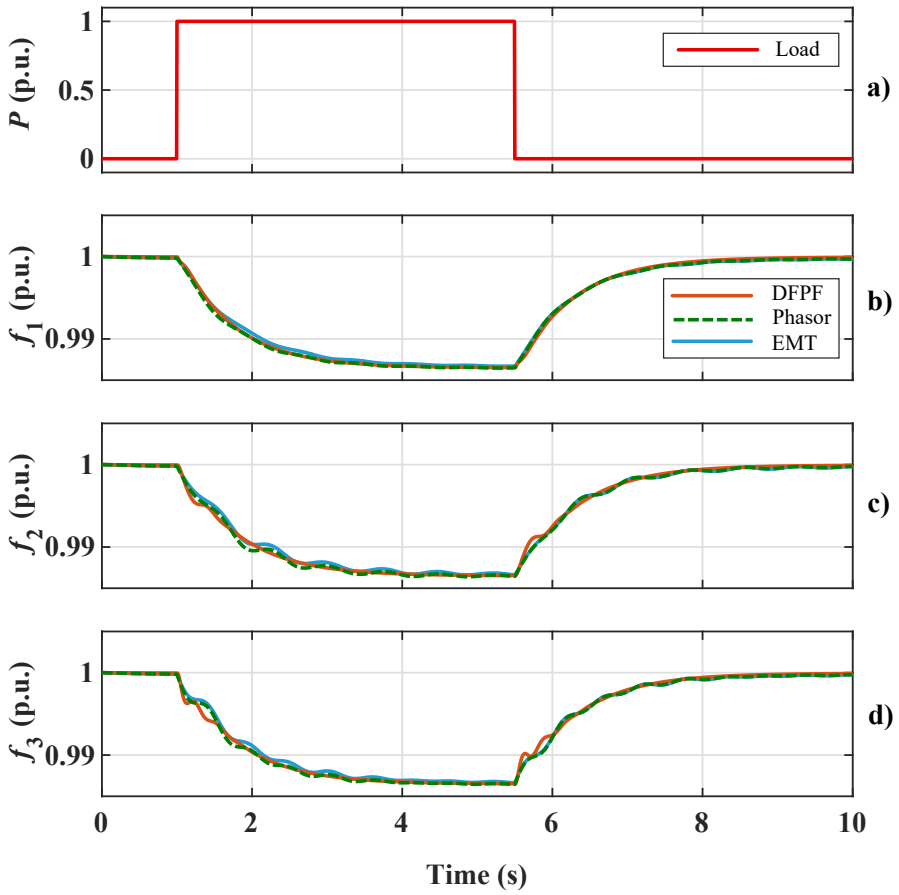

Figure 2.9: DFPF, Phasor and EMT simulation result comparison of three SGs' frequency for a 1 p.u. active load step in the nine node scenario.

The frequency response of the three SGs is equal in steady-state, but it presents slight differences during frequency transients with respect to the EMT and Phasor simulations. These variations arise from the resolution of the electrical part of the power system. In the case of EMT and Phasor simulations, the system is simulated through solving line voltages and currents, preserving the intrinsic dynamic characteristics of the power system topology. Meanwhile, in the DFPF simulations the obtained node voltages are based on the power dispatch of each system node, and only the electromechanical response of the frequency is represented. All in all, it can be considered that the obtained response with the DFPF tool is sufficiently

accurate to represent frequency transients in power systems, and neglecting the faster transients of voltages and currents makes it possible to improve the simulation speed as will be demonstrated subsequently.

The configuration and the time required by each method to carry out the simulation is also provided in Table 2.5. Although a variable-step simulation is employed for the EMT and Phasor simulations, they require much smaller simulation step sizes compared to the DFPF tool to provide an accurate solution. This has a direct impact on the time required by each method to solve the simulation, and it can be observed that in this test the DFPF tool is faster than the rest of the methods.

Table 2.5: Simulation settings and required time for Test A

Simulation Method	Step (T_s)	Max. Step	Min. Step	Simulation Length	Required Time
EMT	Variable	0.1ms	auto	10s	12.7s
Phasor	Variable	0.1ms	auto	10s	9.68s
DFPF	Fixed	5ms	5ms	10s	< 0.5s

Test B – Integration of RES and Varying Load Profiles

In the previous section the proposed DFPF tool is validated under very simple testing conditions. However, the real advantages of the proposed DFPF tool come when it is employed at larger time scale simulations. The purpose of this test is to analyse the performance of the proposed DFPF tool more in detail for larger time spans, and to study the effect of RES-based generators and loads in the system frequency. The SG parameters are the same as in Test A (Table 2.4). In addition, a PV and a WP generation plant is connected to nodes 5 and 6, respectively. A dynamic active power load is also connected at node 8. These systems can be seen in Figure 2.7. It must be pointed out that even if RES-based generation systems and the load are represented via time-domain power profiles, it is up to the user to adapt the model fidelity depending on the study to be carried out in each case.

Figure 2.10 a), b) and c) show the active power profiles of the RES-based generators and the active power load profile for a 20min simulation. Figure 2.10 d) shows the frequency response of the first SG for the DFPF, Phasor and EMT simulation method.

Although the obtained frequency results are almost equal in the three cases, it should be taken into account that the accuracy of the obtained results depend on the employed simulation settings. In order to perform a fair comparison between the three simulation approaches, their performance for different simulation step sizes (T_s) is evaluated below.

Since the Phasor method and the DFPF tool are oriented to studying the electromechanical dynamics of power systems, their performance is compared against the EMT simulation, which provides the most detailed model representation.

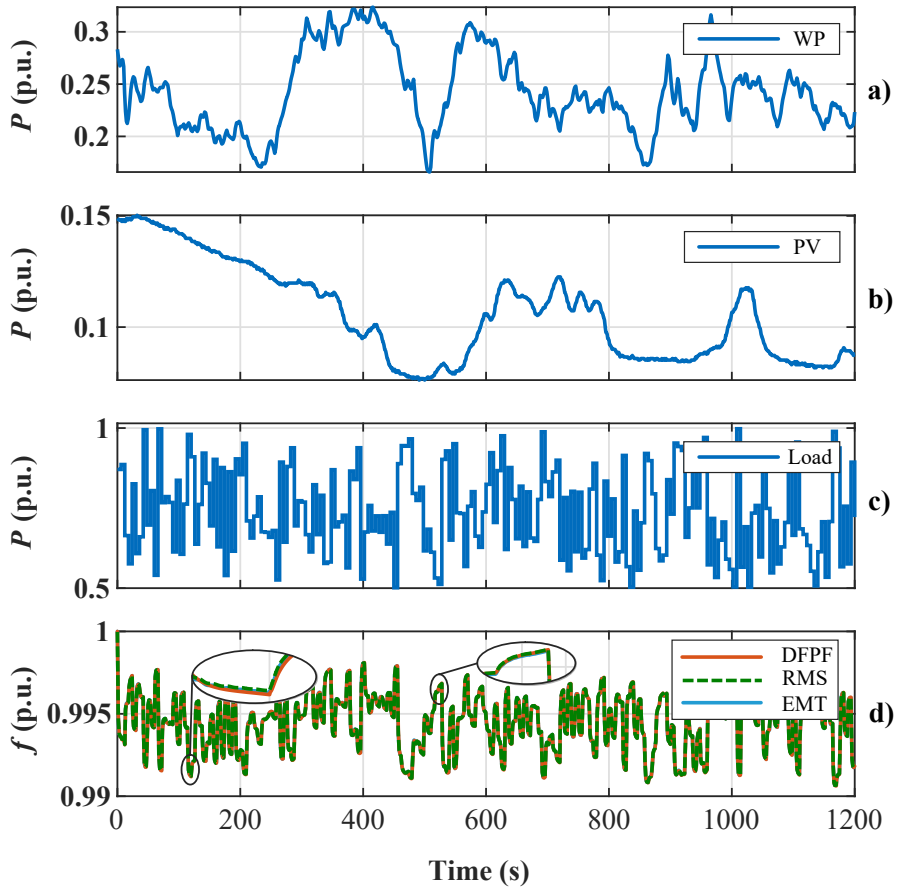

Figure 2.10: a) WP generation profile, b) PV generation profile, c) active power load profile and d) first SG's frequency for DFPF, Phasor and EMT simulations.

On the one hand, the average value of the frequency deviation is calculated for different T_s values, and the results are illustrated in Figure 2.11 a). The frequency deviation of the DFPF is almost equal for all the simulation steps, meaning that increasing the step size does not penalise the accuracy of the simulation within the shown parameter range. In addition, the frequency deviation of the DFPF tool is similar to the one of the Phasor simulation for a 0.4ms step size.

On the other hand, Figure 2.11 b) illustrates the time required by both tools to simulate the 20min profiles for different T_s values. For instance, for $T_s = 5$ms the DFPF tool requires 23s, while the the Phasor simulation requires 1min and 30s for $T_s = 2$ms. It is also important to highlight that the time step of the Phasor simulation cannot be increased beyond 2ms to accelerate the simulation, since the inaccuracy of the variables causes the system to become unstable for the tested conditions.

Table 2.6 gathers the simulation configuration and the time required by each method to simulate the 20min profiles. Considering that the same accuracy is required in the simulation

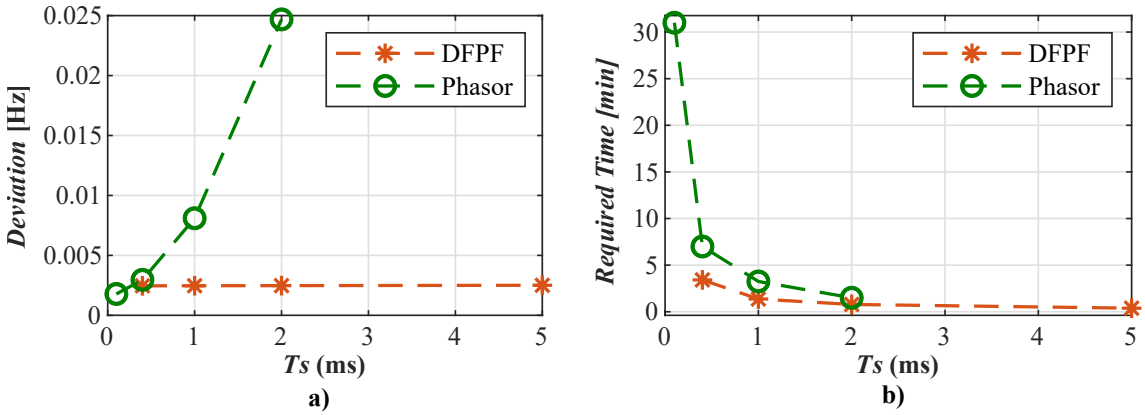

Figure 2.11: a) Mean value of the difference with the EMT simulation of DFPF and Phasor methods and b), required simulation time of each simulation method. Both depending on the simulation step size T_s.

results, a 0.4ms and 5ms step is selected for the Phasor and DFPF tool, respectively. In such conditions, the Phasor simulation requires 7min, whereas the DFPF tool requires 23s to complete the simulation. It means that the DFPF is capable of simulating the system approximately 18 times faster than the Phasor method while obtaining a similar accuracy in the results. As a reference, the EMT simulation requires slightly more than one hour to complete the simulation with a variable step and a maximum step size of 0.1ms.

Table 2.6: Simulation settings for EMT, Phasor and DFPF simulations in Test B

Simulation Method	Step (T_s)	Max. Step	Min. Step	Simulation Length	f deviation	Req. Time
EMT	Variable	0.1ms	auto	20min	-	1h 1min 15s
Phasor	Fixed	0.4ms	0.4ms	20min	3 mHz	7min
DFPF	Fixed	5ms	5ms	20min	2.5 mHz	23s

The main reason for such a difference in the time required by each method to simulate the 20min profiles is the way in which the electrical part of the system is solved. The EMT method is the slowest one because the electrical part is modeled by means of differential equations in order to be able to represent the electromagnetic transients. In the Simulink Phasor method, power system differential equations are replaced by algebraic equations in order to solve the system faster than in the case of EMTs, but still they are more complex than in DFPF simulations. In the DFPF tool all voltages are calculated from power flow equations, which are developed considering a single-line representation of the system. This allows to increase the time step and significantly reduce the time required to simulate the system. The maximum time step in this case will be limited by the speed of frequency transients (i.e. the rate of change of frequency (RoCoF)), which directly depends on the total inertia of the system.

With these results, it can be stated that the DFPF method is highly suitable to represent

frequency dynamics in power systems with relatively low required simulation time, due to its capability to carry out simulations with larger step sizes. This enables to simulate larger time spans, evaluating the steady-state power supply effect on different devices. For example ESS units and their SoC under different loading conditions, the effect of different generator parameters on power system dynamics such as generators' inertia (or virtual inertia), or prime movers' delay.

Test C – Generator Parameter Evaluation

The low simulation times required by the DFPF tool are an advantage compared to other tools or methods for various reasons. On the one hand, larger time span simulations can be carried out to analyse the performance of higher-level energy management strategies that provide some kind of frequency regulation service. Some examples include the so-called enhanced frequency response in Great Britain or frequency restoration reserve in Italy. On the other hand, multiple simulations can be carried out either sequentially or in parallel to evaluate the effect of control parameters or physical properties in the dynamic response of the grid. This is essential to study the impact of integrating new devices into the grid, such as energy storage or generation systems, or electronic power converters interconnecting different parts of the grid as demonstrated by the authors in [35]. The aim of this test is to illustrate the effect of varying two critical parameters on the frequency stability of the previous power system scenario.

First, the H_1 inertia parameter from the first SG is modified from the nominal inertia value given in Table 2.4, until reducing its value eight times. To observe the effect of this variation, a 1 p.u. load step is applied at node 8 of the system, and the result is shown in Figure 2.12 a). Although the rest of the generators and system parameters are kept equal, the reduction of this generator's inertia causes a much steeper RoCoF under the same load perturbation.

Then, for a second test a weaker grid scenario is set up by reducing the inertia of each generator six times. Besides, a time delay modeled by a *transport delay* (T_D) and a *first order filter* are introduced to all the prime movers of SGs (refer to Figure 2.8). For generators 2 and 3 the *transport delay* and the time constant of the filter are set to a value of 0.1s. For the first SG, the filter's time constant is set to 0.25s and the value of the *transport delay* (T_{D1}) is the parameter whose effect is studied in the test. T_{D1} goes from zero to 0.75s in steps of 0.25s. The results in Figure 2.12 b) show that when the the delay of the prime mover is bigger, the frequency nadir of the system reaches a lower value, and the the response after the disturbance becomes more oscillatory.

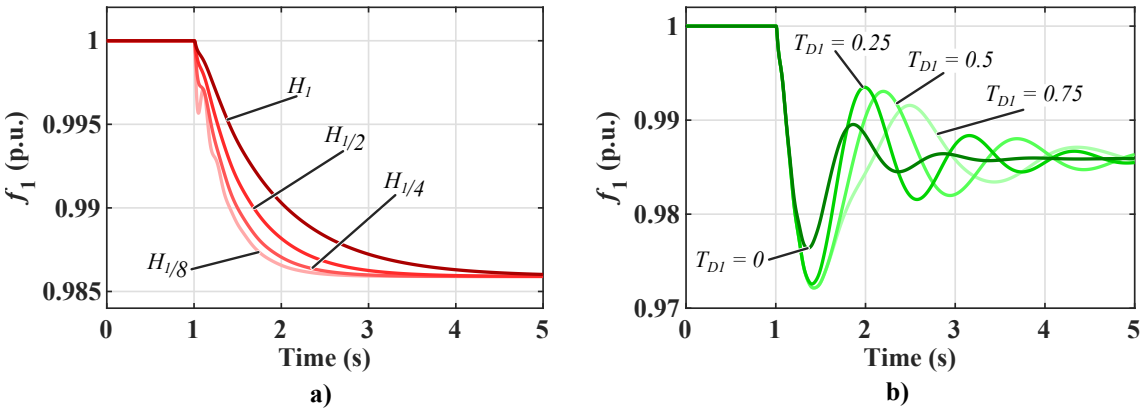

Figure 2.12: a) Variation of the inertia of the first SG (H_1) and b) variation of the prime mover's delay (T_{D1}) with six times less system inertia, both for a 1 p.u. active load step at node 8.

2.4 Simulation of a Hybrid AC/DC Power System in the DFPF tool

Once we have validated the performance of the DFPF tool, the upcoming section shows the capacities of the proposed tool to represent the transient behaviour of power systems with ac and dc subgrids. The purpose is to highlight the potential use of the tool for studying the integration of different types of grid-connected generation, ESS and load units, asd well as for analysing the interconnection of power systems of different natures through ICs.

2.4.1 Description of the Hybrid AC/DC Scenario

The selected scenario represents the interconnection of the Nordic power system with the Continental European grid and the integration of two wind power plants through an MTDC system acting as an energy hub. A simplified diagram of the test scenario is illustrated in Figure 2.13.

The Nordic grid is based on a 32 bus power system proposed by CIGRÉ task force 32.02.08 in [36], and the Continental grid is represented with a European HV transmission network benchmark proposed by the CIGRÉ Task Force C6.04.02 in [37]. Each grid model includes three synchronous generators to represent the aggregated dynamic response of the system. One of the generators in each grid acts as the slack, meaning that it is responsible for setting the voltage and frequency of the grid. The rest of synchronous generators operate as grid-forming units, supporting the control of the frequency and contributing in the primary regulation. Considering that the purpose of the tool is to study frequency and voltage transients, these generators are represented with a simplified model including the swing-equation, the governor and the active voltage regulator as it has been explained previously in 2.3.1. The loads are

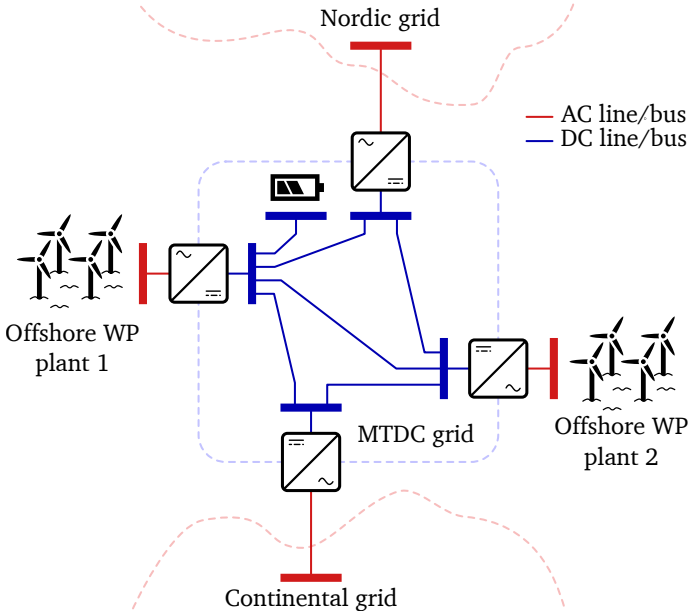

Figure 2.13: Simplified diagram of the hybrid ac/dc benchmark scenario.

different depending on the test case, so they are detailed in the following sections.

The topology of the two WP plants consist of simplified 5 bus grids as represented in Figure 2.14.

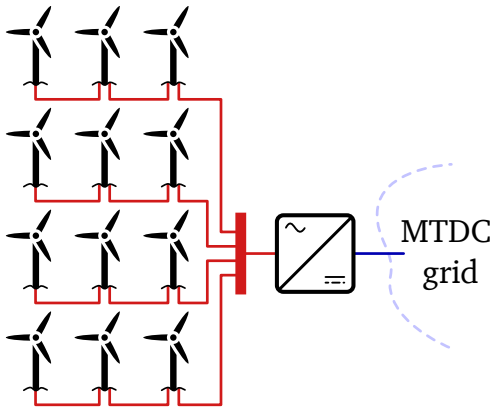

Figure 2.14: WP plant ac grid topology.

One of the turbine strings is defined as the slack to set the voltage and frequency of the grid, and it is modelled as an aggregated grid-forming device capable of generating or absorbing power, assuming that the string would include some type of ESS. The rest of turbine strings are represented as grid-following devices using an equivalent power profile directly connected to the coupling node.

The four ac grids are interconnected by means of a 5-bus MTDC grid. A small-scale energy storage system is used as the slack of the dc grid to set the voltage and to facilitate the

transmission of power between the ac grids.

In Table 2.7 the constants of inertia of the grid-forming elements connected to these five grids are gathered. As it can be observed, the aggregated inertia (H_C) at the Continental grid is 26s, whereas the Nordic (H_N) is 2.6s. The WP plants and the MTDC grid are weaker in terms of equivalent inertia (H_{WP1}, H_{WP2} and H_{DC} respectively) because the number of grid-forming units and their rated power is lower.

Table 2.7: Inertia constants of the grid-forming units in the test scenario

Grid	Inertia constants		
Nordic	$H_{N_1} = 1$s	$H_{N_2} = 0.6$s	$H_{N_3} = 1$s
Continental	$H_{C_1} = 10$s	$H_{C_2} = 6$s	$H_{C_3} = 10$s
WP plant 1		$H_{WP_1} = 0.5$s	
WP plant 2		$H_{WP_2} = 0.5$s	
MTDC		$H_{DC} = 0.5$s	

The ICs between the MTDC grid and the rest of ac grids are controlled with a dual-droop strategy to support the primary regulation of the entire system [11]. When there is a power variation in any of the grids, the interlinking converters will interchange power so that all the devices contribute to restore the power balance in steady-state.

2.4.2 Simulation Results

Test A – Interconnection of the Nordic and the Continental Grids

This use case consists of two different tests: first the Nordic and the Continental grids are simulated in parallel but isolated from each other; secondly, the two grids are connected via the previously described MTDC grid. In this case no WP generation is considered, and the loads consist of two steps applied at the Nordic and the Continental grid to observe the transient behaviour of their frequency while avoiding the influence of other generation or loads.

The results are depicted in Figure 2.15. The step-shaped loads are equal for both tests, so they have been illustrated once. Similarly, the voltage of the MTDC grid is only shown for the case where the Nordic and the Continental grid are interconnected (test B).

As expected, the frequency signals show that when the two systems are decoupled, a load perturbation in one of them does not influence the other. However, when the two grids are interconnected via the MTDC grid, and thanks to the dual-droop control implemented in the ICs, both grids contribute to the primary regulation when there is a sudden power perturbation, reducing the frequency deviations in overall. Thanks to this interconnection, power perturbations occurring at any point in the system are shared by all the elements participating in the primary regulation.

The frequency and voltage curves also illustrate that the proposed DFPF tool is capable of

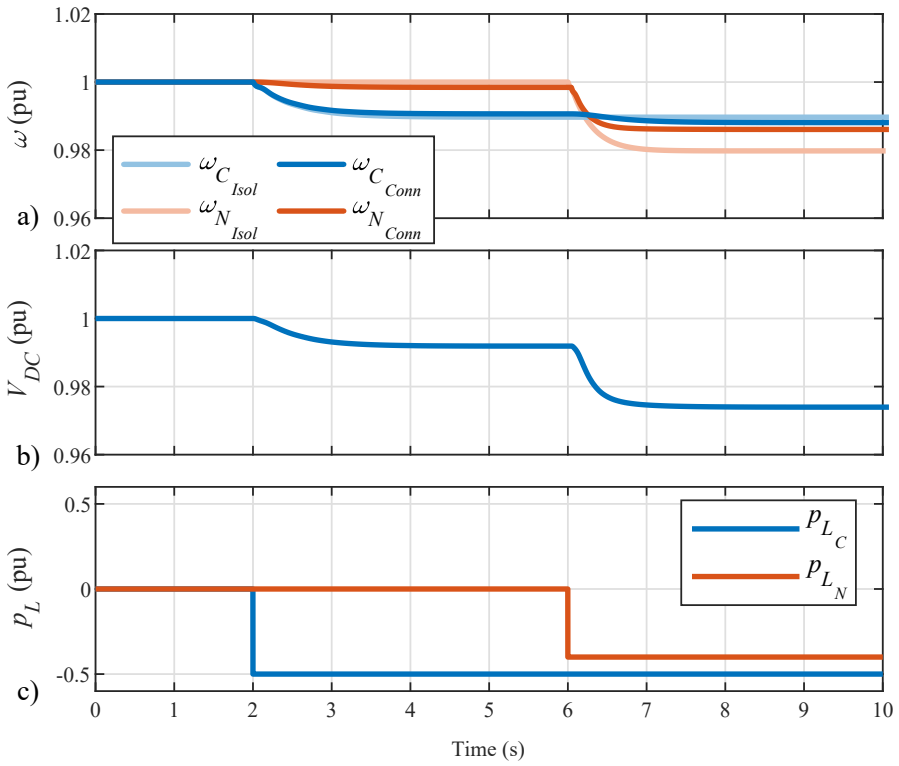

Figure 2.15: Test 1: a) Nordic and Continental grid frequencies (at the IC connection node), b) MTDC slack node voltage and c) Load step-shaped profiles.

simulating the transients associated to electromechanical oscillations for the ac as well as the dc grids.

Test B – Integration of Offshore WP Plants and Non-expected Disconnection of the Continental grid

The second use case consists of simulating the entire system shown in Figure 2.13, also considering the two WP plants. In this case the objective is to study the time-domain evolution of the frequency and voltage under dynamic generation and load power profiles. In addition, a sudden disconnection of the Continental grid is provoked at $t = 100$s to showcase how the DFPF tool can be employed to evaluate the impact of planned or unplanned grid/area connections or disconnections in the system performance. The results of this test are represented in Figure 2.16.

Most of the generation is located in the WP plants and the loads are located at the Nordic and the Continental grid, so the frequencies of the WP plants are higher than the other two ac grids. Another reason for this behaviour is the power transfer capacity of the ICs interconnecting all the grids to the MTDC grid, as this capacity defines the droop gains that determine how much power is transferred through the ICs.

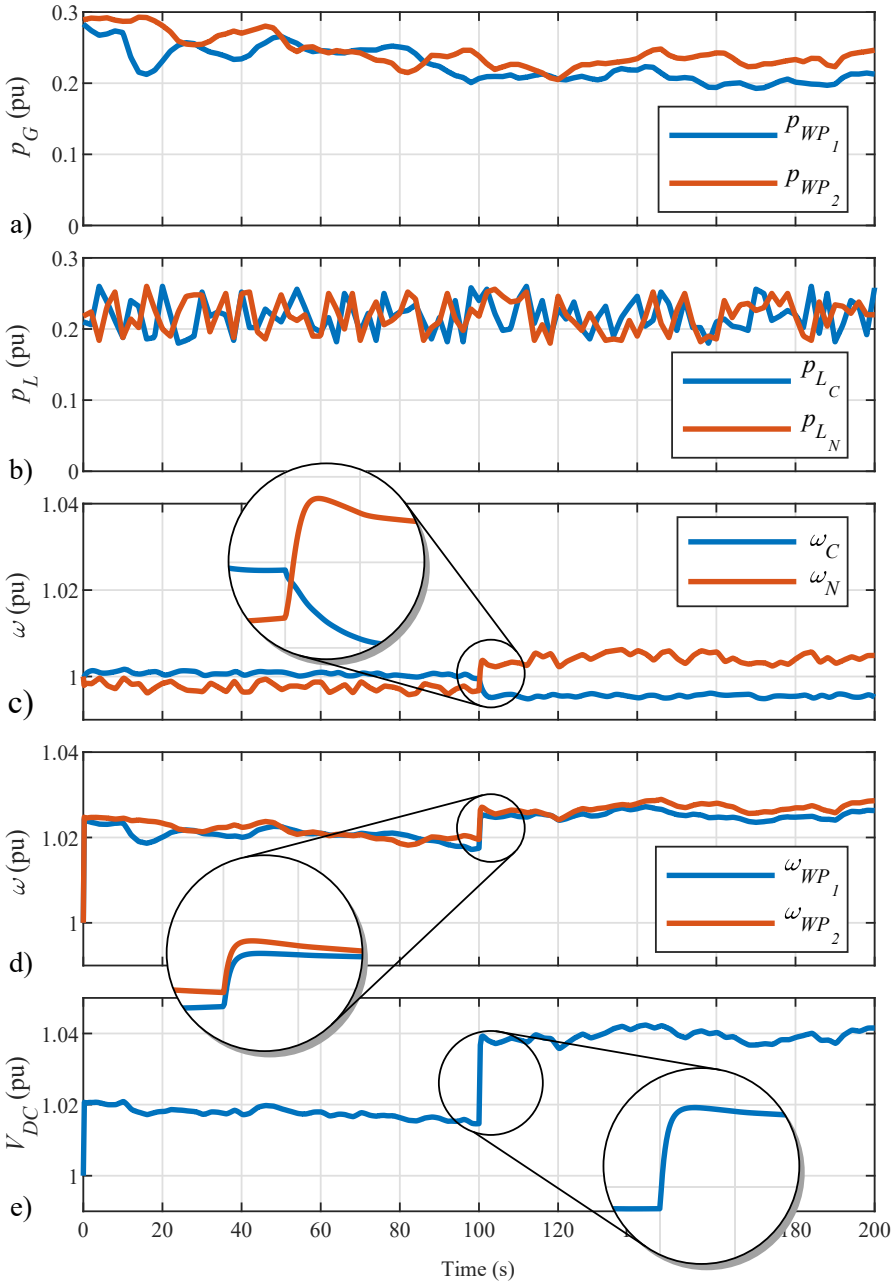

Figure 2.16: Test 2: a) Dynamic generation profiles, b) Dynamic load profiles, c) Nordic and Continental grid frequencies (at the IC connection node), d) WP plant frequencies, and e) MTDC slack node voltage.

At the instant $t = 100$s the Continental grid is suddenly disconnected from the rest. The frequency of this grid decreases relatively slowly thanks to the high mechanical inertia of the three generators (Figure 2.16). However, since the Continental grid has lost the power coming from the WP plants, its frequency decreases to a lower steady-state range of operation. On the contrary, since all the power generated by the WP plants is transferred via the MTDC grid to

the Nordic system, the frequency of this grid increases with respect to the previous operation range. However, the transient behaviour after the disconnection is much faster than in the Continental grid because the overall inertia of the Nordic grid and the rest of grids is much lower.

2.5 Conclusion

The DFPF tool represents frequency and voltage variations of ac, dc, and hybrid ac/dc power systems by combining a static load flow solver with simplified dynamic models of grid-connected devices; i.e., the electromechanical models of SG-based generators and the most representative control loops of grid-connected converters that relate the flow of power with the grid's frequency and voltage. However, we must clarify that the DFPF tool is not suitable to represent electromagnetic phenomena of power systems, since the static load flow solver cannot contemplate it and hence, employed models for grid-connected devices do not require the implementation of inner voltage and current control loops. The tool has been developed using the MATLAB Simulink® environment, and it requires a very low computational burden to solve the system. Thus, it is capable of carrying out long-term dynamic simulations for relatively large and interconnected power systems in a time efficient manner. Furthermore, the programming of differential equation-based models of grid-connected devices or nonlinear control functions can be easily implemented using the graphical interface and the library elements of the Simulink software.

The precision of DFPF tool has been validated against Simulink Phasor and EMT simulation methods in a 9 node ac standard power system. Then, the tool has been used to simulate a hybrid ac/dc power system scenario where two WP generation plants are linked with two ac power systems via a MTDC grid. The obtained results have shown that the proposed tool is suitable not only to study the dynamic behaviour of modern power systems, but also to evaluate the performance of devices that participate in the frequency or voltage regulation. Moreover, it can be concluded that the tool might be also useful to assess the impact of the integration of renewable energy sources, energy storage systems, variations in the total system inertia or the contribution of electronic power converters to the regulation of the frequency and the voltage.

Last but not least, the DFPF tool facilitates to interconnect power systems of different natures using simplified IC models, which makes possible to study the performance of the IC control and its impact on the interconnected systems. Thus, the DFPF tool has been used to test and validate the IC controls proposed in the presented thesis document in Chapters Chapter 4 and 5.

Chapter 3

Interlinking Converter Control Techniques for the Provision of Transient Support on Interconnected Grids

The replacement of synchronous generation by converter-interfaced devices on power systems entails the reduction of the inherent inertial response when power variations occur. In this sense, the contribution of power converters to the transient or inertial response of power systems has been identified as a key factor to ensure the correct and stable operation of modern power systems. This chapter is focused on analysing and explaining the contribution that existing IC control techniques can make to the frequency and voltage stability of interconnected ac and dc systems, respectively.

The first part of the chapter provides the basic technical background on control techniques of grid-connected devices, and the second part is focused on specific IC control strategies that can be used to improve the transient behaviour of interconnected grids.

3.1 Technical Background

In the following sections, we explain the main control layers that define the operation of a power system, so that we are able to identify in which control layer do we need to take action to support the power system(s). We also explain the most generalised classification criteria for converter control strategies, but focusing on ICs. Afterwards, we interpret the equivalence between ac and dc power systems in terms of control and physical properties. This way, we lay the foundations to comprehend the different IC control strategies that are reviewed in Section 3.2, and the ones proposed in the upcoming Chapters 4 and 5.

3.1.1 Hierarchical Control Layers on a Power System

The control of frequency on power systems has been traditionally carried out in three different layers [3]:

- **Primary control**: this layer provides **active power balance to the system** to respond to the constantly changing loading conditions. When a load variation occurs in the electric system, the primary controllers adjust the mechanical power input of the different generators participating in this control layer, so the input mechanical and output electrical power are balanced keeping the system stable. However, the primary movers (governed by the primary controllers) do not respond instantaneously under load variations, so in the gap of time it takes the generation to equalise the demand, the mismatch active power is released from (or absorbed by) the kinetic energy storage of rotating masses coupled to the grid. These masses—also known as grid-coupled inertia—are composed by grid-connected SGs and the turbines attached to their shafts. Hence, when this rotating inertia releases or absorbs power, the system frequency varies. For a given load variation, the bigger the power system inertia is, the lower the acceleration of the system will be. Thus, in the first instance, **load variations drive the frequency of the system out of its nominal value**.

  In classical power systems, the response time of the primary regulation depends on the dynamic properties of the primary movers. In other words, very powerful turbines that need to open valves, burn fuel, or adjust the pressure of the thermal process require more time than, for example, a hydroelectric power plant to readjust the flow of water that controls the mechnanical power input of the generator. In any case, it is essential to maintain the trade-off between inertia and primary response time of generators in order to keep the system stable. The most popular control at this layer is the well-known *droop* control and it is usually composed by a proportional controller that keeps a linear proportion between the mechanical power input in the generator and the frequency deviation. In this manner, all the grid-connected generators can see the frequency deviation and

readjust their power output, achieving the **load sharing** based on local measurements and in a communication-less manner. This operation has been extended to grids of different types, such as microgrids of different natures or even dc systems, where the dc voltage is adjusted according to the droop coefficient and power output.

In electric systems, the operating reserve refers to the generation capacity available by the system operator to meet the loading demand in a short interval of time [38]. The generation capacity that is online but unloaded, and can respond within a few minutes is known as **spinning reserve**. More precisely, the **frequency-response** spinning reserve is the one that responds to frequency variations in few seconds time, and contributes to keep the system frequency at first instance [39]. Thus, a high spinning reserve ensures a good primary regulation capacity and a more robust power system to face load variations and generation outages. In large grids where the power generation is mainly carried out by traditional power plants, the primary regulation capacity usually is relatively good. This is due to the fact that generators can work below the nominal power, and they have a primary energy reservoir to be used whenever the system requires more power generation. In the case of RES, the power generation capacity might not be constant—and hence non-dispatchable—since it depends on factors like sun irradiation or speed of wind (on PV and WP plants respectively) and hence, the primary regulation might be more complicated for RES-based power plants. ENTSO-E classifies the generators or power plants according to their power capacity and voltage level [40], and the regulation requirements are common for each type of generator.

- **Secondary control**: once the primary control layer has accomplished its target and if the new loading condition persists over time, the frequency value will continue being different from the nominal one. With a slower response, the secondary control starts **restoring the frequency of the affected area** by modifying the set-points of the generators that are performing the primary regulation. This control layer usually reacts after 30 seconds, and can restore the grid frequency to its nominal value within a 15 minute interval.

  The secondary control is usually performed by an automatic central controller controlled by the system operator, and sends a specific updated set-point to all the generators participating in this regulation layer, so the references for the primary controllers are updated to restore the grid to its nominal value and still share the load among the different generators. This control layer makes use of the available spinning reserve to achieve its target [41].

- **Tertiary control**: after previous two layers have reacted, the available spinning reserve margin might not be sufficient, or might not be properly distributed to face new contingencies or loading conditions in the system. Therefore, **the purpose of the tertiary**

control is to restore the available reserve. In order to achieve so, the system operator orders single producers (even ones not involved in the primary and secondary regulation layers) to stop the operating generators or even to start-up new ones.

Besides, the operator might coordinate generation plants to reduce transmission line congestion and improve other aspects such as the system efficiency, cost, etc. Fault management, resource optimisation and market participation are contemplated in this control layer as well.

At modern power systems where the rotating inertial SGs are replaced by power electronic converter-interfaced generation units, the inertia of the system is drastically reduced. This involves the overlapping of the dynamic response of **low-level** controllers of grid-connected converters with the remaining system's inertia, as Figure 3.1 illustrates. The low-level control includes the loops that define the dynamic behaviour of grid-connected power converters under different grid events. It is worth noting that this layer depends on local measurements of the converter and it can operate in a time span from a few milliseconds to seconds. For example, a control loop for the emulation of inertia would belong to the low-level control of a generator, and voltage and current inner loops are also considered to be part of the low-level control.

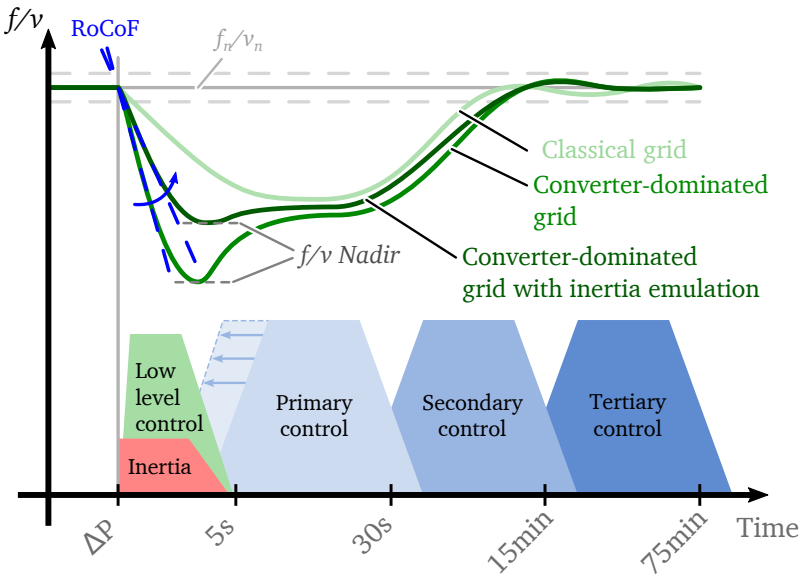

Figure 3.1: Participation of inherent inertia, low-level control and the hierarchical control layers in the regulation of frequency at a converter dominated grid.

Depending on the power system properties, employed type of generators and prime movers, the control layers and their reaction time might differ from one system to another. We would like to denote that as Figure 3.1 shows, the response time of primary control is reduced in converter-based systems, like ESS providing this service.

As it will be detailed later in section 3.1.4, the voltage in dc power systems can be considered to be equivalent to the frequency in ac ones. Thus, Figure 3.1 illustrates that the frequency or voltage dynamics are different when a load variation persists over time depending on the grid type. At classical grids where SGs are predominant, the RoCoF and the frequency nadir will be smaller than at those who are governed by converter-interfaced generators that do not inherently provide any inertial response and neither do implement inertia-emulation controls. DC power systems usually present a high rate of change of voltage (RoCoV) since they are mainly formed by converter-based generators. In any case, the provision of mismatch power in the time gap between the load disturbance and the reaction of the primary control is of vital importance to keep system stable [2].

3.1.2 Contribution of ICs to Hierarchical Power System Control

The previously explained control layer classification for power systems is applicable for grids and microgrids of different scales and natures. The different grid-units (SGs, converter-interfaced generators, loads, etc.) can participate at different control layers, and in the same manner, ICs can also take part by contributing to them. Shen *et al.* in [42] explain some of the functionalities of ICs on these control layers, and in Figure 3.2 we provide a complete perspective of the possible IC contribution to each control layer.

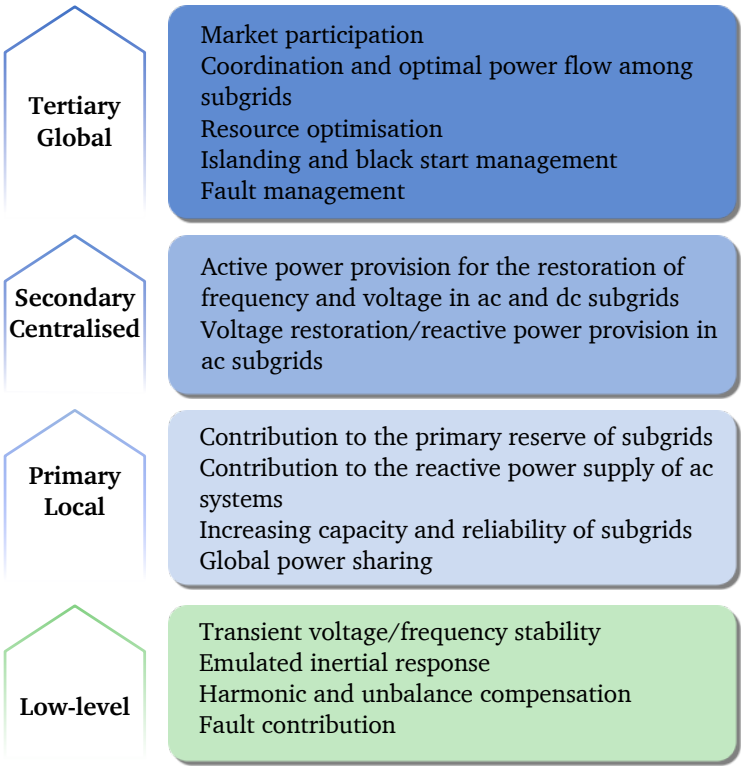

Figure 3.2: Possible contribution of ICs to the different control layers of interconnected subgrids.

With regard to **tertiary control**, ICs can take part on the global energy management strategy of the entire system, where resources and system efficiency are optimised. Besides, the voltage source capacity and the control over the power flow can contribute to the black start operation and fault management.

When the **centralised secondary control** restores the frequency of a power system to its nominal value, it updates the references of the generators performing the primary regulation. If the frequency is below the nominal value, the secondary control requires to employ part of the spinning reserve to accelerate the system until it reaches its nominal frequency value [41]. At IC-interconnected systems where the spinning reserve is low, IC units can be coordinated with the secondary control, so that active power is transferred transiently from one grid to another to restore the frequency of the affected subgrid. This way, the spinning reserve usage of interconnected grids can be optimised. When ICs are connected to ac grids, they can also provide reactive power and voltage control, acting as static synchronous compensators (STATCOMs).

Since ICs are able to exchange energy between subgrids, they can also contribute to the **primary regulation** of interconnected systems. The active power exchange between subgrids in the primary layer is achieved by observing the subgrids at IC terminals, and acting according to the adopted strategy. Many primary regulation techniques have been proposed for ICs in the literature, and in [11] we provide a detailed classification.

When IC control strategies are designed for ICs, we must not forget that in the act of supporting one grid, the contrary will be affected. This is specially notable when high amounts of active power are transferred (transiently and in steady-state). Thus, each IC application and system requirement needs to be studied in detail. The most important aspects that need to be considered when designing IC controls (specially low-level ones) are:

- **Robustness of interconnected subgrids:** the amount of spinning reserve, power capacity, and the amount of systems' inertia will determine the constrains for the secure power transmission between two subgrids.

- **IC topology and conversion stages:** depending on the nature of interconnected grids, the amount of conversion stages and converter topology, employed control philosophy might be different. Depending on the aforementioned aspects, some IC loops will be mandatory. For instance, if a two-stage IC is required with a intermediate dc bus, the regulation of such bus by one of the stages must be accomplished.

- **IC functionality:** once the constrains of the interconnection and the topology are defined, the main control loops must be defined according to the role of the IC. For instance, inner control loops will be completely different when a IC is compensating harmonic currents or providing inertial-response to interconnected systems.

3.1.3 Classification of Grid-Connected Converter Controls

While tertiary and secondary controls require a global perspective of the power system, primary and low-level controls focus on the local operation of the converter. Besides, the primary and low-level control layers are the ones that determine the transient response of the grids when load variations occur, hence this thesis has been focused on studying them in detail and proposing new control alternatives.

Depending on how the primary and low-level control layers operate with respect to the grid, converter (and hence IC) control strategies can be classified accordingly. In this case, we follow the classification provided by authors in [43–45], but we apply this criteria to ICs.

Grid-Forming Control

A grid-forming control is able to set the grid voltage and/or frequency by itself without the necessity of any other grid-connected device. In this group we consider converters that simply act as voltage sources, droop-operated units with inner voltage and current proportional-integral (PI) loops, or units with other low-level controls like synchronous machine emulation (SME) controls that imitate the behaviour of a grid-connected SG.

For example, a power converter interfacing a ESS may act as voltage and frequency reference for all the distributed generation (DG) units in an ac microgrid system. Similarly, the same converter could provide primary regulation and virtual-inertia in a bigger system with more grid-forming units connected in parallel.

When the grid-forming concept is applied to ICs, it must be noted that in most cases an IC unit can only set the voltage at one of its sides, while the voltage at the other side needs to be fixed externally. However, a grid-forming IC can be configured as a grid-supporting device towards the opposite grid, as we explained in [11] and report in section 3.2.

Grid-Supporting Control

In this category, we consider the control strategies that actively support the frequency or voltage (transiently and in steady-state) of ac and dc grids respectively, but operate as current sources. Thus, grid-supporting control strategies are not able to set the voltage of the power system by themselves (in the way grid-forming controls do), and require other devices to do so. The grid-supporting control detects the status of the grid and generates the corresponding reference to support it, keeping the synchronisation with the power system and ensuring the corresponding power delivery.

In the case of ICs, grid-supporting controls are configured to observe the status of the interconnected grids, carrying out the primary and/or low-level controls accordingly. This support can be done only by observing one subgrid or both of them. The latter corresponds to

the so called *dual grid-supporting* operation, already defined in [11] and further explained in Section 3.2.2.

Grid-Following Control

These type of controllers (also known as *grid-feeding* controls) deliver a certain amount of active and reactive power to an already energised grid, but unlike grid-supporting controls, they do not respond under grid variations or transients. Hence, they do not contribute to support the frequency or voltage of power systems, and they can be represented as ideal current sources where the delivered power responds to higher level control or algorithm reference, such as a maximum power point tracking (MPPT) technique in the case of RES. The low-level control of a grid-following unit needs to be synchronised with the existing power system.

The grid-following operation of ICs would correspond to the most simple IC operation. In this case, the power exchange between interconnected grids would respond to an external reference that the system operator would provide according to its necessities, i.e. to secondary or tertiary control layers. Hence, there would not be any primary regulation based on local measurements nor any transient support to the system. Therefore, IC control strategies in this category have not been further studied in the framework of this research project.

3.1.4 Analogy Between AC and DC Power Systems

Although ac and dc grids manifest obvious differences, there exist some analogies that can be taken to facilitate the management of power systems. In this section, we aim to identify these analogies and lay the foundations to employ a common framework to develop control strategies applicable at both ac and dc systems. Apart from understanding the analogies between conventional grid-connected devices, this analogy will enable to lay the foundations to develop IC control approaches regardless of the current nature of the interconnected subgrids.

As we mentioned in Chapter 1, the consumed and generated power in any power system needs to be balanced in order to keep the system stable and the frequency constant. Thus, the total amount of generated active power needs to cover the loading and the system losses:

$$\sum p_{gen} = \sum p_{load} + \sum p_{loss} \tag{3.1}$$

It is well known that in classical **ac systems** the power demand is adjusted through primary control, and this layer usually takes a few seconds to readjust the input mechanical power to the SG when a new (electrical) loading condition occurs in the system. Thus, the mismatch active power is released or absorbed by rotating kinetic masses attached to the shaft of synchronous rotating elements, and causes a variation in the system's angular velocity. The

amount of stored kinetic energy E_k in a rotating inertial element J is expressed as:

$$E_k = \frac{1}{2} J \omega^2 \tag{3.2}$$

where ω is the angular velocity of the rotating mass and J is the inertia. Thus, the grid-connected SG and the turbine system attached to its shaft present an equivalent inertia value J.

The inertial value of a grid-connected rotating element, is usually expressed by its per-unit value H, as described in [1]:

$$H = \frac{1}{2} \frac{J \omega_b^2}{S_b} \tag{3.3}$$

where ω_b represents the base frequency of the ac system, and S_b represents the base power of the system. The value of H is given in seconds, and represents the time required by the inertial element to be decelerated from nominal frequency to zero (or vice versa), when the nominal power is applied.

The mathematical expression that describes the electromechanical behaviour of SGs in a p.u. notation is known as the *swing equation* [1]:

$$2H \frac{d\omega}{dt} = \frac{P_m}{\omega} - \frac{P_e}{\omega} - K_d \Delta\omega \tag{3.4}$$

where ω is the frequency, P_m and P_e are the mechanical and electrical power, and K_d represents the damping factor of the generation system. This equation can be also represented in terms of a torque balance as:

$$2H \frac{d\omega}{dt} = T_m - T_e - K_d \Delta\omega \tag{3.5}$$

This equation shows how the resulting frequency variation and dynamic behaviour on a grid-connected generator mainly depends on its inertial value H, and the applied mechanical and electrical torque balance $T_m - T_e - K_d \Delta\omega$ on its shaft.

At **dc power systems**, when a power mismatch occurs between the generated and demanded power, there are two types of devices that are able to provide an inherent "inertial" response [46]: a capacitor directly connected to the dc bus or a dc generator.

If the **dc generator** is analysed, we can denote that the provided electromotive force (EMF) of a dc machine—expressed as E (in volts)—is proportional to the rotational speed of the generator:

$$E = K\omega \tag{3.6}$$

where K is the constant that links the rotational speed ω and the electromotive force E. The dc generator presents a rotational energy, with a energy storage capacity like the one described in (3.2). Thus, the dynamic behaviour of a dc generator is expressed as:

$$\frac{2H}{K}\frac{dE}{dt} = T_m - T_e - K_d\Delta\omega \tag{3.7}$$

where the voltage at its terminals E will be a direct reflection of the rotor's speed ω. When a power variation occurs at the grid side, the electrical power (and therefore the torque) of the dc machine will increase causing the deceleration of its shaft. The inertia of the machine will oppose to that variation by releasing electrical power and the EMF of the dc machine will decrease proportionally to the machine speed.

In the case of the dc bus-connected **capacitor**, the stored energy on a given capacitor C in form of electrostatic energy can be expressed as:

$$E_c = \frac{1}{2}Cv^2 \tag{3.8}$$

where v represents the capacitor voltage. This equation shows clear similarities with (3.2). Thus, we can deduct that the dc bus capacitance is equivalent to a rotating inertia, and the per-unit equivalent inertial value for dc system capacitance can be hence calculated as:

$$H_{dc} = \frac{1}{2}\frac{CV_b^2}{P_b} \tag{3.9}$$

where V_b represents the base dc voltage and P_b the base power of the system. This equivalent inertia value is also provided in seconds, and it expresses the capacitor discharge time when nominal power is applied.

The equation that describes the behaviour of a dc bus-connected capacitor with a parallel damping resistance R is described below

$$2H_{dc}\frac{dv}{dt} = I_{C_i} - I_{C_o} - \frac{\Delta v}{R} \tag{3.10}$$

Figure 3.3 shows the simplified dynamic model representation of the elements described above. Apart from showing the similarities between the different elements, it describes how active power is transferred from *inertial* elements to the corresponding ac and dc grids.

Table 3.1 summarises the equivalences identified for ac and dc grid-connected elements.

Virtual Inertia

As we have explained before, converter-interfaced devices do not provide an inherent inertial response under power variations. Figure 3.4 a) suggests that if a SG-based generation

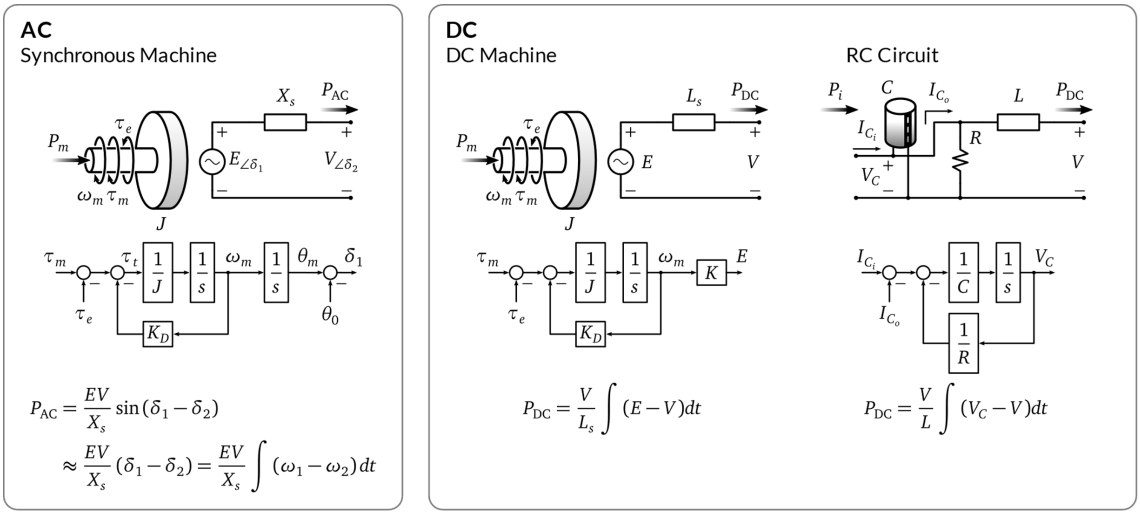

Figure 3.3: Dynamic models and equations describing the power exchange for grid connected devices providing inertial behaviour in ac and dc systems, described in [46]. (a) synchronous machine, (b) dc machine, and (c) resistor-capacitor (RC) circuit.

Table 3.1: Variable analogy for grid-connected ac and dc elements

	AC	DC	
	SG	Generator	Capacitor
Energy Storage Variable	J	J	C
Stored Energy Equation	$E_k = \frac{1}{2}J\omega^2$	$E_k = \frac{1}{2}J\omega^2$	$E_c = \frac{1}{2}Cv^2$
Dynamic Equation	$\sum\tau = J\dot{\omega}$	$\sum\tau = J\dot{\omega}$	$\sum I_c = C\dot{V}_c$
Power Transfer Variable	ω	E	V_c

unit is connected to the grid using a power converter, the inherent inertia of the machine will not react under variations unless the converter is controlled to carry out this function.

Similarly, grid tying devices such as power transformers or tie lines couple the dynamic response of the interconnected grids (inertial response, primary regulation capacity, etc.). However, when two grids are tied using one or various ICs, these grids are decoupled from each other [47], as Figure 3.4 b) suggests. Hence, to ensure the stability and an adequate power quality of modern ac/dc power systems, the contribution of grid-connected converters to improve the transient response of frequency and voltage under power perturbations is crucial.

The most widespread solution to cope with a weak inertial response is simply to mimic the dynamic behaviour of traditional grid-connected generators. For **ac systems**, these techniques basically implement the electromechanical dynamic equation of SGs (i.e. (3.5)) within the converter controllers and imitate their dynamic behaviour under load variations. These controls adopt many different names such as virtual synchronous generators (VSG), virtual synchronous machines (VISMA or VSM) or SME techniques. Among the SME techniques pro-

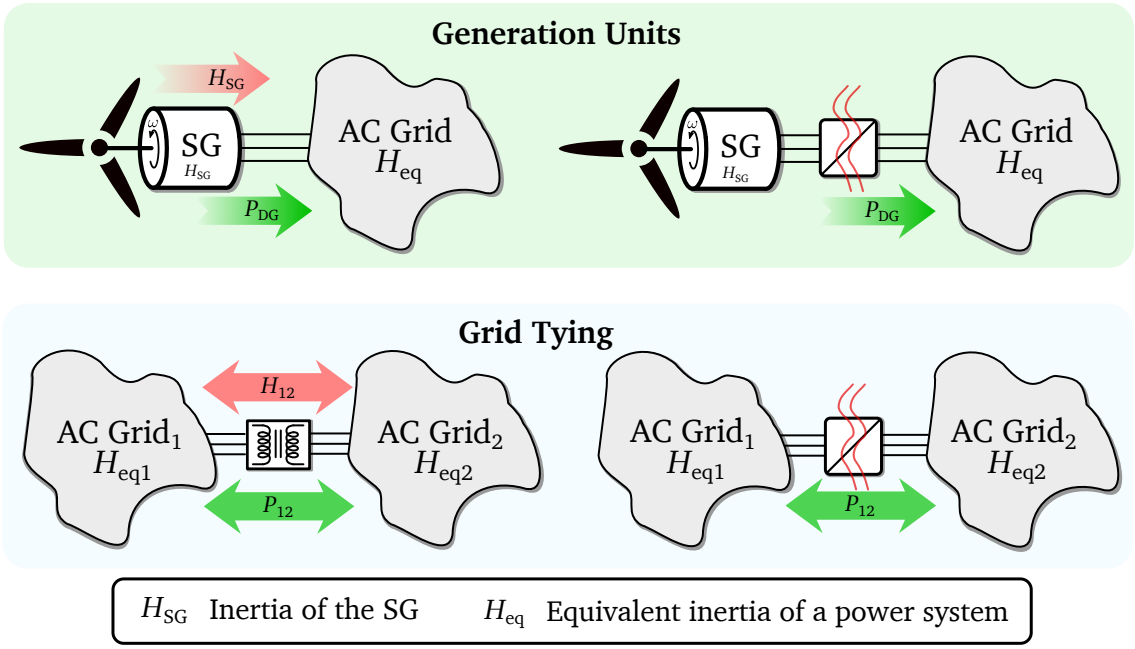

Figure 3.4: Dynamic (primary and inertial) response decoupling of power electronic converters.

posed in the literature, some of the most widespread control types include the **synchronverter**, the **current-controlled virtual synchronous machine (CCVSM)** and the **voltage-controlled virtual synchronous machine (VCVSM)** [48].

The **synchronverter** control is the simplest proposal among the SME controls. It consists of a frequency regulation loop based on the *swing-equation* (3.5) which provides the reference angle, and a reactive power control loop that provides the voltage amplitude of the converter. This technique does not require a phase-locked loop (PLL) synchronisation unit to operate, and neither does employ any inner voltage or current control loops that protect the converter from overloading or failure conditions. Authors in [49] have reviewed the different proposals for this control technique.

Other SME versions like the **CCVSM** and the **VCVSM** present more complex control structures. An example of the **CCVSM** can be found in [50], whereas the **VCVSM** has been thoroughly analysed in [51]. Although the dynamic response of these techniques under sudden power variations is defined by the well known *swing equation*, they include additional inner loops such as a virtual winding of a SG in the case of the **CCVSM**, or a steady-state virtual impedance in the **VCVSM** control. Both control approaches offer more controllability over electric variables but in contrast, tuning their control parameters is more complex than in the **synchronverter** [52].

In recent years, many control techniques that provide virtual inertia have been proposed for different applications, such as microgrids [53–58], RES units [4, 59–64], ESSs [65, 66],

HVDC and transmission systems [67–70], vehicle to grid applications [71–74] or ICs (as we will see in later in Section 3.2).

As we have previously mentioned in 3.1.4, grid-connected capacitors and dc-generators are able to provide inertial support in **dc systems**, so by implementing the equations of such devices (3.10) and (3.7) in converter controllers, dc inertia can be emulated. On the one hand, **virtual-capacitor (VC)** controls have been proposed for different power systems such as dc microgrids [75–79], dc railway systems [80] or HVDC transmission systems [81–84]. On the other hand, **virtual dc machine (VDCM)** control proposals [85] can be found for microgrid applications [86–89] as well as for dc distribution grids [90].

The aforementioned control techniques that imitate the behaviour of ac and dc grid connected generators and dc capacitors, provide virtual inertia to corresponding systems through voltage source converters operating as **grid-forming** units, as we explained in 3.1.3. However, virtual inertia can be provided to either ac and dc systems by providing active power transiently through a converter operating as a **grid-supporting** unit. This is achieved by reversing Eqs. (3.5), (3.7) or (3.10), so by observing the derivative of the frequency or the voltage and applying the virtual inertia term, the equivalent transient power setpoint for the grid-connected converter is obtained [91–95], leading to the **derivative-based** inertia-emulation controls. These strategies require a frequency estimation PLL unit or a voltage measurement in order to apply the derivative term and apparently they are not so complicated to implement [96]. Nevertheless, special care must be taken when derivatives are applied in such cases because electrical noise can cause active power reference peaks. Thus, frequency and voltage signals are usually treated by filtering, limiting their rate or adjusting the sampling of the signals [35].

Unified Control Framework for ICs

The analogy between ac and dc systems opens the possibility to extend the concept of virtual inertia from ac to dc grids, although there are some differences such as the fact that the frequency of ac systems needs to be estimated (e.g. by a PLL), while the dc voltage can be directly measured at the connection point. Besides, the frequency in steady-state is equal for all the nodes of an ac power system, whereas the dc voltage is different across the nodes due to the voltage drop through power system lines.

However, the similarities identified in the previous section make it possible to develop IC control techniques to couple power systems of very different characteristics (voltage levels, rated frequencies, ac or dc, etc.). As we have expressed in (3.3) and (3.9), the variable that represents the energy storage (either inertia or capacitance) can be converted to a per-unit representation H that enables the development of a generalised controller regardless of the nature of the power system. This requires to convert the grid measurements to a per-unit notation in order to set a common IC control framework that unifies both interconnected grids.

Two approaches can be followed to carry out this normalization. The first one converts measured ac frequency f_{meas} and ac-and-dc voltage v_{meas} as follows:

$$f_{pu} = \frac{2f_{meas} - (f_{max} + f_{min})}{f_{max} - f_{min}} \tag{3.11}$$

$$v_{pu} = \frac{2v_{meas} - (v_{max} + v_{min})}{v_{max} - v_{min}} \tag{3.12}$$

It is very common to set the droop control gains of generators and ESSs according to the voltage/frequency boundaries of the power system and the rated power of the device [97–99]. For such cases, this p.u. conversion approach provides a -1 to 1 reflection of the grid measurement. A p.u. value of -1 means that the lower limit of the measurement has been achieved (and hence the loading limit), 0 indicates the nominal value and a 1 expresses the higher limit has been reached.

On the other hand, a simpler p.u. conversion can be done by dividing the voltage and frequency by their base values:

$$f_{pu} = \frac{f_{meas}}{f_b} \tag{3.13}$$

$$v_{pu} = \frac{v_{meas}}{V_b} \tag{3.14}$$

The latter usually provides values closer to 1 p.u., and negative results are not contemplated. We consider this approach to be more suitable for large power systems, where the generation capacity might be time variant or non constant.

Employing any of the aforementioned p.u. conversion approaches, the variables of interconnected grids become comparable, and different IC controls can be proposed and implemented regardless of the current nature of the interconnected grids, as Figure 3.5 depicts. In this case, p.u. voltages v_{pu} and frequencies f_{pu} of the interconnected systems are represented with a general name x.

3.2 IC controls for the Provision of Virtual Inertia and Transient Support of Interconnected Systems

It is expected that in the future ICs will be requested to provide AS towards the interconnected systems, as several official entities such as ENTSO-E are recommending for grid-connected converters [100–102]. Some of the ASs recently proposed in the literature for ICs include the

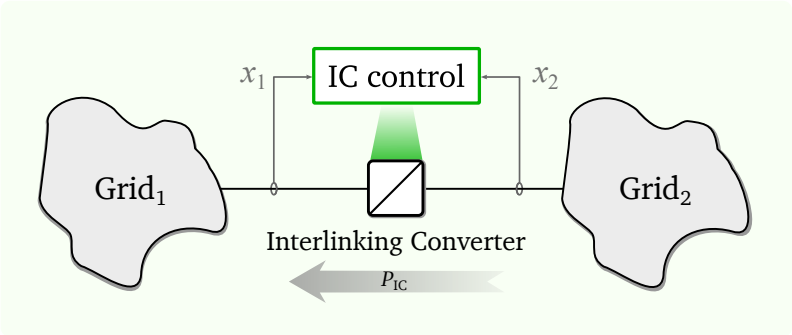

Figure 3.5: Illustration of the IC unified framework using p.u. grid measurements.

reactive power provision and ac voltage support [103–106], the harmonic current compensation [107–110] or the unbalance compensation [111–115].

In this section, we carry out an in-depth literature revision about the IC controls that provide transient support for the interconnected grids. The classification we propose is organised depending on how ICs provide the transient response, rather than the nature, scale or topology of the interconnection. Therefore, IC applications from bulk transmission systems to microgrids have been considered. Besides, communication-based IC controls have been left out of the classification, since we consider that the transient support must be handled locally (i.e. employing a local controller and local measurements). We must point out that the primary regulation control layer is not exclusively covered in this document, and the reader is referred to the article we presented in [11] where we provide an extensive review of the most relevant primary regulation techniques for ICs.

The classification we employ for IC controls that provide transient support is shown in Figure 3.6. First, we distinguish two different control groups, namely **grid-supporting** and **grid-forming** controls, based on the criteria provided in 3.1.3. Then, we further split these groups based on whether the transient support is provided for only one or both interconnected grids. In order to gather the control techniques according to the controller type they employ, we distinguish three subgroups. Two main groups are referred to what we have explained in 3.1.4, considering that transient support can be provided by providing virtual inertia in two main ways: using **SME – VC/VDCM**, or using **derivative-based** controls. However, we have observed that other control approaches can be also employed to contribute to the transient response of the interconnected power systems without imitating the inertial behaviour of a SG, and hence, these control strategies have been gathered in the third group named as **others**.

More details about employed controllers of reviewed IC techniques are provided in the upcoming sections, but by observing Figure 3.6 we can say that derivative-based controllers are implemented as grid-supporting IC controls, while SME – VC/VDCM controls work as single grid-forming ICs. In the mid-point between the grid-supporting and grid-forming operation (the single grid-forming and dual grid-supporting operation), the IC control proposal from

Chapter 5 takes place, and it does not use a *swing-equation* based controller to provide transient support and grid-forming capability to interconnected grids. Besides, we have seen that the grid-forming controls that provide transient support on ICs are limited to single-grid operation, since the dual grid-forming operation is not achievable in power converters, except for modular multilevel converter (MMC) converters, and yet no control proposal has been published as we will see later.

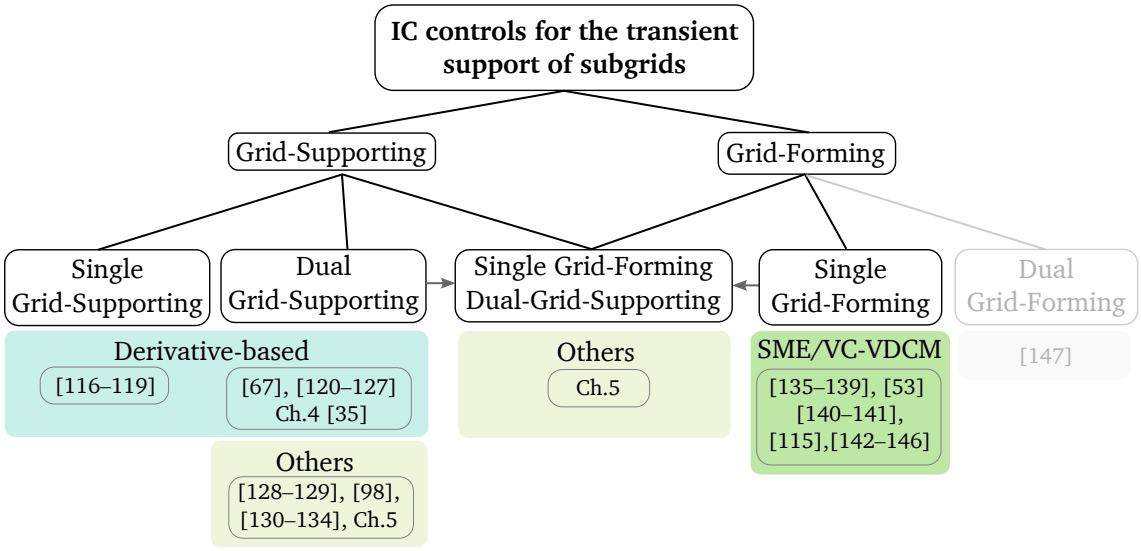

Figure 3.6: Literature review classification diagram.

3.2.1 Single Grid-Supporting Control Strategies

These techniques only provide transient support for one of the interconnected grids as Figure 3.7 suggests. Thus, while the one that is being observed receives active power support, the contrary is employed as a mere energy reserve.

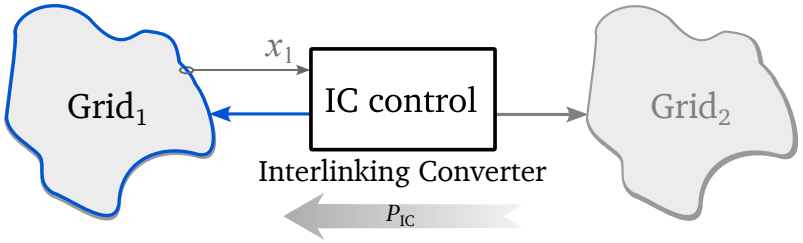

Figure 3.7: Illustration of the single grid-supporting IC control.

The authors in [116] propose a **derivative-based** control strategy that provides virtual inertia from a HVDC link to an ac system by observing first and second derivatives of frequency. A similar control approach is proposed in [117], where the frequency derivative is observed to provide inertial support from an HVDC grid to an ac power system by using a MMC.

In [118], Melath *et al.* propose a derivative-based IC control that supports the ac microgrid on a hybrid ac/dc microgrid link. In the ac microgrid there is a SG, so the purpose of this control is to take advantage of the grid-connected kinetic energy storage capacity as far as possible. The IC controller observes the ac grid frequency, and when it goes below or above some specified boundaries it applies the derivative-based emulation of inertia, extracting power from the dc microgrid and providing transient power to the ac system. According to the authors, this operation enables to reduce the investment on ESS while a reliable operation of the ac system is ensured.

In [119], Shen *et al.* propose a control technique that provides ac frequency support from a HVDC link. The authors implement a flexible inertia-emulation control (FIEC), which observes two aspects of the frequency to flexibly adjust inertia and provide transient power to the ac system. On the one hand, a variable inertia term is adjusted by observing the frequency derivative, and applying an exponential function. On the other hand, a second inertia term is adjusted according to the frequency deviation. By employing these two terms the provided virtual inertia is optimised, since larger frequency rate variations require more inertia, while a lighter inertia enables a faster restoration of the system's frequency.

3.2.2 Dual Grid-Supporting Control Strategies

IC controls in this category provide transient support to both interconnected grids. For that purpose, they need to observe the interconnected systems and generate an active power reference accordingly (see Figure 3.8).

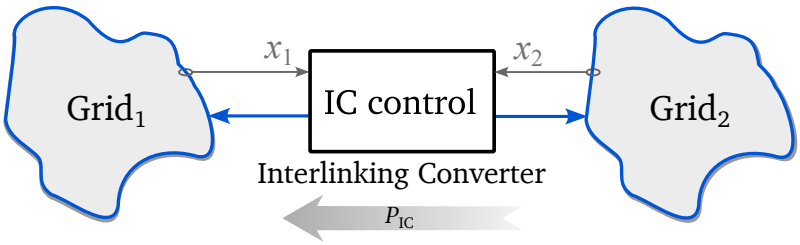

Figure 3.8: Illustration of the dual grid-supporting IC control.

Although some of the controls in this group consider the intermediate dc capacitor as a power source for the provision of inertial response, we would like to denote that none of the reviewed techniques employ a large storage system within the IC to provide a different active power for both sides of the IC during transients that lasts more than some milliseconds.

Considering the IC control techniques that employ the *swing equation* on its derivative form, Rakhshani *et al.* study these controllers for HVDC-AC links in [67, 120]. Authors state that although in the presented proposals the energy is obtained from additional ESSs, it could also be extracted from neighbouring grids.

In [121], He *et al.* propose a flexible control strategy for a hybrid ac/dc shipboard system. A derivative-based inertia-emulation loop is implemented for the IC, which is coordinated with the different ESS units connected to the ac and dc grids. This control is denominated as *flexible power control loop* and a *cross-zone* power compensation is carried out, extracting power actively from ESSs from one grid when the contrary presents a load increment and vice versa, so inertial and primary support is provided to both interconnected systems. In [122], same authors propose a control strategy following the same principles as in the previous case, but for a microgrid scenario. The main agent of this control strategy is the IC, since it enables the power flow between both microgrids. However, the proposed technique acts over all the DG and ESS units of both microgrids such as PV panels, micro turbine generator, wind turbine generator (WTG) and hybrid energy storage (HES) systems. We consider important to denote that the proposed strategies by He *et al.* in [121] and [122] are designed ad-hoc for each scenario, where a central controller is used without any communication link, and it might be more difficult to integrate at systems with other types of energy assets.

The proposed IC controls in [123, 124] observe the ac frequency and dc voltage of a hybrid microgrid link and obtain a power reference for each subgrid. For that purpose, they apply a derivative-based inertia-emulation control loop. In [125], the frequency of a distribution subgrid and voltage of a dc microgrid are observed for the bidirectional inertia support in a hybrid microgrid, but in this case only one grid is supported at a time. The supported grid is selected according to which grid requires more support in terms of primary regulation, and a derivative-based inertia-emulation is applied.

Zhu *et al.* in [126] propose a point-to-point HVDC link for asynchronous ac grid interconnection. While the first stage of the IC is in charge of dc bus voltage regulation, the second one regulates the active power flow with the second ac grid. Taking into account that the presented control strategy does not use any communication link, the authors employ an *information extraction loop* to estimate the frequency of the first ac grid on the second stage of the IC. Since the droop gain that defines the frequency of the first ac grid and the dc bus voltage reference is known, the second converter can estimate the frequency of the first grid. Then, a derivative-based inertia-emulation loop is applied for each grid's frequency. This controller only supports one ac grid at a time, based on a priority selection algorithm, i.e. the one that presents the highest RoCoF. This controller employs a dead zone for the frequency and a hold time to prevent unnecessary execution of the control. In [127], employing a similar scenario than in [126], a bilateral inertia and damping control is proposed. In this case, the IC is able to provide transient support for both interconnected grids simultaneously. The inertia-emulation is realised by varying the dc capacitance voltage via the dc regulating stage, and the damping emulation is achieved by coordinating the active power flow via the power regulating stage.

In [128, 129], Zhang *et al.* propose a bidirectional virtual inertia support IC control for a hybrid ac/dc microgrid. The proposed IC control combines two main loops for the emulation

of inertia. On the one hand, synchronverter loop is implemented to obtain the equivalent ac microgrid frequency response, and a VC loop obtains the equivalent dc voltage response. Then, both frequency and voltage p.u. values are compared, and the difference is fed to a PI regulator, which provides an active power reference for inner IC voltage and current control loops. From our point of view, although this technique might provide some transient support to interconnected systems, we do not consider that the bidirectional inertia support is performed simply because the equivalent active power provision of the *inertial* elements cannot be achieved. In other words, larger inertial values in the control loops will cause lower virtual RoCoF/V values, and hence lower active power support to interconnected systems, which is contradicting the principle of inertial grid-connected devices.

Last but not least, we briefly analyse the dual grid-supporting controls that provide transient support to interconnected grids but they do not employ the *swing equation* to achieve so. Most of the reviewed techniques hereafter do not consider the improvement of the dynamic response of interconnected systems in their proposals, and mainly focus on power sharing properties. However, we consider that they contribute to the transient response of grids, since they employ controllers that go beyond proportional controllers (which would correspond to *droop* or *dual-droop* approaches) and they provide power under grid transients. The authors in [98, 130, 131], for instance, propose IC control strategies that aim to equalise the interconnected microgrids by exchanging active power among them. By using a PI controller, the per-unit value of the frequency and voltage (for ac and dc microgrids respectively) are equalised. Similarly, in [132] the per-unit errors of a hybrid microgrid are equalised. In [133], Shi et al. apply the *virtual transformer* philosophy but instead of using a per-unit value to equalise the voltages of the interconnected grids, a constant voltage proportion is employed to perform the power exchange. In [134], the authors propose a proportional power sharing technique where instead of using the IC terminal measurements, ac and dc subsystem common voltages are estimated to achieve a better active and reactive power sharing. One of the main drawbacks of the aforementioned control is that it requires to know the structure and parameters of the interconnected systems.

Finally, in Chapters 4 and 5 we propose two IC control strategies that can work as dual grid-supporting units for the improvement of the transient response of interconnected systems. The former control is denominated as dual inertia-emulation (DIE) control (presented in [35]), and consists of two-derivative-based loops in order to provide a IC power reference for the contribution of virtual inertia for both interconnected systems. This technique can be easily implemented along with a primary regulation control technique, contributing to the primary response as well. The latter, named as virtual power line (VPL) control, makes the IC behave as a power transmission line but enables to interconnect power systems of different natures and properties. Thus, this control approach unifies the primary and the transient responses of interconnected grids, improving both of them by making all the generators respond under

load variations. Proposed IC controllers are explained in detail, and simulation results that prove their performance and compare them against other solutions are provided in chapters 4 and 5.

3.2.3 Single Grid-Forming Control Strategies

In this section we gather the IC control techniques that provide transient support and work as grid-forming units for one of the interconnected systems. These IC controls employ one of the interconnected grids as a power source to set the voltage at the contrary one, as Figure 3.9 illustrates.

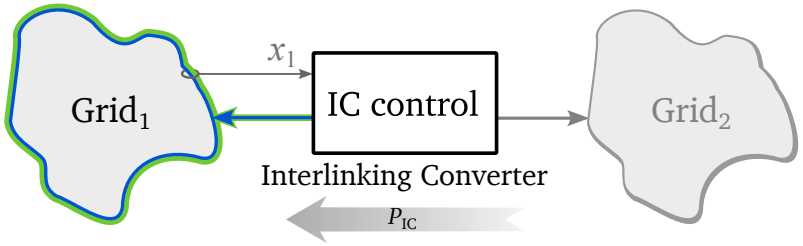

Figure 3.9: Illustration of the single grid-forming IC control.

Alsiraji *et al.* employ a SME loop on a hybrid ac/dc microgrid IC in [135]. In this case, the IC works as a grid-forming unit for the ac microgrid, without taking into account the voltage transient support for the dc microgrid. Additional inner voltage and current PI loops enable to control electric variables so that the IC can be protected from over currents and over voltages. In [136], Li *et al.* use a SME control loop to perform the emulation of inertia towards the ac microgrid. This control uses a non-ideal proportional-resonant controller and the emulation of inertia contributes to stabilise the ac side of the interconnected hybrid ac/dc microgrid. Similar approaches that support the ac microgrid are provided in [53, 137–141].

The authors in [115] propose a control strategy that, in addition to being able to compensate phase unbalances on hybrid ac/dc microgrids, they also include a SME loop that coexists with the unbalance compensation control. It is important to highlight that an adaptive inertia variable is implemented which depends on the frequency deviation, providing more inertia when frequency deviation is larger.

Contrary to the previously analysed IC control strategies with virtual inertia capability, the authors in [142] propose a *virtual capacitor* control for the capacitance emulation at the dc microgrid on a hybrid ac/dc microgrid scenario. To perform the primary regulation and achieve the power sharing between two microgrids, a *proportional power sharing* technique is used. The results provided show the effectiveness of this control technique over a normalised droop control during load transients in the dc system. We consider that this control technique is interesting for cases in which the dc microgrid presents poor transient response while the ac grid is coupled to the main ac grid.

In [143], Zeyan *et al.* propose a control strategy with bidirectional inertial support in a hybrid ac/dc microgrid with a two stage IC, so one stage refers to the dc/dc stage and the second one corresponds to the dc/ac inverter. The proposed control strategy has two main parts. On the one hand, the dc/ac stage of the IC is controlled with a SME technique, providing inertial support towards the ac microgrid. On the other hand, the dc/dc stage is in charge of controlling the voltage of the intermediate dc stage capacitor. The presented control technique for the intermediate dc capacitor voltage control uses a hyperbolic tangent based trigonometric function, which is naturally an asymptotic function and by employing it the minimum and maximum intermediate capacitor deviation voltage values can be set. The aim of the proposed control technique is twofold. First, it aims to keep the intermediate stage dc capacitor voltage value into acceptable boundaries for the IC operation on the ac microgrid support. Then, it optimises (reduces) the current surge from the dc microgrid comparing to conventional dc bus voltage controls. This control is denominated by the authors as **adjustable inertia for the dc microgrid**, reasoning that smoother currents are surged from the dc microgrid using the proposed control than using fixed voltage control or linearly reduced dc bus voltage. Authors state that implementing this control the dc microgrid voltage is improved comparing to other techniques when loading conditions in the ac microgrid change. Nevertheless, the proposed control does not correspond to a **VC** or **VDCM** control that provides virtual inertia for the dc microgrid, because when a power variation occurs in the dc microgrid, the proposed control technique will not respond providing any power to the dc system. Therefore, we consider that it can not be classified as an adjustable dc inertia, nor does it correspond to a dual inertia-emulation technique despite of its benefits under some concrete conditions.

Zhang *et al.* in [144] propose a control approach for ICs on networked ac and dc microgrids. In the proposed benchmark system, two ac microgrids and two dc microgrids are networked through a MTDC system by using ICs. In first place, the power sharing among droop-governed microgrids is obtained by equalising per unit frequency-and-voltages of the different systems. Then, an adaptive virtual inertia and governor gain control that improves the ac frequency and dc voltage of ac and dc microgrids is proposed. The control principles are the same for ICs that interface the ac and dc systems with the MTDC grid. ICs in charge of supporting ac grids employ the SME control while the ones supporting dc systems employ the VDCM loop. In both cases, virtual inertia and governor gain values are defined by hyperbolic tangent functions, so when RoCoF and RoCoV values are large, inertia and governor gain values will be large and vice versa. Thus, by adequately varying these parameters, an improved bidirectional transient support is achieved on the networked system.

The authors in [145] propose an IC control for a hybrid ac/dc microgrid where a virtual rotor (and hence a virtual inertia) is employed. The dynamic equation of this virtual rotor is implemented through a synchronverter loop which sets the ac reference angle of the IC. The active power regulation is achieved by comparing the dc and ac microgrid values, and the

resulting value is fed to the virtual rotor loop. Thus, we can say that this control behaves as a SG for the ac subgrid when there is a load variation, but when the dc system requires transient power it behaves as a dc machine that needs to be accelerated to provide power to the dc system. A similar approach is proposed by the authors in [146] for a hybrid ac/dc microgrid.

3.2.4 Dual Grid-Forming Controls

The dual grid-forming control with ICs is—following our definition of IC—limited to MMCs, since they do not employ additional ESS systems beyond the required module capacitors to operate. These converters can employ each module's internal capacitor energy storage to set the dc voltage and ac frequency of both sides of the converter. Authors in [147] state that MMCs can be employed to provide virtual inertia to interconnected grids, even if they do not specifically propose any control. We believe that MMCs could be employed to provide transient support for both interconnected grids and still operate as dual grid-forming controls, but further research is still required in this topic. The conceptual form of this controller is shown in Figure 3.10.

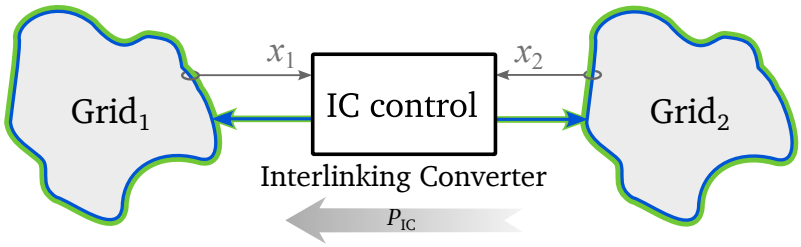

Figure 3.10: Illustration of the dual grid-forming IC control.

3.2.5 Single Grid-Forming and Dual Grid-Supporting Controls

During the literature review, we have not found any control that provides transient support to interconnected power systems and can be included in this category. However, in Chapter 5 we propose a virtual power line control for ICs that can work as a grid forming unit for one of interconnected grids, and supports both of them in transient and steady state as Figure 3.11 suggests. The full control proposal is addressed in Chapter 5 and simulation results that verify the validity of the proposed control are provided as well.

3.3 Summary

After reviewing the different control techniques for ICs that provide transient support to interconnected systems, we summarise the most relevant features of each strategy in the following Tables 3.2 and 3.3 for grid-supporting and grid-forming controls respectively. Besides,

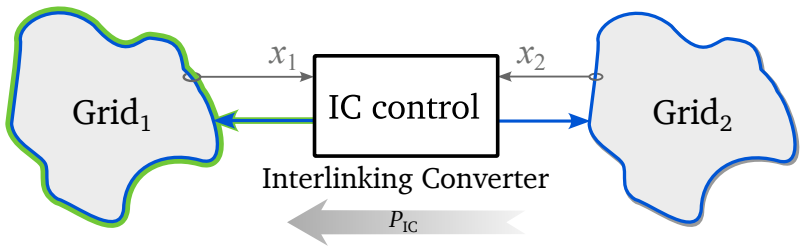

Figure 3.11: Illustration of the single grid-forming and dual grid-supporting IC control.

the most relevant conclusions of the literature review are gathered below:

- Most of the IC control techniques for the provision of transient support under load variations are proposed for hybrid microgrid environments due to the fact that they are usually formed by converter-interfaced devices with a poor inertial response. However, the penetration of RES in traditional ac systems is demanding the interconnection of different power systems via HVDC links, where ICs will play a crucial role in the power transmission, ancillary service market and in the contribution of systems' stability and robustness. Thus, we have seen that the number of publications that propose IC control strategies for high-voltage and transmission applications shows an upward trend in the last years.

- If the features of grid-supporting controls are observed in Table 3.2, we can deduct that most of the proposals employ **derivative** based solutions for the emulation of inertia. Since they are not required to form the grid, this method is the most straightforward to obtain an active power reference that supports the subgrids. Regarding the controls not based on the implementation of the swing equation, we can say that these proposals are mainly focused on the power sharing among subgrids, and the contribution to the transient response is not analysed in detail.

- Grid-forming proposals employ the SME and VC loops for the provision of virtual inertia, and they support only one grid, which in most of the cases corresponds to the ac grid. Under our classification criteria, ICs do not present a large internal energy storage capacity, so the dual grid-forming approach is limited to MMC converters. However, this operation is on an early stage of maturity and controls for the contribution to the transient response have not been covered yet. Similarly, single grid-forming and dual grid-supporting proposals are almost non-existing, but we consider that this can be a very interesting control philosophy since ICs could be employed to form new grids avoiding the necessity of exclusive devices to do so, and yet support both sides of the interconnection. The advantages of these types of controllers are further studied in Chapter 5.

Table 3.2: Summary of IC grid-supporting control techniques for the provision of transient support on interconnected grids.

Ref.	Controller	Inertia Loop	Link's Nature	Inertia support to:	Scale
[116]		Derivative	ac/dc	ac	Transmission
[117]	Single GS	Derivative	ac/dc	ac	Transmission
[118]		Derivative	ac/dc	ac	Microgrid
[119]		Derivative	ac/dc	ac	Transmission
[67]		Derivative	ac/dc	ac & dc	Transmission
[120]		Derivative	ac/dc	ac & dc	Transmission
[121]		Derivative	ac/dc	ac & dc	Microgrid
[122]		Derivative	ac/dc	ac & dc	Microgrid
[123]		Derivative	ac/dc	ac & dc	Microgrid
[124]		Derivative	ac/dc	ac & dc	Microgrid
[125]		Derivative	ac/dc	ac or dc	Distribution
[126]		Derivative	ac/ac	ac1 or ac2	Transmission
[127]	Dual GS	Derivative	ac/ac	ac & ac	Transmission
Ch.4		Derivative	any	both	any
[128]		Other	ac/dc	ac & dc	Microgrid
[129]		Other	ac/dc	ac & dc	Microgrid
[98]		Other (PI)	ac/dc	ac & dc	Microgrid
[130]		Other (PI)	ac/dc	ac & dc	Microgrid
[131]		Other (PI)	ac/dc	ac & dc	Microgrid
[132]		Other (PI)	ac/dc	ac & dc	Microgrid
[133]		Other (PI)	dc/dc	dc & dc	Microgrid
[134]		Other (PI)	ac/dc	ac & dc	Microgrid
Ch.5		Other	any	both	any

Table 3.3: Summary of IC grid-forming control techniques for the provision of transient support on interconnected grids.

Ref.	Controller	Inertia Loop	Link's Nature	Inertia support to:	Scale
[135]		SME	ac/dc	ac	Microgrid
[136]		SME	ac/dc	ac	Microgrid
[137]		SME	ac/dc	ac	Microgrid
[138]		SME	ac/dc	ac	Microgrid
[139]		SME	ac/dc	ac	Microgrid
[53]		SME	ac/dc	ac	Microgrid
[140]	Single GF	SME	ac/dc	ac	Microgrid
[141]		SME	ac/dc	ac	Transmission
[115]		SME	ac/dc	ac	Microgrid
[142]		VC	ac/dc	dc	Microgrid
[143]		SME	ac/dc	ac	Microgrid
[144]		SME/VDCM	ac/dc	ac & dc	Microgrid
[145]		SME	ac/dc	ac & dc	Microgrid
[146]		SME	ac/dc	ac & dc	Microgrid
[147]	Dual GF	–	ac/dc	–	Transmission
Ch.5	SGF & DGS	Other	any	both	any

Chapter 4

Dual Inertia-Emulation Control Strategy for ICs

This chapter presents a novel control strategy for ICs named dual inertia-emulation (DIE) control, that improves the dynamic response of tied grids by emulating inertia at both sides of the converter, and which can be employed at any IC regardless of the interconnected grid type (ac or dc). The proposed control is tested by means of DFPF simulations of WSCC 9-bus and IEEE 14-bus benchmark systems. The obtained results demonstrate that the proposed technique increases the equivalent inertial response of the interconnected grids, hence reducing frequency oscillations, RoCoF, and improves the frequency nadir.

4.1 Introduction

The purpose of this chapter is to propose and validate a novel control technique for ICs. We named this technique *dual inertia-emulation* (DIE) control, since it enables to achieve the inertia-emulation for both sides of the IC. The DIE control observes the grids at the IC terminals, and always supports the most damaged grid by extracting power from the contrary one. The conceptual form of this technique was first introduced in [46], and in this chapter we go a step further by demonstrating that it does indeed improve the transient behaviour of the interconnected grids. One of the main advantages of this control is that, since it is based in a per unit notation (see 3.1.4), it can be equally employed for ICs interconnecting ac or dc grids. Moreover, the controller parameters can be adjusted independently based on the type and strength of the interconnected grids to prioritise the support of the most weak side. As we demonstrate in upcoming sections, this technique can be easily incorporated to a classical controller, e.g. like one of the reviewed techniques in [11] performing the primary regulation. The DIE control does not require any communication link and it can operate autonomously, so this feature makes the IC operation more reliable and ICs can be connected in parallel.

The principles of the DIE technique are provided in the upcoming Section 4.2. Section 4.3 explains the simulation scenario that has been chosen for the validation of the proposed technique, and different test case simulation results are provided. Finally, Section 4.4 concludes the chapter with the most important remarks of the DIE proposal study.

4.2 Dual Inertia-Emulation Control

4.2.1 Operation Principle

As we have explained in 3.1.4, most of the existing techniques for the emulation of inertia on ac systems are based on the well known *swing equation*, and it is repeated here for convenience [1]:

$$2H\frac{d\omega}{dt} = T_m - T_e - K_d\Delta\omega \tag{4.1}$$

where H is the per unit inertia constant, ω is the per unit frequency, T_m and T_e are the mechanical and the electrical torques and K_d is the damping factor.

This equation can be also written in terms of mechanical and electrical power (P_m and P_e, respectively), and it leads to the *derivative-based* inertia-emulation as follows:

$$2H\frac{d\omega}{dt} = \frac{P_m}{\omega} - \frac{P_e}{\omega} - K_d\Delta\omega \tag{4.2}$$

The DIE technique is based on the unified control framework presented in section 3.1.4,

and it can be included in parallel to a primary regulation loop like the ones gathered by the authors in [11]. For instance, it can be set up in parallel to a dual-droop (DD) loop and then cascaded to a current reference calculation (CRC) stage and a classical current controller (CC) as shown in Figure 4.1.

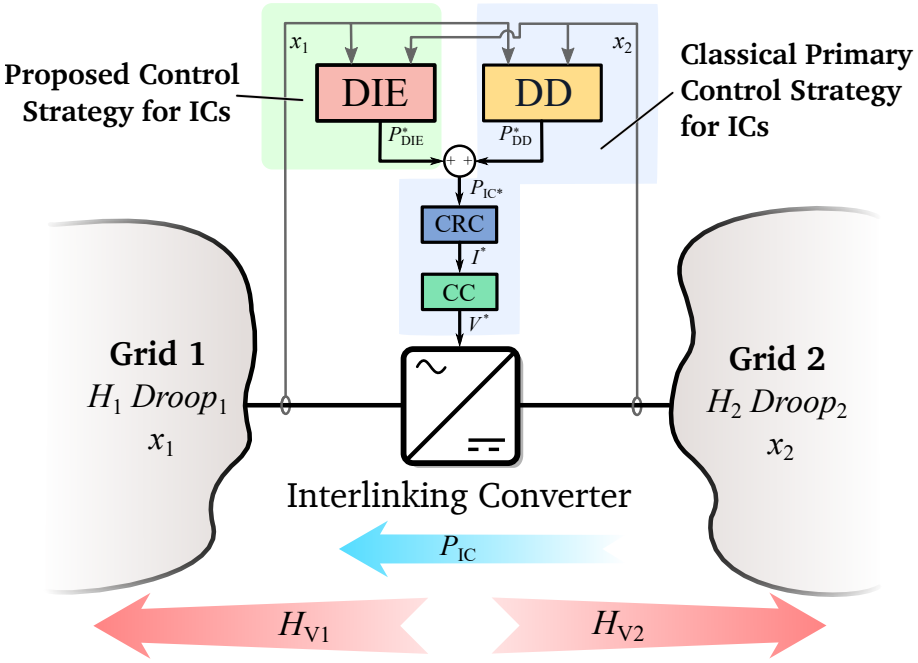

Figure 4.1: Representation of the IC with the proposed dual inertia-emulation technique and classical control approach.

The inertia-emulation of the proposed technique is built on the swing equation in (4.2), and the purpose is to generate a power reference from a grid voltage or frequency variation, similar to the response of a SG in an ac grid or a bus-connected capacitor in a dc one by employing the grid derivative *df/dt* like in [148]. Since most of the times such techniques include a droop gain for power-sharing purposes, equation (4.2) can be simplified by neglecting the damping term (which is almost equivalent to the droop), leading to:

$$-2H_V\omega\frac{d\omega}{dt} = P^* \tag{4.3}$$

where H_V is the per-unit virtual inertia value and P^* is the obtained power reference. The (−) sign is introduced because for a negative grid evolution, the control strategy needs to respond with a positive power to the system and vice versa.

Basically, this technique observes the grid derivative (frequency on ac grids and voltage at dc ones) and provides a power reference which is proportional to the emulated inertia H_V. Implementing this technique, different ICs can be connected in parallel to perform the inertia-emulation. The provided power by each IC will depend on the H_V control parameter and the

grid derivative that each IC controller senses, achieving the power sharing in a communication-less and autonomous manner. By providing a transient response under frequency or voltage variations, we provide more time for other devices (generators, energy storage systems, etc.) to carry out the primary regulation of the system.

In the case of the DIE technique, (4.3) is implemented twice (hence the use of the term “dual"), one for each of the interconnected grids. Figure 4.2 represents the main structure of the DIE loop, where the two normalised inertia-emulation branches can be observed. We would like to denote that the DIE control concept has been proposed for ICs regardless or their topology of number of stages, so depending on the use case the required control loops must be implemented (e.g. the intermediate dc bus on a two-stage IC). Taking into consideration that the DIE belongs to a dual grid-supporting control technique, it requires to observe the grids at both sides of the IC in order to transfer active power from one grid to another. Thus, a PLL unit for ac grids and a voltage measurement unit for dc systems will be mandatory.

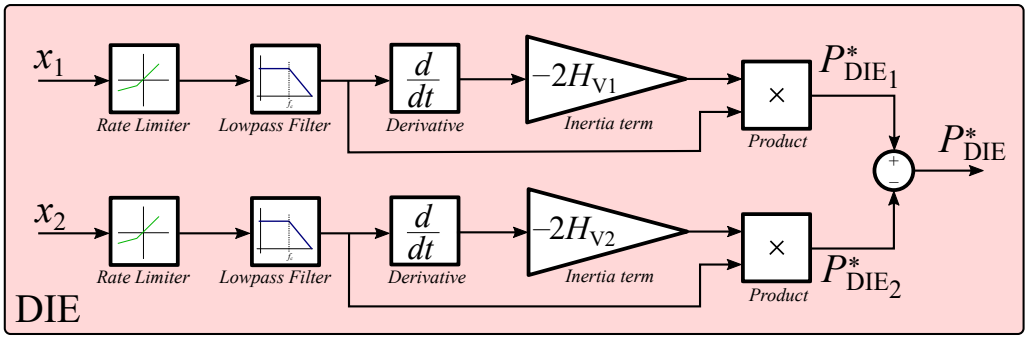

Figure 4.2: Detailed Dual Inertia-Emulation control loop for ICs.

The power references for each grid are calculated employing (4.3) as follows:

$$P^*_{\mathrm{DIE}_1} = -2H_{V_1} x_1 \frac{dx_1}{dt} \quad P^*_{\mathrm{DIE}_2} = -2H_{V_2} x_2 \frac{dx_2}{dt} \tag{4.4}$$

where the subscript on parameters from equation (4.4) represents the number of the grid (i.e. grid 1 or 2), x represents the per-unit frequency (for ac grids) or the voltage (for dc grids) of the grid and H_V is the emulated inertia.

The two power references from (4.4) are then subtracted to obtain the final power reference for the converter:

$$P^*_{\mathrm{DIE}} = P^*_{\mathrm{DIE}_1} - P^*_{\mathrm{DIE}_2} \tag{4.5}$$

By observing (4.5), it can be deducted that the inertia-emulation will be performed for the most damaged subgrid, extracting power from the contrary one. If a simultaneous load variation occurs in both grids, the power reference will tend to be cancelled.

In most cases the measured grid signals (voltage and frequency) exhibit electric noise,

spikes or oscillations, leading the derivative-based controller to respond under such perturbations and providing disproportionate power references. This is specially critical when the IC is connected to ac grids, inasmuch as the frequency cannot be directly measured and needs to be estimated using a PLL. A great deal of research is currently being conducted in this path regarding the frequency estimation under non ideal grid conditions or voltage dips and although we are conscious of this fact, this study is out of the scope of this research. Therefore, we have considered that the grid position can be correctly estimated for the proposition of the DIE control strategy.

In order to avoid issues with grid frequency estimations and voltage measurements (for ac and dc subgrids respectively), we first filter the grid voltage or frequency by means of a rate limiter and a low-pass filter (Figure 4.2). As in the case of the PLL, it is worth noting that the selection of the parameters of these blocks will strongly depend on the environment where the IC is implemented, keeping the commitment between the grid dynamic measurement (which relies on the robustness of the grids) and the filtering of undesired electric noise.

Regarding the virtual inertia coefficients H_{V_1} and H_{V_2}, we must choose them according to the capacity and robustness of each grid, as will be explained in Section 4.3.

4.2.2 Supporting the transient response of grids

By including two independent inertia-emulation loops in the controller, it is possible to decouple the extent to which we want to support each of the grids in terms of inertial response. This is an interesting feature when one of the grids is much stronger than the other one, or when we want to transfer the inertial response between two grids.

Lets assume for instance that an IC is interconnecting two grids with an equivalent inertia H_1 and H_2 as shown in Figure 4.1. The power variations in each grid are considered as an aggregated power variation named ΔP_1 and ΔP_2 (considering load as negative power), and the power of the IC is considered to be positive when flowing from grid 2 to grid 1. Then, the differential equations that model the dynamic response of the grid frequency or voltage can be written down as follows:

$$x_1 \frac{dx_1}{dt} = \frac{1}{2H_1}(\Delta P_1 + P_{\text{IC}}) \quad x_2 \frac{dx_2}{dt} = \frac{1}{2H_2}(\Delta P_2 - P_{\text{IC}}) \tag{4.6}$$

Assuming that x_1 and x_2 will be close to their rated values, from (4.6) it is clear that if the IC does not provide any power—i.e. $P_{\text{IC}} = 0$—the rate of change of the voltage or frequency depends on the inertia of the grid and the amplitude of the power perturbation.

If we neglect the effect of the DD loop (or any other present primary regulator) to simplify the analysis and consider that the current controller is fast compared to the inertial response (i.e. $P_{\text{IC}} = P^*_{\text{DIE}}$), when we control the IC with the proposed DIE technique we get the following

expressions by introducing (4.5) into (4.6):

$$\begin{aligned} x_1 \frac{dx_1}{dt} &= \frac{1}{2(H_1 + H_{V_1})} \left(\Delta P_1 + 2H_{V_2} \frac{dx_2}{dt} x_2 \right) \\ x_2 \frac{dx_2}{dt} &= \frac{1}{2(H_2 + H_{V_2})} \left(\Delta P_2 + 2H_{V_1} \frac{dx_1}{dt} x_1 \right) \end{aligned} \tag{4.7}$$

These expressions show that, for the same power perturbations, the dynamic transients of the frequency or voltage now also depend on the virtual inertia introduced by the DIE loop. This means that we are capable of improving the transient response of the grid by emulating a certain amount of inertia H_{V_1} and H_{V_2}.

As one would expect, when the IC transfers a certain amount of power to support one grid, the second grid will also suffer a perturbation according to P_{DIE} and the inertia of the second grid. However, as it will be demonstrated in the upcoming section, in the case that two neighbouring grids are tied using a tie line or a power transformer, the power disturbance happening in one grid is completely coupled to the neighbouring grid. Therefore, by employing the DIE technique we can choose the coupling level of the disturbance by properly setting virtual inertia control terms according to the robustness of the interconnected grids by the IC. In a sense, we can say that the DIE enables to transfer the inertial response of the interconnected grids in a controllable manner, thus extending the benefits of using ICs to interconnect different power systems. In the case of a simultaneous power variation in both grids, the DIE technique will always support the most damaged one by emulating more inertia to this side.

4.3 DIE Control Validation

4.3.1 DIE Testing Scenario

We propose a testing scenario comprised by two standard ac (initially syncronised) systems to validate the proposed control strategy. The first system corresponds to a modified 9-node WSCC system [34] (referred from now on as System 1), and the second one is a modified 14-node IEEE system [149] (System 2). Figure 4.3 shows the single-line diagram of these two systems interconnected via an IC. The employed parameters, IC control strategy or grid-tying elements are detailed on each test case.

Even though the proposed control concept can be employed for the interconnection of different types of grids (hybrid interconnections, ac grids with different frequencies or dc grids with different voltage levels), in this case both tied grids are ac. The reason for choosing two ac grids is that, in addition to comparing the DIE technique to other control approaches, it also enables to compare its performance to power transformers or tie lines.

This scenario has been implemented in a DFPF simulation as described in Chapter 2, where two ac subsystems and the link between them (i.e. the IC with its corresponding control or the

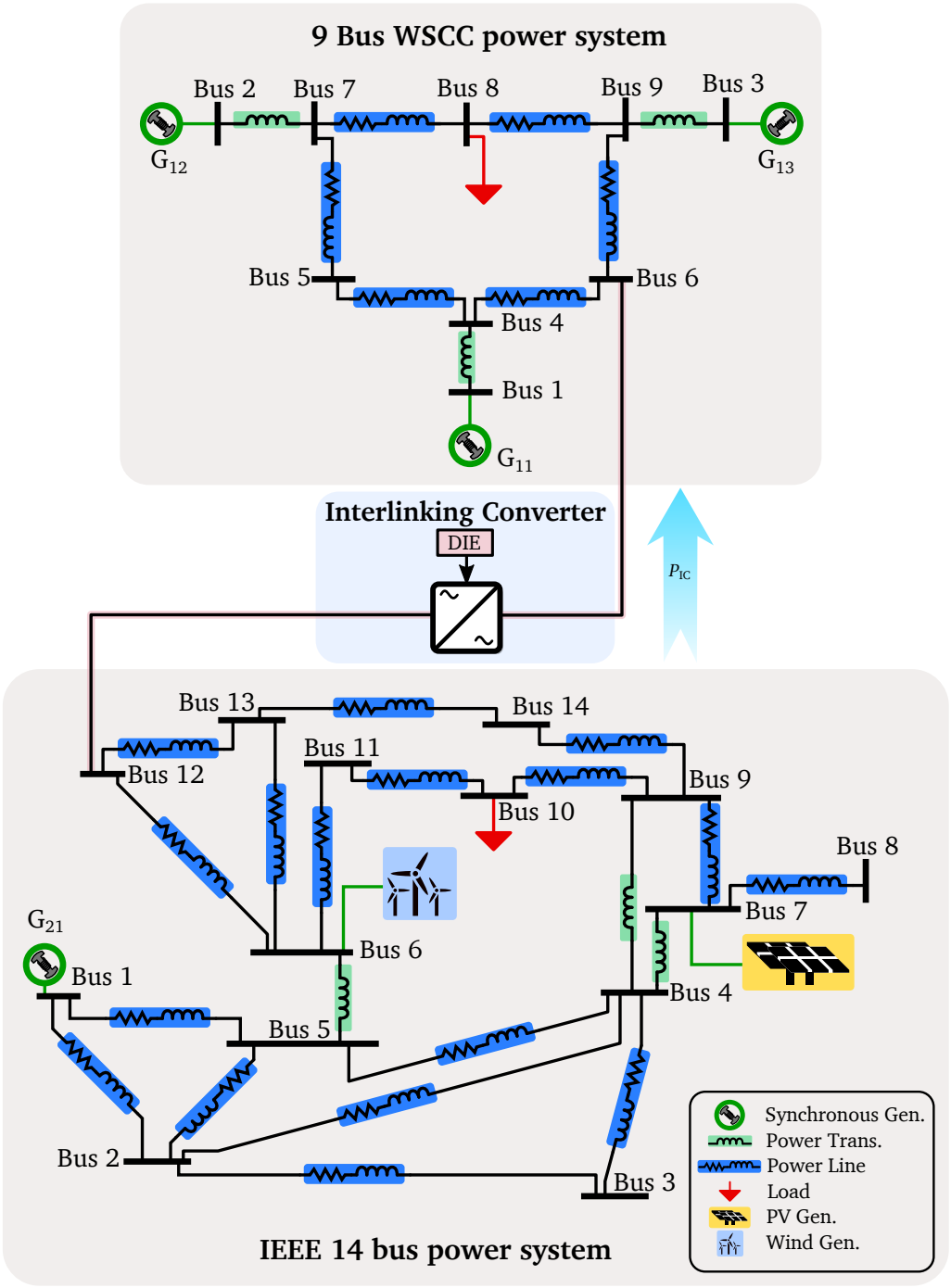

Figure 4.3: Proposed simulation scenario for testing the DIE technique on an IC tying two electric grids.

power transformer) have been simulated in the same Simulink model file. The line data from Figure 4.3 has been gathered from [34] and [149] for Systems 1 and 2, respectively, and the same base power and voltage magnitudes have been employed for the per unit conversion in both systems (230 kV and 100 MVA). The specific generated/consumed power and controller

parameters are detailed in each test case.

4.3.2 DIE Operation Concept

In this test we show the effectiveness of the proposed technique in a simplified scenario. Both grids are modelled with a single synchronous generator at the first node. The parameters are represented as N_{ij}, where N denotes the name of the parameter (inertia, damping, reactance, etc.). The power system is expressed by subscript i, and j represents the generator (G) number. For this test case, G_{11} and G_{21} are the only operative generators on the scenario from Figure 4.3 and they are configured with equal inertia (H_{11} and H_{21}), droop coefficients (D_{11} and D_{21}) and synchronous reactances (X_{s11} and X_{s21}). In order to show the operation concept of the DIE technique in a clearer way, we have modelled the droop of both grids as an instantaneous gain—i.e. as a first order filter with zero time constant ($\tau_{11} = \tau_{21} = 0$). The parameter values for this test are gathered in Table 4.1.

Table 4.1: System and IC parameter values for the simplified simulation scenario.

Device	Parameter	Value [p.u.]
System 1 G_{11}	H_{11}	1
	D_{11}	10
	X_{s11}	0.1
	τ_{11}	0
System 2 G_{21}	H_{21}	1
	D_{21}	10
	X_{s21}	0.05917
	τ_{21}	0
IC - DIE	H_{V_1}	1
	H_{V_2}	1

In order to illustrate the operation concept of the proposed DIE technique we have carried out two tests. On the first one we have simulated both systems decoupled from each other, and on the second one we have repeated the same test by interconnecting them via a DIE-controlled IC. In both simulations, a 0.2 p.u. step-shaped load power has been introduced, first in System 1 (at $t = 1$s) and then in System 2 (at $t = 11$s). The DIE technique is tested using equal virtual inertia values ($H_{V_1} = H_{V_2} = 1$)

Figures 4.4 a) and b) show the frequency of each grid for both tests. When a power step occurs on any of the two grids, the RoCoF of the perturbed grid is improved thanks to the DIE-controlled IC. The IC improves this dynamic response by transferring power from the opposite grid. Therefore, the frequency of the opposite grid also suffers a small transient due to the load variation.

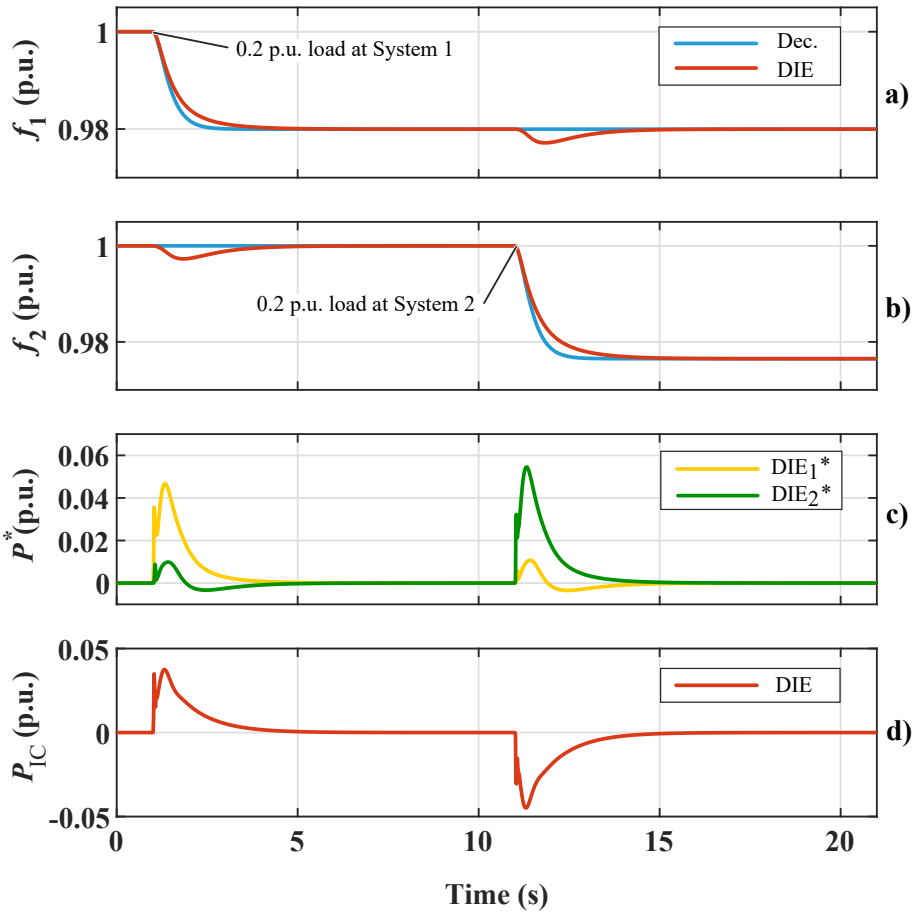

Figure 4.4: DIE operation concept test: a) Frequency of System 1, b) Frequency of System 2, c) Power references of the DIE control branches, and d) Power transferred by the IC

This can be also seen in Figure 4.4 c), where the power references for each grid on the DIE technique are illustrated. The transferred power by the IC, calculated from these two references, is shown in Figure 4.4 d). When the 0.2 p.u. load is introduced at System 1, power flows transiently from System 2 to System 1. Similarly, when power is demanded in System 2, power flows from System 1 to System 2 via the IC. Since both systems have equal inertia, we are emulating the same inertia at both sides of the IC (i.e. $H_{V_1} = H_{V_2}$) and the load perturbations have the same amplitude, the power transferred by the IC is very similar but with opposite sign for each load variation. The small differences are caused by the topologies employed at Systems 1 and 2.

4.3.3 DIE Test Cases

In this case we test the performance of the proposed control under more realistic conditions and compare it not only with other IC control approaches, but also with other grid-tying devices such as power transformers.

In order to consider the dynamic response of generators in the following simulations, we have applied a time delay to the droop controllers of the generators of both grids. Besides, we will analyse the DIE technique for the case in which the IC is tying one strong grid and a relatively weak grid. System 1 is a robust grid with high equivalent inertia and droop coefficients ($H_1 = 6$ and $D_1 = 30$), representing a classical power system. On the other hand, System 2 represents a weaker grid in terms of inertial and primary response (with $H_2 = 1$ and $D_2 = 10$), which could be the case of a power system with a higher penetration of renewable energy sources and electronic power converters. The DIE and DD technique parameters have been designed to support more the weaker System 2. We have defined the emulated inertia of the DIE as $H_{V_1} = 0.33$ and $H_{V_2} = 2$.

Table 4.2 summarises the rest of parameters that have been used to carry out the set of tests under this section.

Table 4.2: System and IC parameter values for the test cases.

Device	Variable	Value [p.u.]
System 1 G_{11},G_{12},G_{13}	H_{11},H_{12},H_{13}	2
	D_{11}, D_{12}, D_{13}	10
	X_{s11},X_{s12},X_{s13}	0.1
	$\tau_{11}, \tau_{12}, \tau_{13}$	0.5
System 2 G_{21}	H_{21}	1
	D_{21}	10
	X_{s21}	0.05917
	τ_{21}	0.5
IC - DIE	H_{V_1}	0.33
	H_{V_2}	2
IC - DD	D_{d_1}	3.33
	D_{d_2}	10

Case 1 – Decoupled grids vs tied grids with a DIE-controlled IC

Weak grids in terms of equivalent inertia are prone to oscillate when there is a sudden power perturbation in the grid. This is mainly caused by the time delays of the generators that are carrying out the primary regulation of the frequency. The purpose of this test is to show how, by interconnecting two grids with an IC controlled with the proposed technique, we are capable of transferring the inertial behaviour to damp the frequency oscillations caused by a power variation.

Figure 4.5 a) and b) illustrate the frequency response of System 1 and System 2, respectively. Since System 1 is strong and the inertia emulated at this grid with the DIE technique

is relatively small, there is no difference in the frequency when a load step is applied in that system (at $t = 1$s). This can be also observed in Figure 4.5 c), where it can be seen that the IC provides almost no power during this transient. This means that System 2, which is much weaker than System 1, is very slightly affected by a perturbation in System 1.

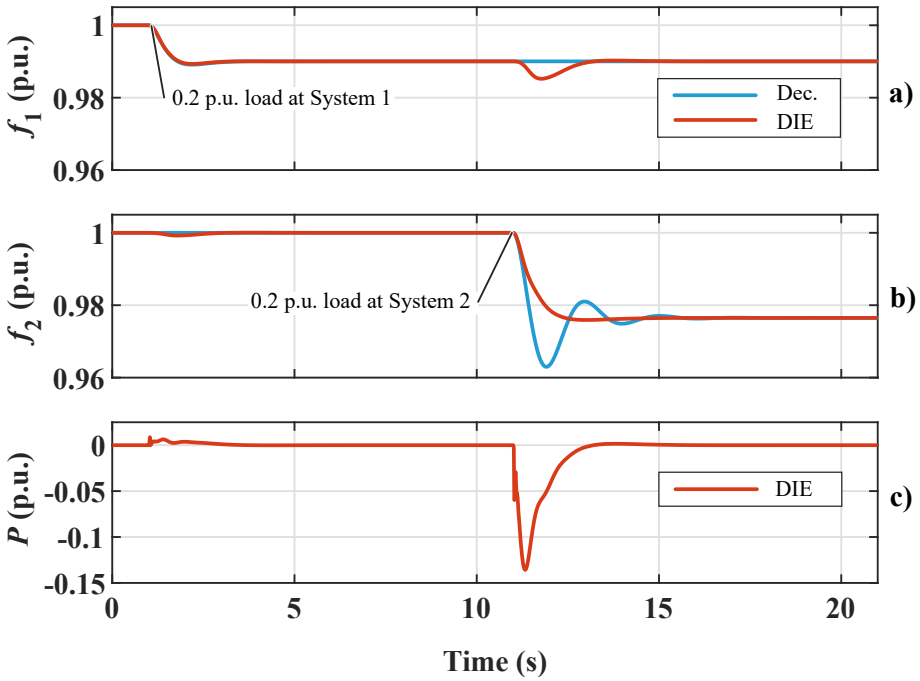

Figure 4.5: Case 1: a) Frequency of System 1, b) Frequency of System 2, and c) Power transferred by the DIE-controlled IC.

On the other hand, when there is a sudden power variation in System 2 (at $t = 11$s), the frequency response is significantly improved when the two systems are connected via the DIE-controlled IC. In this case, the IC transmits power transiently to decrease the RoCoF, to damp the frequency oscillation and to improve the frequency nadir. As explained in previous sections, this improvement is achieved by extracting power from System 1, which suffers a small frequency perturbation at that instant.

Case 2 – Tied Grids using DIE Technique vs Power Transformer

When a power transformer or a tie line is used to connect two power systems, all the devices participating in the regulation of the grid share the power perturbations occurring at any point of the system. This means that the droop coefficients and inertia are aggregated. The main drawback of these classical interconnections is that there is no control over the power that flows between the two systems, since it directly depends on the phase (voltage for dc) difference on the device terminals and its impedance. ICs are an interesting solution to increase the degrees of freedom of the system operator, since the power flow can be actively

controlled. Moreover, in this section we show that by controlling the IC with the proposed technique, we can damp the frequency oscillations after a sudden power variation.

The results of this test are illustrated in Figure 4.6. In these curves we can see how the inertia and droop values of both systems are aggregated for both cases (with the transformer and a DIE-controlled IC). When a power variation occurs at any of the grids, both systems respond to it, improving the RoCoF and the steady-state deviation compared to the decoupled scenario.

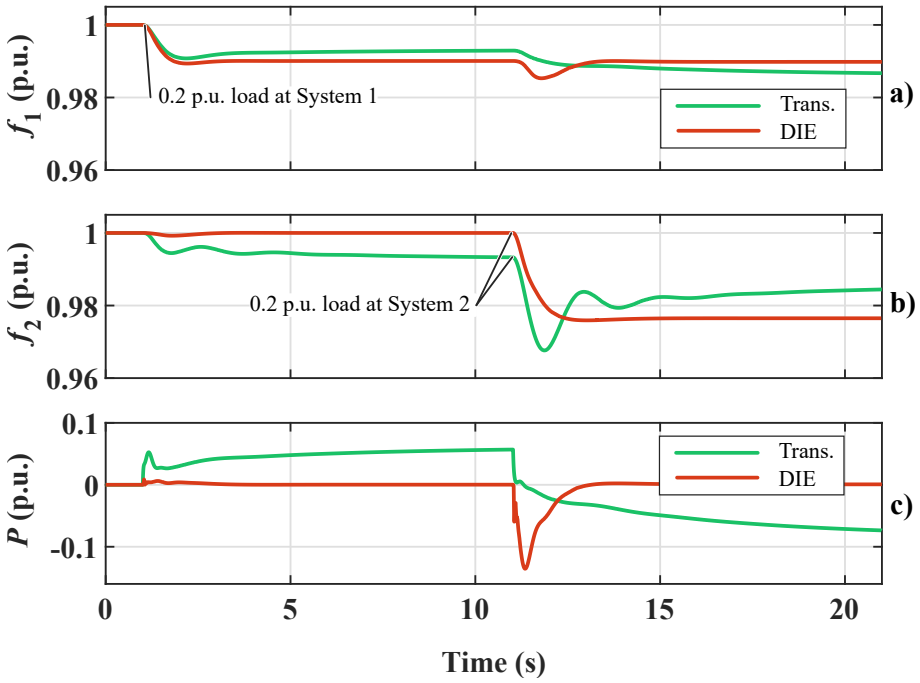

Figure 4.6: Case 2: a) Frequency of System 1, b) Frequency of System 2, and c) Power transferred by the interlinking device (transformer or DIE-controlled IC).

One of the main differences between interconnecting two systems with a transformer or a DIE-controlled IC is that the steady-state value of the frequency is not equal for the same power perturbation. This is because, in the first case, the frequency deviation is dependent on the droops of all grid-connected devices. As the transformer tightly couples both systems, their frequency deviations are equal in steady-state. However, when we replace the transformer by an IC, the frequency deviation of the system will be dependent on the droops of the devices connected to that system and the droop of the IC. Since in this case we are only observing the effect of the loop and the IC does not have any droop or primary controller, the steady-state frequency deviations are higher compared to the scenario in which the systems are connected through the transformer. The incorporation of a droop regulator is studied in the next section.

On the other hand, the transient response of the frequency is significantly improved thanks to the inertial response transmitted by the DIE-controlled IC. When the power perturbation occurs in System 2—which is weaker than System 1—we can clearly see how the frequency

oscillations are damped and the frequency nadir is improved. From this analysis we can conclude that, in addition to enabling the control of the power flow, ICs can be a potential solution to improve the sudden frequency variations occurring in the grid by tuning the virtual inertia terms (H_{V_1} and H_{V_2}) of the technique.

Case 3 – Tied Grids using dual inertia-emulation + dual droop (DIE-DD) Technique vs Power Transformer

The previous tests have shown the benefits of using a DIE-controlled IC over a power transformer in terms of damping, frequency nadir and oscillatory response. However, we could also see that from the point of view of primary regulation the proposed technique is not as effective as connecting the systems with a transformer.

As we have mentioned at the introduction, the proposed technique can be easily implemented along with a primary regulation control technique such as the ones reviewed in [11]. Therefore, in this test we repeat the simulations of the previous section but considering that the IC also includes a dual droop controller, in the configuration shown in Figure 4.1. Therefore, the IC will run two power controllers in parallel. While the loop will provide the power reference under a transient power perturbation, the steady-state power response will be determined by the DD loop. For this test we have maintained the parameter values related to the grid and the IC controller gathered in Table 4.2.

As in the previous test, when grids are tied using a power transformer, the frequencies of both grids (Figure 4.7 a) and b)) converge to the same value. However, when we incorporate the DD loop to the IC controller, we can see that the steady-state frequency deviations are reduced compared to the case in which we only have a loop. This reduction is more significant in the case of System 2, which is an expected outcome considering that we are trying to support more the weakest system. This phenomena can be clearly observed in Figure 4.7 c); when the power load step is introduced at $t = 1$ s, a small quantity of power is transferred by the IC, while at $t = 11$s a notable power spike is transferred to actively damp the frequency response at System 2.

At this point we should also highlight that, if opposite sign power disturbances occurred at both sides of the IC at the same time, the DIE-DD-controlled IC would support both systems at the same time by compensating the generation excess from one system with the demand of the other system.

Case 4 – DIE-DD vs DD Technique on a real test case

The last test consists of evaluating the proposed technique under a more realistic scenario in terms of the generated and consumed power. For that purpose we have integrated different renewable energy-based generation systems and loads at both grids, which are placed as shown

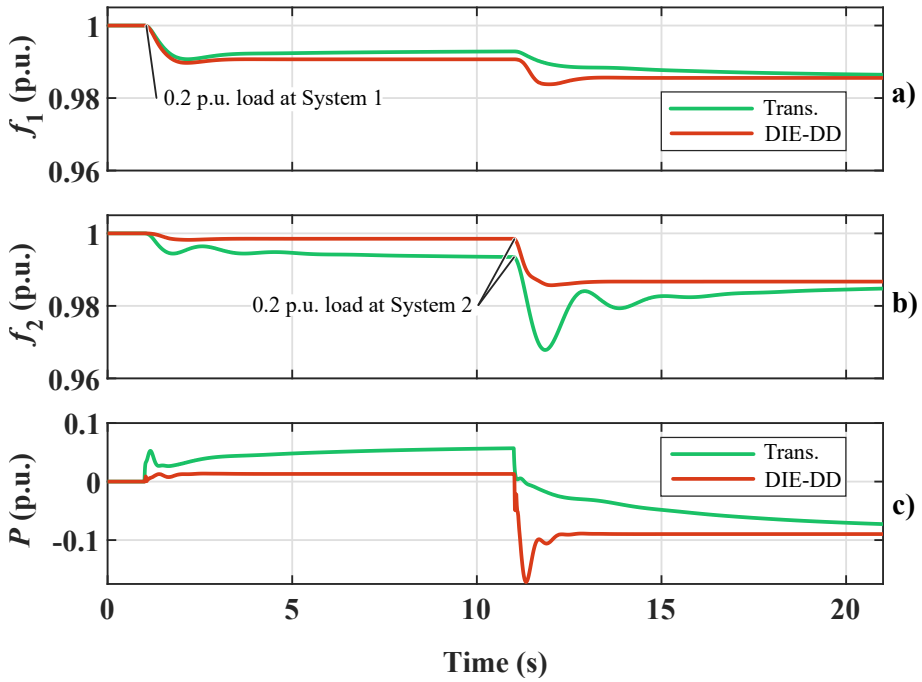

Figure 4.7: Case 3: a) Frequency of System 1, b) Frequency of System 2, and c) Power transferred by the interlinking device (transformer or DIE-DD-controlled IC).

in Figure 4.3. The 20 minute dynamic profiles of these elements can be observed in Figure 4.8. Moreover, since our purpose is to study the effect of the proposed loop, the comparison is based on a DD-controlled IC with and without that loop.

The controller values and grid conditions remain as shown in Table 4.2. Figure 4.8 a) and b) show the WP and PV generation profiles at System 2, while Figure 4.8 c) and d) show the aggregated loads applied at Systems 1 and 2, respectively. Lastly, Figure 4.8 e) and f) illustrate the evolution of grid frequencies of Systems 1 and 2 for the DD and DD-controlled IC cases.

From these results we can see that the frequency of System 1 is similar for both IC control approaches. This is because, as in test case 3, we have configured the loop to support more System 2, since it is weaker than System 1. The main difference in both controllers can be observed in Figure 4.8 f), where the evolution of the frequency is much smoother with the loop than without it. This illustration clearly shows how the frequency overshoot (and hence the nadir) are improved by employing the technique. As an example, if the the second zoom of Figure 4.8 f) is observed, the RoCoF is decreased from -1.077 Hz/s to -0.82 Hz/s and the frequency nadir level is improved a 64% when the technique is employed (being 100% the frequency gap on steady-state before and after the load variation). Moreover, the frequency oscillations of that grid are significantly damped, improving the frequency transient behaviour.

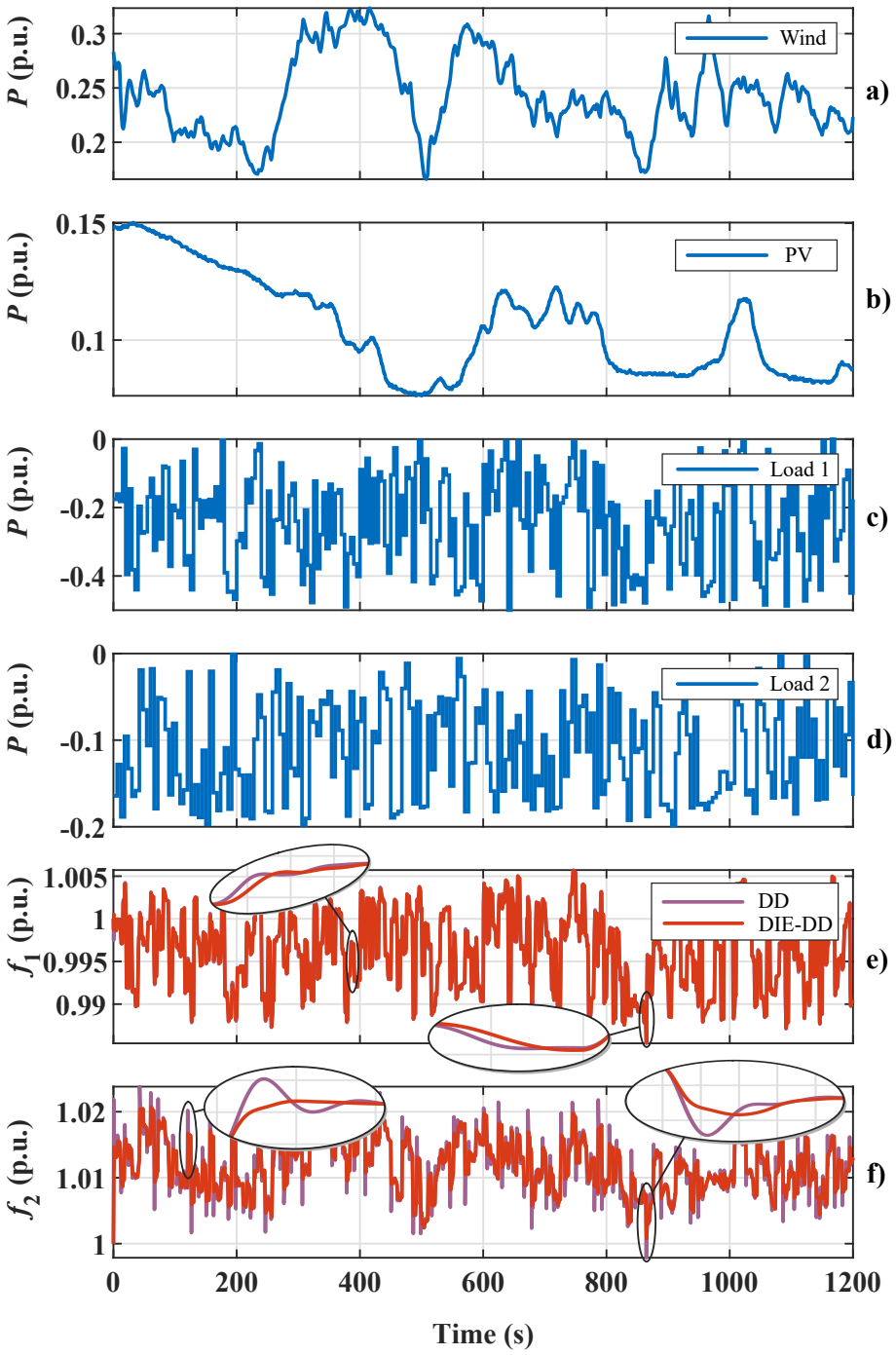

Figure 4.8: Test case 4: a) Wind Power generation at System 2, b) PV generation at System 2, c) Power load profile at system 1, d) Power load profile at System 2, e) Frequency of system 1, and f) Frequency of System 2.

4.4 Conclusion

The derivative-based DIE control strategy enables to provide inertial support to both interconnected grids without any communication network. In addition to improving the transient response of tied grids under power variations, the proposed technique enables to adjust the response of each side of the converter independently. The employed grid measurements in the DIE control are normalised using per unit variables, so it facilitates the interconnection of power systems with different current natures. Besides, it can be easily incorporated to other controllers such as primary regulation loops.

The simulation results have shown how, when a power variation occurs in one grid, the technique supports that grid by transferring power transiently from the grid on the other side. Therefore, we can say that this technique transfers the inertial response of the interconnected grids, so that all the devices participating in the regulation of the grids share the power variations occurring at any part of the system. Although the transient stability of the proposed technique has not been directly analysed, simulation results have shown that it is improved by employing the technique. Besides, the improvement of the RoCoF, frequency nadir and oscillation damping has been demonstrated by means of a simplified scenario and a more realistic scenario with time-varying generation systems and loads, where one grid was stronger than the other in terms of inertia and primary reserve.

Chapter 5

Virtual Power Line Control for Interlinking Converters on AC, DC and Hybrid Grid Links

In this chapter we propose the so-called virtual power line (VPL) control for ICs, whose purpose is to couple the dynamics of different and incompatible electric systems analogously to a classical transmission line with the aim of achieveing a more robust and reliable power system. The VPL control employs local measurements and it does not require any communication link to operate.

We propose two VPL control variants: the dual grid-supporting VPL control and the single grid-forming VPL control. Both support the frequency and/or voltage of the interconnected grids under power perturbations, and the latter provides grid-forming capabilities for one of the interconnected systems. This feature avoids the necessity for additional grid-forming devices at this grid. The performance of the proposed VPL control is tested and compared at four different power system scenarios, and the results demonstrate how transient and steady-state responses are improved while the power flow happens through ICs from generation to consumption grids as if all devices were part of the same electric system.

5.1 Introduction

In our view, the most relevant advantage of traditional power system tying methods is that they couple the interconnected grids in terms of inertial (transient) and primary (steady-state) responses. This means that under load and generation variations, all the grid-connected generators respond to keep the voltage and frequency stable. Besides, a very meshed grid provides more paths for the power to flow, significantly increasing the power transmission capability and the reliability of the system. In other words, when a power line is employed, it implies the extension of the grid to another area setting the voltage and/or frequency at the interconnection point. If we analyse this aspect from the point of view of grid-connected converter control (see section 3.1.3), we can say that a power line works as a grid-forming unit for the new area, where no other grid-forming unit is mandatory to operate the grid.

Among the IC controls already proposed in the literature, to the best of the authors' knowledge none of the existing techniques replicate the behaviour of a power transmission line and extend it to hybrid ac/dc, non-synchronised ac, or dc interconnections of different voltage levels. As we have reviewed in 3.2.2, there have already been proposed *dual grid-supporting* control techniques that are able to equalise the interconnected grids by using PI or other type of controllers, but many aspects need to be covered to replicate and extend this control concept to other types of interconnections. For instance, the reviewed techniques do not offer grid-forming capabilities and they mainly appear focused on specific microgrid interconnections, lacking a generalised IC control approach to be employed at any type of interconnection. In what regards to the provided results, they are mainly focused on the power sharing feature and other aspects such as the synchronisation/coupling of the interconnected grids, the improvement of the transient response, the control performance under system failure or grid scenarios apart from microgrid interconnections are not covered.

In this chapter, we present a new control strategy for ICs named *virtual power line* (VPL) control, which takes advantage of the features offered by a traditional power line. This means that the inertial as well as the primary response of the interconnected grids are coupled. The control concept can be employed not only to interconnect synchronised grids, but also to interconnect non-synchronised ac grids and grids with different voltage levels (either ac or dc). We propose two variants of the VPL control in this paper. On the one hand, the *dual grid-supporting* VPL (DGS-VPL) technique is oriented to the interconnection of grids which are already in place, with the aim of supporting them as an equivalent power line would do. On the other hand, the *single grid-forming* VPL (SGF-VPL) control offers the ability to form new power systems from existing ones while supporting both interconnected systems. This feature increments the systems' reliability, makes the islanding or black start operation possible, and might help in the investment reduction/deferral on new grid-forming units. The VPL control does not require any communication or coordination with other grid agents for its operation,

and its application range goes from high-power transmission-level links to microgrid links, as we demonstrate in the upcoming sections.

5.2 Virtual Power Line Control

The principle of operation of the proposed VPL control is inspired by the advantages offered by traditional grid-tying devices such as transmission lines or transformers (Figure 5.1). These include the coupling of the inertial and the primary regulation response of the interconnected systems, so that all devices participating in the grid regulation respond under power perturbations at any location in the system.

In this section we first revise the operation principle of an inductive transmission line for ac-ac and dc-dc connections. Based on a generalisation of this power transmission, we describe the proposed VPL control approaches. Taking advantage of the control flexibility offered by ICs, we extend this concept to other connections beyond typical ac-ac and dc-dc system interconnections.

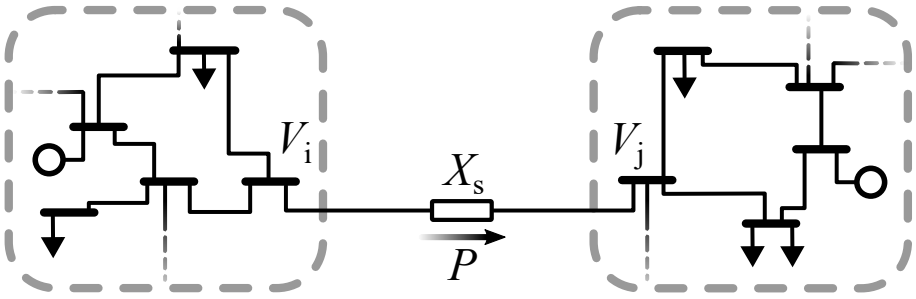

Figure 5.1: Two power systems tied by a power transmission line.

5.2.1 Power Line Tying Two AC Systems

If the power systems depicted in Figure 5.1 were ac, then the voltage at a node (V) would represent the magnitude and angle of this voltage ($V\angle\theta$). If the two grids are interconnected at nodes i and j, the active power flowing through the line can be obtained as follows:

$$P_\mathrm{ac} = \frac{V_\mathrm{i} V_\mathrm{j}}{X_\mathrm{s}} \sin \underbrace{\left(\theta_\mathrm{i} - \theta_\mathrm{j}\right)}_{\delta} \tag{5.1}$$

where X_s is the impedance of the line, and V_i, V_j and θ_i and θ_j represent the voltage amplitudes and angles of the nodes i and j, respectively.

If we consider that the angle difference δ between V_i and V_j is very small, we can assume

that $\sin(\delta) \approx \delta$, hence $\sin\left(\theta_{\mathrm{i}} - \theta_{\mathrm{j}}\right) \approx \theta_{\mathrm{i}} - \theta_{\mathrm{j}}$, and (5.1) can be simplified as follows:

$$P_{\mathrm{ac}} \approx \frac{V_{\mathrm{i}} V_{\mathrm{j}}}{X_s} \int \left(\omega_{\mathrm{i}} - \omega_{\mathrm{j}}\right) dt \tag{5.2}$$

Assuming that the voltage amplitude of the nodes is relatively constant, the transferred active power depends mainly on the angle difference $\theta_{\mathrm{i}} - \theta_{\mathrm{j}}$, which is obtained by integrating the frequency difference between the two nodes (i.e., $\omega_{\mathrm{i}} - \omega_{\mathrm{j}}$).

When two power systems are tied using an inductive line, their frequency in steady-state will be the same and the voltages at the interconnection terminals will be almost the same, considering that the voltage drop at the line will be relatively small. Thanks to the interconnection, when a power perturbation occurs at any of the two grids, all the generators will take part in the power response, increasing the system's robustness and primary reserve compared to the decoupled grid scenario.

5.2.2 Power Line Tying Two DC Systems

If the interconnected systems in Figure 5.1 were two dc systems, the node voltages V_{i} and V_{j} would correspond to dc voltage amplitudes. In such cases, the active power transfer from node i to node j depends on the voltage difference at their terminals and the inductive value of the line (to simplify the analysis, the initial current through the line is not considered):

$$P_{\mathrm{dc}} = \frac{V_{\mathrm{i}}}{L_{\mathrm{s}}} \int \left(V_{\mathrm{i}} - V_{\mathrm{j}}\right) dt \tag{5.3}$$

Thus, when there is a voltage difference in the terminals of the interconnection line, the active power will increase or decrease, and when V_{i} and V_{j} are equalised the active power will converge to a constant value.

5.2.3 Virtual Power Line Control for ICs

In this section we describe the control principles of the proposed two VPL control variants for ICs, which will emulate the behaviour of classical transmission lines while enabling the interconnection of any type of grid regardless of its nature or voltage level. It must be noted that in this study the lower-level control loops are not considered, since they will be different depending on aspects such as the IC topology, the nature of the interconnected systems or the voltage limitations.

From (5.2) and (5.3) it can be deducted that the active power transfer through an inductive line is directly related to the frequency in ac power systems and to the voltage in dc ones. Based on this premise, an equivalence can be formulated to control devices connected to dc grids analogously to the ones connected to ac grids, as explained in 3.1.4. The VPL control

concept is a generalisation of this equivalence for the interconnection of any type of grid (ac or dc, different frequency or voltage levels, etc.).

The first step is to convert ac frequencies and dc voltages to their corresponding per-unit values (see 3.1.4). These variables are henceforth referred as x_{i} and x_{j}, where x represents frequency in ac grids and voltage in dc ones. Assuming that voltage amplitudes are close to 1 p.u. either in ac or dc grids, the equation that describes the power transfer through a *virtual power line* interconnecting nodes i and j can be formulated as:

$$P^{*}_{\mathrm{VPL}} = \frac{1}{Z_{\mathrm{VPL}}} \underbrace{\int \left(x_{\mathrm{i}} - x_{\mathrm{j}}\right) dt}_{\delta_{\mathrm{v}}} \tag{5.4}$$

where Z_{VPL} is the virtual impedance parameter of the VPL.

When two power systems with same characteristics are tied using a classical power line, they are inherently synchronised. However, this synchronisation cannot be naturally achieved when the interconnected power systems present different characteristics and thus, the VPL control works on a virtual synchronous reference frame. This frame is established when the VPL control is initialised. x_{i} and x_{j} per unit variables are considered as the equivalent rotating frequencies or equivalent dc voltages of the interconnected power system nodes, as equation (5.4) describes from the equivalence with (5.2) and (5.3).

Based on (5.4), two different VPL control approaches are proposed hereafter.

5.2.4 Dual Grid-Supporting VPL Control (DGS-VPL)

The proposed DGS-VPL control loop and its conceptual implementation in a IC are depicted in Figure 5.2. The DGS-VPL control loop directly implements equation (5.4) to obtain the power reference P^{*}_{VPL}. Then a CRC and an inner CC are implemented to regulate the power to be transferred from one grid to the other. Hence, we can apply the DGS-VPL control loop to carry out ac-ac, dc-dc or hybrid interconnections. Since this technique is not able to fix the voltage (grid) at none of its terminals, but supports both sides of the IC we can consider it as a DGS IC control according to the classification provided in 3.2.

In case of that one or both interconnected grids are ac, the voltage amplitude can be fixed to a certain value, or voltage and/or reactive power support control strategies similar to the ones studied in [103–106] can be implemented in parallel to the VPL control, although they are not covered in this manuscript.

All in all, the DGS-VPL control generates an active power reference to virtually synchronise the interconnected power systems. This means that the controlled variables (frequency in ac and voltage in dc systems) will converge to the same per-unit values, as we demonstrate it in Section 5.3. Moreover, since a power reference is calculated, the DGS-VPL technique can be

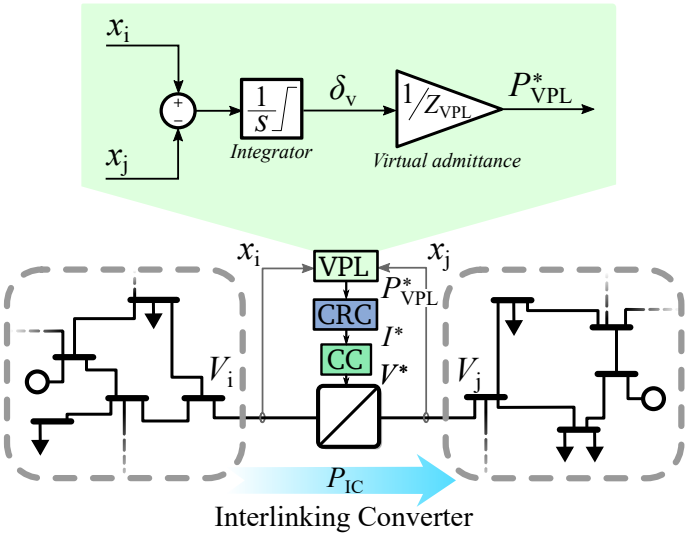

Figure 5.2: Representation example of a IC with the DGS-VPL control tying two power systems.

easily implemented without modifying the inner control loops of the IC. This is an advantage when the inner control is not accessible to the user, or when the converter manufacturer prefers not to modify that inner control structure.

5.2.5 Single Grid-Forming-VPL Control (SGF-VPL)

With the SGF-VPL strategy, in addition to supporting the interconnected power systems as with the DGS-VPL, the IC is controlled as a grid-forming device at one of its sides (hence, it has been categorised as a *single grid forming & dual grid-supporting control in section* 3.2.5). Depending on whether the formed grid is dc or ac, the implementation of the SGF-VPL is slightly different, as explained hereafter.

DC SGF-VPL Control

This VPL control variant is able to generate a dc grid at the terminals of the IC from a existing grid. If (5.4) is taken as reference, x_i corresponds to the p.u. value of the grid that is already set by other devices, and x_j corresponds to the p.u. value of the system created by the DC SGF-VPL control. Thus, if the value of x_j is isolated in (5.4) we obtain that:

$$x_j \approx x_i - \frac{d}{dt}(P_{IC} Z_{VPl}) \tag{5.5}$$

It must be noted that the measured IC power (P_{IC}) is here considered as positive when the active power flows from node i to j.

The detailed control scheme that incorporates equation 5.5 to form dc systems from a existing grid (either ac or dc) is shown in Figure 5.3 a). The voltage drop across the VPL

impedance is calculated by deriving the measured IC power (P_{IC}) and the virtual impedance (Z_{VPL}) value. Then, this value is subtracted to the p.u. value of the existing grid (x_i) and we obtain the p.u. reference for the newly formed dc grid x_j. In last place, we multiply the dc base value of the new grid to obtain the dc voltage reference value, which will be fed to the inner IC voltage control loops.

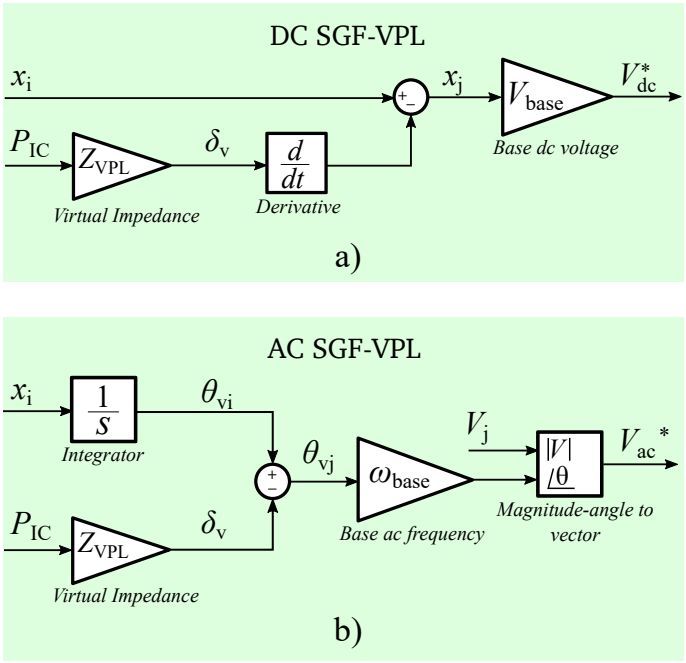

Figure 5.3: Detailed SGF-VPL control scheme a) to form dc grids and b) to form ac grids.

With the DC SGF-VPL control, the obtained voltage response and IC power transfer will be the same as the one that is obtained when two grids are tied by a power line. When there is no power demand in any of the grids, the p.u. value of x_i will be equal to x_j. However, when there is a power flow through the IC, x_i and x_j will evolve according to the value of Z_{VPL}.

AC SGF-VPL Control

Since the SGF-VPL control is equivalent for creating ac and dc systems, the structure from Figure 5.3 a) can be employed to obtain the reference frequency for an ac system. In such case, instead of using the base dc voltage, the base ac frequency should be employed in the last gain block. We would like to denote that if we want to be grid-forming for an ac grid, the IC will require the instantaneous reference angle position of the voltage vector and thus, a continuous integrator must be added as well to the final stage in Figure 5.3 a).

However, taking into consideration practical implementation aspects and with the aim of avoiding derivatives in control loops, we have considered to reformulate equation (5.4) as

follows:

$$\int x_{\mathrm{j}}\, dt = \int x_{\mathrm{i}}\, dt - (P_{\mathrm{IC}} Z_{\mathrm{VPl}}) \tag{5.6}$$

In this case, x_{j} corresponds to the p.u. frequency of the newly formed ac system. We keep the integral in the equation because the grid-forming control requires the instantaneous angle position of the ac voltage, which is obtained by integrating x_{i} and x_{j}. The virtual p.u. angles corresponding to these variables can be defined as follows:

$$\theta_{\mathrm{vi}} = \int x_{\mathrm{i}}\, dt$$

$$\theta_{\mathrm{vj}} = \int x_{\mathrm{j}}\, dt$$

Hence, we can reformulate (5.6) as:

$$\theta_{\mathrm{vj}} = \theta_{\mathrm{vi}} - (P_{\mathrm{IC}} Z_{\mathrm{VPl}}) \tag{5.7}$$

Figure 5.3 b) shows the implementation of the AC SGF-VPL controller. In order to obtain the absolute value of the angle, in the last step we multiply θ_{vj} by the base frequency of the ac system.

The voltage amplitude and the reactive power control at the AC SGF-VPL approach can be defined by classical voltage or reactive power control schemes and since we consider that these strategies are already addressed in the literature they are not contemplated in the actual study.

5.3 Performance of the VPL control

The aim of this section is to show the operation and assess the performance of the proposed VPL control variants under different power system scenarios. Taking into account that the VPL concept couples the interconnected grids, in the upcoming sections we study aspects like the transient and steady-state frequency response or the amount of transferred active power.

We describe the specific simulation scenarios for testing the proposed VPL controls in each case, and the tests have been carried out employing the DFPF tool presented in Chapter 2.

5.3.1 Test I: DGS-VPL on a Hybrid AC/DC Grid Link

In order to show the operation principle of the DGS-VPL control, we have set up a hybrid ac/dc simulation scenario where the ac grid corresponds to a 14 node IEEE system inspired by [149] and the dc one to a 9 node WSCC grid based on [34]. For the sake of simplicity, in

this test only one generator has been considered at each grid. At the ac grid, a simplified SG model has been employed, which includes the swing-equation, the governor with a classical primary regulator and the active voltage regulator as in 2.3.2. On the other hand, at the dc grid a virtual capacitor control has been implemented in the low-level control of a grid-forming converter as explained in [46]. The primary regulator is equal for both generator models, and is comprised of a droop control with a first order low-pass filter. The aim of this test is not to represent in detail the interconnected grids and their generators, but rather to illustrate the principles of operation of the proposed DGS-VPL control from Figure 5.2.

The parameters of the generators of the interconnected grids are shown in Table 5.1. The most relevant parameters for this test are the inertia of generators (H), the droop gain of the primary regulators (D), the time constants of the primary regulators' delay (τ), and the VPL impedance Z_{VPL}.

Table 5.1: System and IC parameter values for the simplified hybrid simulation scenario.

Device	Parameter	Value [p.u.]
System 1 G_1	H_1	3
	D_1	30
	τ_1	0.4
System 2 G_2	H_2	3
	D_2	30
	τ_2	0.4
IC - VPL	Z_{VPL}	0.01

Figure 5.4 a) shows the p.u. frequency at grid 1 and the voltage at grid 2 for a 0.5 p.u. active power load step applied at $t = 0.5$s on the ac system and at $t = 10.5$s on the dc system (see Figure 5.4 c)). Thanks to the interconnection through the DGS-VPL-controlled IC, the frequency and voltage of the interconnected grids converge to the same value in steady-state. Figure 5.4 b) shows how the virtual delta angle δ_{v} varies its value when active power load steps are applied in both systems, causing an active power transfer between the interconnected grids, proportional to the inverse of the Z_{VPL} value.

With the aim of studying more in depth the effect of the value of Z_{VPL} in the response of the interconnected systems, in Figure 5.4 d) and we show the frequency and voltage response of the generators from systems 1 and 2 at the previously stated loading conditions but for values of Z_{VPL} ranging from 0.1 and decreasing it to 0.002. The results show how, the lower the value of Z_{VPL} is, the more coupled are the interconnected systems. This entails a lower frequency and voltage nadir and a reduction in the RoCoF and RoCoV in the power system where the load variation has occurred. When higher Z_{VPL} values are employed at the VPL control, although the power system that has suffered the load variation presents a higher RoCoF/RoCoV and

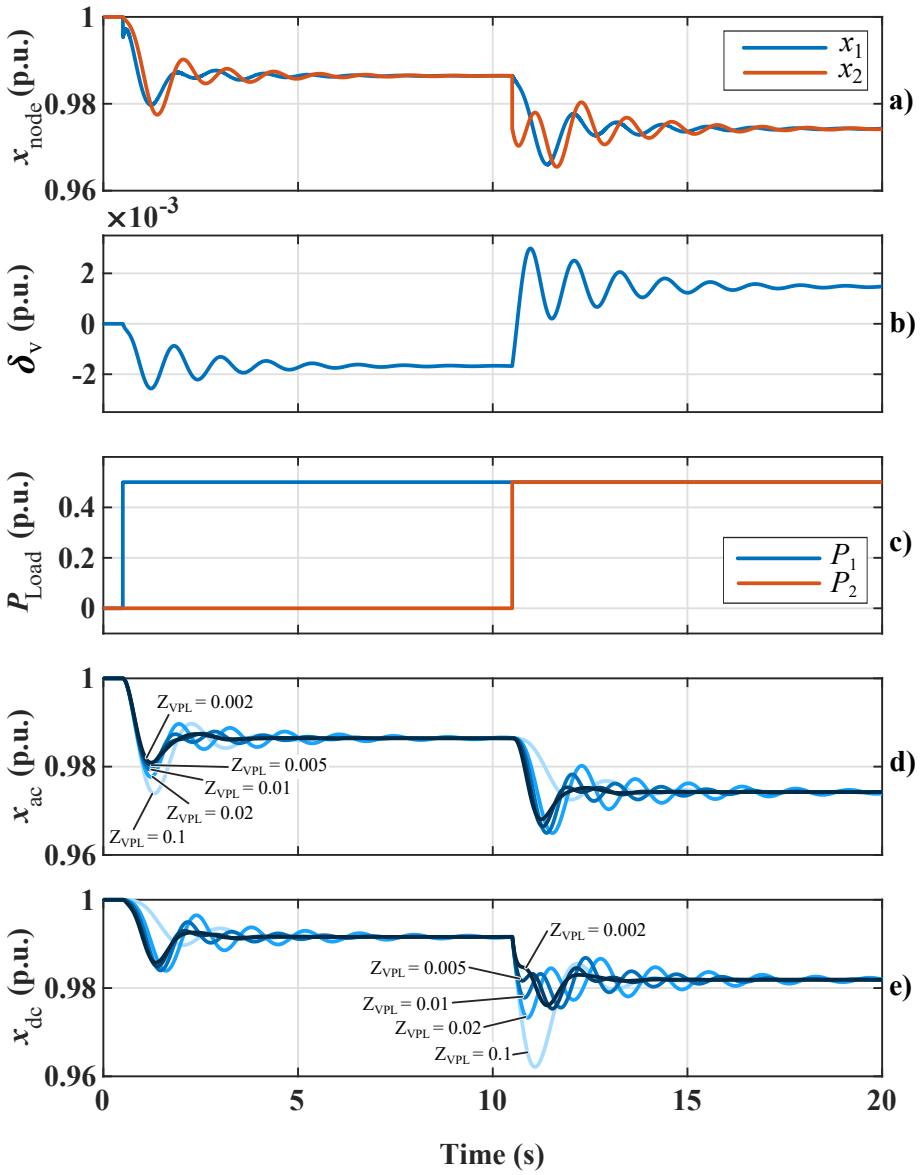

Figure 5.4: VPL operation concept test: a) frequency of System 1 and voltage of system 2 (both in p.u.) b) virtual angle δ_v c) active power profiles at system 1 and 2, d) frequency of the slack node at system 1 for different Z_{VPL} parameters and e) voltage of the slack node at system 2 for different Z_{VPL}

nadir, the contrary grid does not suffer the variation in the same level due to the weaker coupling. In short, when the DGS-VPL control is deployed at an IC, the inertial response and the prime movers' response of the interconnected systems are coupled, and hence all devices participating in the regulation of the system will respond under power perturbations occurring at any location. Another relevant outcome of the tests is that although the point of operation in steady-state will be the same for any Z_{VPL} value, the transient response will vary in each case; lower Z_{VPL} values will entail a stronger grid coupling and hence a bigger transient support

under load variations.

5.3.2 Test II: DGS-VPL vs existing IC control strategies

The aim of this section is to compare the proposed DGS-VPL technique with already existing IC control approaches. Since the proposed DGS-VPL control couples the inertial and the primary responses of the interconnected grids, we compare it to a control strategy that offers similar functionalities. One of the most common IC control strategies that contributes to the primary response of interconnected grids is the DD control [11]. As explained in 4.3.3, the DD control can be combined with the so-called dual inertia-emulation (DIE) technique, so that the IC also participates in the regulation of the transient response of the interconnected grids. In the following tests we will employ the DIE-DD technique as the benchmark for the comparison with the proposed DGS-VPL control.

The test scenario is the same as in the previous section, and the parameters employed in the simulation are gathered in Table 5.2.

Table 5.2: System and IC parameter values for IC control comparison.

Device	Variable	Value [p.u.]
IC - DIE	H_{V_1}	2
	H_{V_2}	2
IC - DD	D_{d_1}	10
	D_{d_2}	10
IC - VPL	Z_{VPL}	0.002

The results of the test are shown in Figure 5.5 for the same load profiles as in the previous case (refer to Figure 5.4 c)). In Figure 5.5 a) we can observe the frequency and voltage amplitude at the interconnection nodes of the ac and dc grid, respectively. In the case of the DGS-VPL, the ac frequency and dc voltage (x_1 and x_2) converge to the same point very quickly due to the relatively low Z_{VPL} value. This means that the interconnected grids will be strongly coupled, and hence the transient response will be benefited from the support of all the devices participating in the regulation of the grid. In the case of the DIE-DD control, the point of operation of each grid in steady-state depends on the D_d droop parameters, and the transient response of each grid is dependent on the virtual inertia constants (H_V) of the DIE algorithm.

Figure 5.5 b) illustrates the active power through the IC. As it can be observed, the power response in the DGS-VPL control is higher both during transients and in steady-state, which is in accordance with the stronger coupling observed in the frequency and voltage waveforms.

In addition to its simplicity, the results demonstrate that one of the main advantages offered by the DGS-VPL control is that the interconnected grids will be inherently coupled. The active power will flow naturally from areas that have more generation to the ones that present

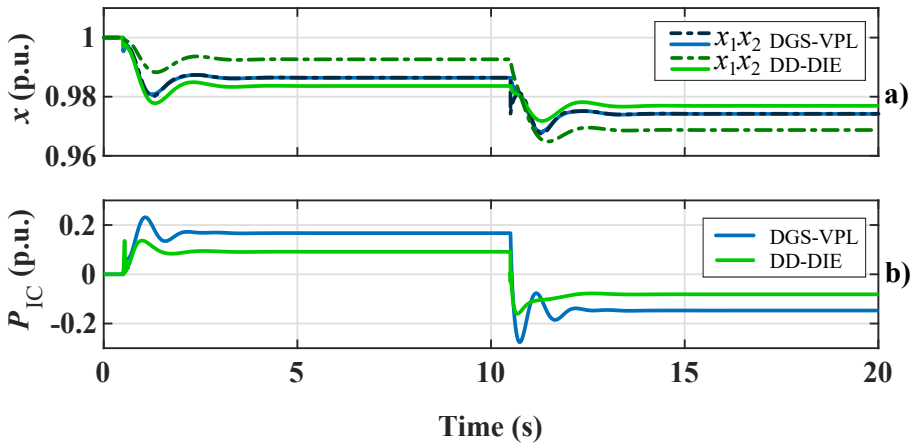

Figure 5.5: VPL operation compared to DIE-DD IC control: a) frequency of Systems 1 and 2 for both IC control approaches b) active power transfer for each control strategy.

a higher power demand, without the need of any external communication or coordination algorithm.

5.3.3 Test III: SGF-VPL control operation

In the previous tests we have compared the grid-supporting variant of the proposed VPL control with a DD-DIE technique. These controllers react under frequency and voltage perturbations, but are not capable of forming a grid by themselves as explained in Section 5.2.5. However, modern converter-dominated power system scenarios require a minimum amount of grid-forming devices to set the system voltage and frequency and ensure a stable operation. Let's consider for instance the offshore ac power system from Figure 5.6, which transmits the generated power through a dc link. In such scenarios, the WP park will require at least one grid-forming unit for its adequate operation. However, wind generators usually operate as grid-following units to extract as much power as possible from the wind. Therefore, at least one of the WP generators, the IC or an external ESS must operate as the grid-forming unit to set the system's ac voltage and frequency. Most of the times, the ESS is the responsible for this task because it can provide or absorb active power from the grid.

Using the scenario in Figure 5.6 as an example, this test aims to show the advantages of the SGF-VPL control over other dual grid-supporting control techniques when the main grid-forming unit fails, which in this case corresponds to an ESS interfaced by a power converter. We simulate the disconnection of this device in two cases: with the IC controlled as a DGS-VPL, and as a SGF-VPL. The employed Z_{VPL} parameter for both tests is the same ($Z_{\text{VPL}} = 0.01$).

Previous to the failure of the main grid-forming unit, the power system operates in stable voltage and frequency conditions, and the grid-forming ESS is being charged by the power generated by the WP turbines. Figure 5.7 a) shows that when the grid-forming unit fails—i.e.

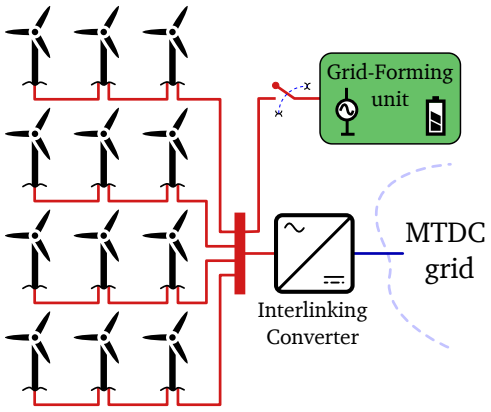

Figure 5.6: AC wind power plant topology example with ac/dc IC link.

suddenly disconnects—at $t = 0.5s$, the DGS-VPL control of the IC is not able to maintain the frequency of the WP system, leading to a system instability caused by the lack of other grid-forming unit in the system. On the contrary, if the SGF-VPL control is deployed at the IC, in Figure 5.7 b) we can see how for the same test conditions the power system does not become unstable because the IC is able to set the system's frequency.

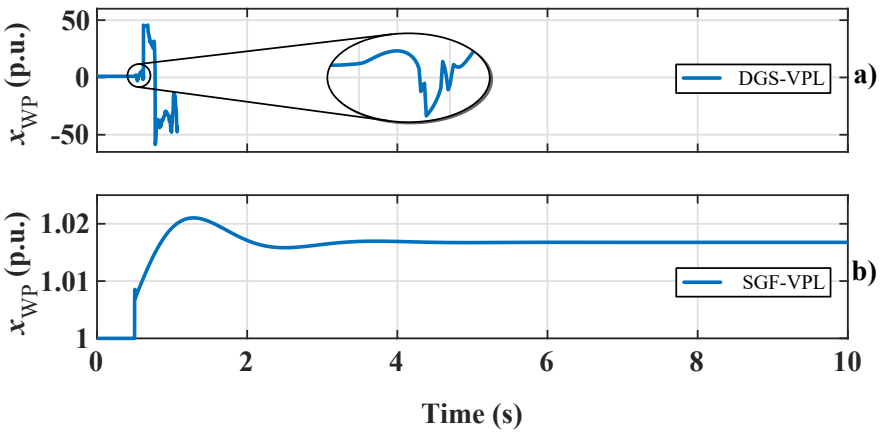

Figure 5.7: Disconnection of the main grid-forming unit from the WP plant with a) DGS-VPL control and b) SGF-VPL control.

These results demonstrate that the proposed SGF-VPL control will be useful to improve the reliability of converter-dominated power systems, since the IC will be able operate as a grid-forming unit at one of its sides. This will help to reduce the number of grid-forming units required in the grid, and can be useful to avoid new infrastructure investments e.g. for the installation of ESSs. Besides, this control will facilitate the black-start of the system, and it will decrease the chances of a possible blackout if the rest of the grid-forming units connected to the system fail.

5.3.4 Test IV: SGF-VPL ICs Forming AC and DC grids in a Multi-Grid System

In this test we show that in addition to the grid-forming capability, the properties of the SGF-VPL control are of high interest for the interconnection of various power systems or different parts of a grid. For that purpose, we have set up a multi-grid power system scenario like the one shown in Figure 5.8, where four ac power systems are tied through a MTDC grid. The main two ac power systems correspond to a 32 bus Nordic grid proposed by CIGRÉ task force 32.02.08 in [36], and a Continental European high-voltage transmission network proposed by the CIGRÉ Task Force C6.04.02 in [37]. Each grid model includes a synchronous generator-based power generation unit to represent the aggregated dynamic response of the grid as in Test III. Besides, two WP ac grids are included, which consist of simplified 5 bus systems as represented in Figure 5.6. In this case, instead of using a dedicated ESS-based grid-forming device, the IC controlled with a SGF-VPL control is responsible for setting the WP ac grid as shown in Figure 5.8. Similarly, the MTDC grid is formed with the ICs by employing the dc variant of the SGF-VPL control. The employed Z_{VPL} parameter is equal for all the SGF-VPL-controlled ICs, with a value of $Z_{\text{VPL}} = 0.01$.

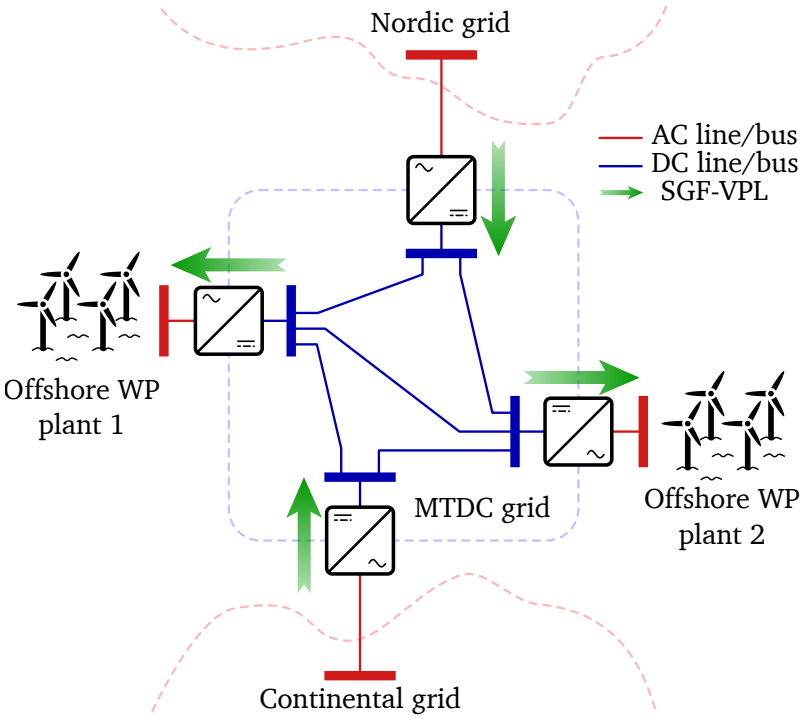

Figure 5.8: Simplified diagram of the hybrid ac/dc benchmark scenario with representation of grid-forming ICs implementing the SGF-VPL.

In Figs. 5.9 a)–d) we can observe the evolution of the frequency of the WP systems, the voltage of the MTDC system and the frequencies of the Nordic and Continental power systems when the aggregated WP generation and load profiles (represented in Figs. 5.9 e) and f) are

applied at the different power systems.

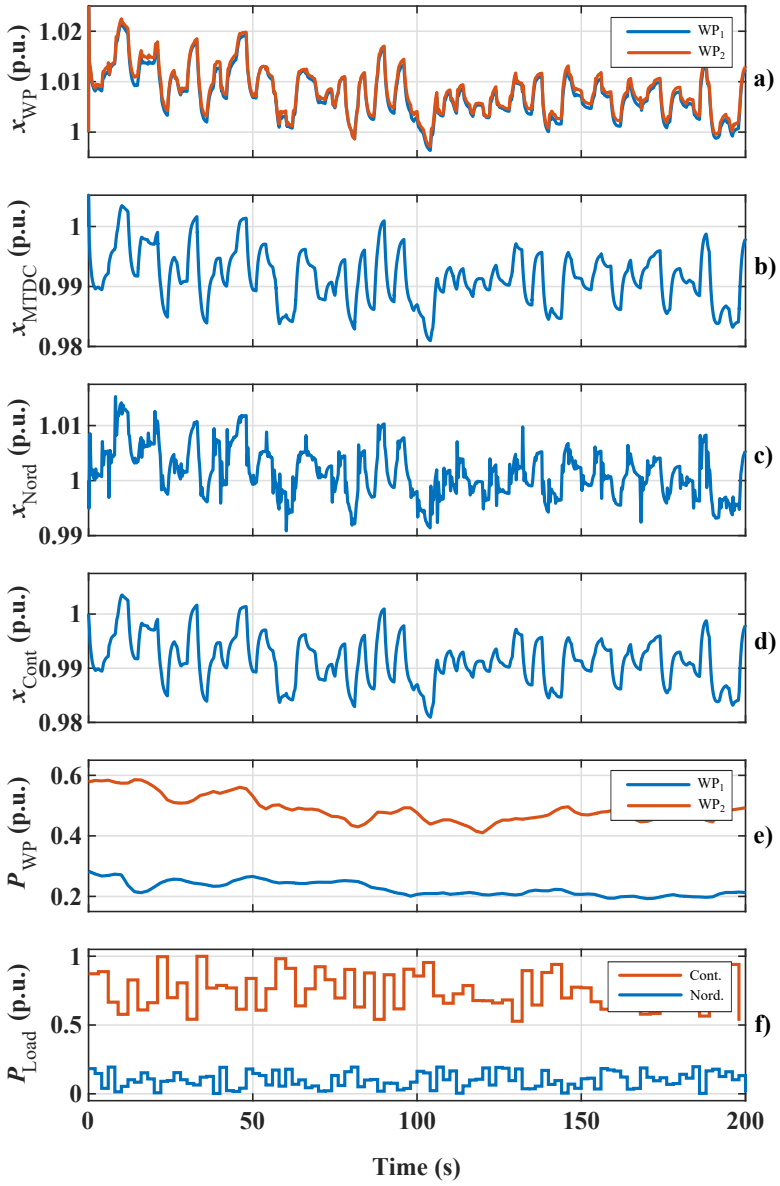

Figure 5.9: a) Frequency of the WP ac systems, b) voltage of the MTDC grid, c) Frequency of the Nordic grid, d) Frequency of the Continental grid, e) Aggregated active power generation of the WP plants, f) Aggregated active power loading of Nordic and Continental systems.

With the aim of coupling all the grids, we control the ICs with their corresponding SGF-VPL technique as illustrated in Fig 5.8. This coupling can be corroborated by looking at the grids' frequencies and voltages. Some differences can be appreciated in the p.u. values of the different grids, which are caused by the voltage drops in the dc system lines. However, all the waveforms present a very similar dynamic behaviour thanks to the coupling provided by the ICs. By looking at Figs. 5.9 c) and d) we can see how the Nordic system is more susceptible

to load variations compared to the Continental system. This happens because the total inertia connected to the Nordic grid is ten times lower than the Continental one.

Figure 5.10 represents the active power transferred by the SGF-VPL controlled ICs in the previous scenario. The ICs that set the voltage and frequency at the WP systems transfer all the active power generation to the MTDC grid as shown in Fig 5.10 a). In contrast, the ICs that are in charge of forming the MTDC system not only transfer the power generated by the WP plants, but they also support the Continental and Nordic grids by supplying active power under sudden load perturbations (Figures 5.10b) and c)).

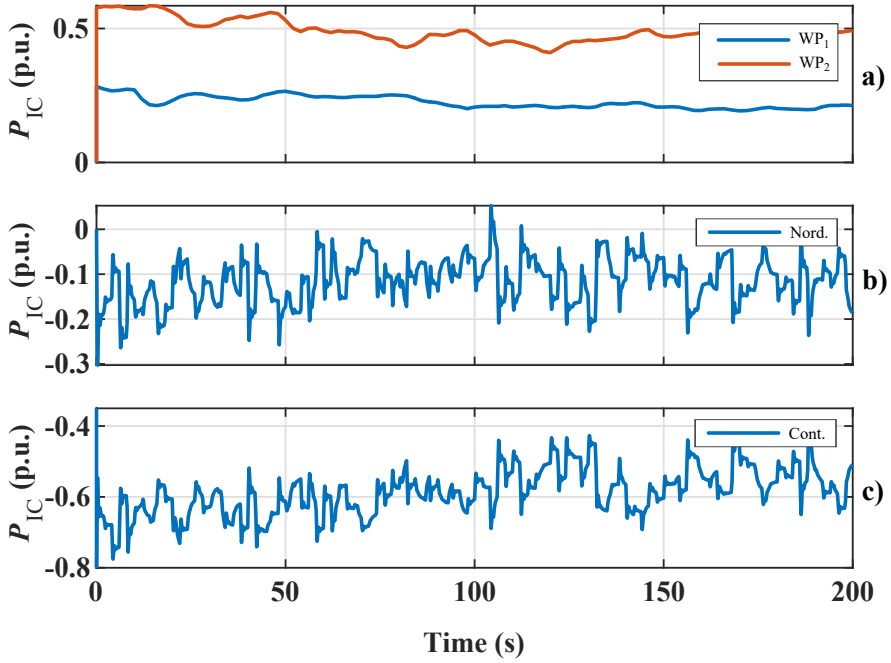

Figure 5.10: SGF-VPL controlled IC power of a) WP-MTDC links, b) Nordic-MTDC link and c) Continental-MTDC link.

The obtained results demonstrate how the VPL control supports the interconnected systems during transients as well as steady-state operation analogously to a classical transmission line. Therefore, when subgrids are tied using VPL-controlled ICs, they can be considered an extension of the same grid. In this sense, the active power flow through ICs will naturally happen from areas with an excess of generation to the parts of the grid with an excess of demand, without needing any communication or coordination among the different ICs. Besides, the VPL control is compatible with any upper-level secondary controller since it employs local measurements to carry out the IC control.

Compared to existing dual grid-supporting control techniques, the SGF-VPL control makes it possible to set the voltage or frequency at one of the sides of the IC. Moreover, unlike other grid-forming techniques proposed in the literature, the SGF-VPL control is capable of sup-

porting both sides of the IC under power perturbations. This improves the coupling between different grids or parts of the grid, which is specially relevant for systems decoupled from strong grids or systems dominated by electronic converters. Apart from the scenarios already described in the paper, the SGF-VPL control can be a feasible solution for ICs operating at high voltage dc (HVDC) links tying ac systems, improving the transient and steady-state coupling of the interconnected ac and dc buses.

5.4 Conclusion

In this chapter we have presented a virtual power line (VPL) control concept for interlinking converters, which enables to tie different and incompatible electric systems—i.e., ac-ac links with different frequencies and voltages, hybrid links and dc-dc links with different voltage levels—analogously to a transmission line interconnecting two compatible grids. This control concept makes it possible to couple the transient and steady-state operation of the interconnected grids by employing only local measurements, improving the system's overall reliability. The VPL control can be deployed at different grid links and it does not require any communication link to operate.

We have proposed two VPL control variants: the dual grid-supporting VPL and the single grid-forming VPL control. The former equalises the interconnected systems by transferring active power proportionally to their voltage and/or frequency deviation. The latter extends the VPL concept to offer grid-forming capabilities at one of the sides of the IC, making it possible to set the voltage and frequency of the system without the need of any other grid-forming device. This is an interesting feature because it can be applied at remote grids that do not have any other grid-forming system to reduce or avoid investments in additional devices such as ESSs.

The results have demonstrated how both VPL control variants contribute to equalise the voltages and frequencies of the interconnected systems in steady-state, and improve the RoCoF and RoCoV as well as the frequency and voltage nadir under sudden load variations. Besides, by employing VPL controls the flow of active power between interconnected power systems happens naturally from generation to consumption points as if all devices were part of the same electric system.

Chapter 6

Conclusion and Outlook

In this chapter we collect the most relevant conclusions of the thesis and the future research lines that we consider could be the continuation of our work.

6.1 Conclusions

The massive integration of RESs is deteriorating the transient response of power systems, mainly caused by their stochastic nature, their distributed implementation and the fact that they are connected to the grid via electronic power converters, which do not support the grid unless controlled specifically to do so. In order to tackle these issues, the integration of ESSs has become one of the most interesting solutions because they can be used as an energy buffer to offer several services towards the grid. As a consequence, the grid's classical top-down structure is shifting towards a more distributed system with clusters of RES and ESS that can be managed locally and even operate completely isolated from the main grid.

In this grid of grids scenario, the converters that interconnect the different parts of the system—i.e. ICs—will play a key role to ensure a high-quality power supply to the users. On the one hand, they will make it possible to connect systems of different natures (ac, dc, voltage/frequency levels, etc.). On the other hand, it is possible to control them so that they contribute to the system regulation, enabling the power exchange among subrgids and increasing the systems' reliability and robustness. Thus, ICs will be crucial when traditional tying methods are not suitable and advanced control strategies must be employed in order to act properly under different grid conditions. Lastly, it is envisioned that they will coexist with traditional tying methods.

One of the main contributions of this thesis—presented in Chapter 2—is the development of the DFPF simulation tool, which can be used to represent frequency and voltage variations of ac, dc and hybrid ac/dc power systems. Results have demonstrated that DFPF simulations are a very efficient approach to carry out dynamic simulations of power systems, compared to Simulink® Phasor and EMT simulation methods. This is due to the fact that they have a very low computational cost to be solved, and the required grid-connected device models are very simple. Moreover, the MATLAB Simulink® environment facilitates the implementation of new use cases. In other words, this tool is very effective to study the interconnection of several grids, the implementation of grid-forming and grid-supporting converters, long-term energy studies, or for cases when grid interconnections, system inertia or controllers and parameters need to be tested in large and long-term simulations. Thus, we can conclude that the first objective of the project **[O1]** has been fulfilled, and the results have led to the publication of **[J2]** and **[C1]** articles.

In Chapter 3 we provide a more in-depth technical background about the controller types of grid-connected devices, the analogies between ac and dc power systems, and the most recent IC control techniques that can be employed to improve the transient response of the interconnected systems. A high-level overview of this study has led to the publication of the article **[M1]**.

In this literature review, IC control techniques that provide transient support to intercon-

nected systems have been classified in two main groups according to their mode of operation, i.e. grid-forming and/or grid-supporting. Then, IC controls have been grouped considering if they provide support to one or both of the interconnected systems, and the employed loops for the provision of transient support. In short, we have seen that most of the proposed IC techniques belong to grid-supporting control techniques, and employ *derivative-based* inertia-emulation loops. Regarding the grid-forming controls, most of them employ SME loops to obtain the grid's reference and provide virtual inertia to the grid. In general, most of the techniques are proposed for hybrid ac/dc microgrids in order to tackle the lack of inherent response of power converters, but we observe that this topic is extending to power transmission systems, where more and more converter-interfaced renewable power plants are substituting SG-based generation.

Regarding the bidirectional transient support capability, only grid-supporting controls have been proposed in the literature, and most of the techniques employ *derivative-based* inertia-emulation loops. The dual grid-forming operation has been recently proposed, but specifically for MMC converters, which inherently have more energy stored in the converter topology. In any case, the provision of inertia or transient support has not been reported yet for this type of converters. The literature review carried out in this chapter and the proposed control classification corresponds to the second objective of the thesis **[O2]**.

One of the main conclusions of the literature review is that there is a lack of control strategies to provide transient support to both interconnected systems at the same time. In this sense, Chapter 4 and Chapter 5 have been oriented to proposing new control techniques for ICs that incorporate this feature.

The DIE control technique presented in Chapter 4 has been designed so that the IC provides inertial support to both interconnected grids, while being able to adjust the inertial response for each side of the converter independently. The DIE philosophy can be employed to interconnect grids of different current natures without the need for a communication network with other agents. Simulation results have shown that the DIE control improves the transient response of both interconnected grids, and that it can be easily combined with other controllers such as primary regulation controls. The research work performed in this chapter has been published in the **[J1]** journal article.

In Chapter 5, on the other hand, we have proposed a virtual power line (VPL) control concept for interlinking converters. This control concept makes it possible to couple the transient and steady-state operation of the interconnected grids by employing only local measurements, replicating the behaviour of a classical tying device such as a transmission line. Based on this VPL concept, we have proposed two control variants: a dual grid-supporting VPL and a single grid-forming VPL control. The former equalises the interconnected systems by transferring active power proportionally to their voltage and/or frequency deviation. The latter extends the VPL concept to offer grid-forming capabilities at one of the sides of the IC, making

it possible to set the voltage and frequency of the system. The results have demonstrated how both VPL control variants contribute to reduce the RoCoF and RoCoV as well as the frequency and voltage nadir under sudden load variations. Besides, the flow of active power between interconnected power systems happens naturally from generation to consumption points as if all devices were part of the same electric system. This control concept has been presented in form of a journal paper in **[J3]**, and with this contribution we consider that the last objective of the thesis **[O3]** has been fulfilled.

An additional contribution of the proposed control strategies is that they can be employed regardless of the nature of the interconnected systems, i.e. ac or dc, voltage and frequency levels.

6.2 Future Research Lines

All in all, we believe that ICs will have an important role in modern power system scenarios, so it will be essential to carry out more research work in this field.

The DFPF tool we presented in Chapter 2 enables to evaluate the contribution of different IC controls to interconnected systems in a simple manner, so in our view these simulations are valid in the first stages of development. The results obtained with DFPF simulations show that the proposed controllers improve the frequency and voltage stability in ac and dc grids, by observing the RoCoF, RoCoV and nadir values of power systems. However, the presented work lacks more in-depth analyses that explore, for instance, the small-signal stability limits of the proposed control techniques. For that purpose, the detailed implementation of the proposed IC control concepts at specific test scenarios is a relevant future research line. The inner control loops, measurements, estimations and also the properties of the interconnected systems are some of the aspects that need to be further considered, since they will determine the small-signal stability margins of the systems and will provide detailed information about the impact of the parameters in the power systems' stability.

Although DFPF simulations are able to represent grid dynamics derived from electromechanical oscillations and the effect of most representative control loops, they cannot represent the electromagnetic oscillations due to the fact that they employ a static load-flow based solver. However, the DFPF tool still can be further developed by adding other functionalities such as the simulation of unbalanced systems, or the representation of harmonic currents. Since in the DFPF tool the power system structure is built from a file containing the admittance matrix, it enables to construct large power systems automatically. Thus, we believe that this feature together with the low computational cost of the tool encourages the usage of DFPF simulations on real-time power system simulations. Therefore, we consider that the implementation of DFPF simulations at hardware in the loop (HIL) platforms is a very interesting research line that needs to be explored, and might facilitate the validation of different controllers on more

realistic power system scenarios.

In order to go one step further in the validation of the already proposed and new IC control strategies, we consider that a good continuation for the presented research work would be to carry out an experimental implementation. For instance, the DIE and VPL controls proposed in Chapters 4 and 5 can be applied to any type of interconnection, but the implementation issues that might arise on a real platform may be different depending on the characteristics of the interconnection. The validation of a new IC control strategy on a real power system scenario is hardly feasible since the set up of two power systems and the IC would require a very high cost and effort. Therefore, in our opinion HIL real-time simulations are a good alternative for a first validation of converter controls. Applying this concept to ICs, two power system models and the IC could be implemented in a HIL real-time platform, and the IC control would run in an external controller (also known as control-HIL (c-HIL) simulation). In a second stage, the HIL platform could be connected to a power amplifier, leading to the so-called power-HIL (p-HIL) test bench. This, for instance, would enable to have one of the interconnected grids integrated in the p-HIL platform, and a real IC could interconnect the p-HIL with a real microgrid scenario, or the terminals of another p-HIL platform. By doing so, more detailed conclusions about the implementation issues and the effectiveness of proposed controls on real test cases could be drawn, and the proposed controls could be compared to other approaches already proposed in the literature.

As we have mentioned throughout the document, it is envisioned that ICs will be called to provide AS to the power systems. Hence, the stacking of other kind of services with the transient support will be of high interest, and will help to maximise the contribution of ICs to the AS market. For instance, if an IC is working below the rated power, it can be used to provide other services such as the provision of reactive power or the compensation of harmonics or ac grid unbalances. In this sense, the power limits, the compatibility of control loops and the performance of new controls need to be studied, and this research will certainly lead to new control proposals for ICs.

List of Figures

1.1 History and projection of the global end-use energy consumption according to EIA21[2]. 2
1.2 History and projection of the global primary energy consumption by source11[1]. 3
1.3 Illustration of classical grid top-down topology. 4
1.4 Energy generation pool data of the Spanish power system, provided by Red Eléctrica 5
1.5 Illustration of a modern power system scenario, a hybrid GoG. 7
1.6 Interconnection of: a) synchronised ac grids with same voltage and frequency, b) synchronised ac grids with different voltage and same frequency, c) dc grids with same voltage levels, d) dc grids with different voltage levels using an IC, e) an ac and dc grid using an IC and f) two ac systems using an IC. 8
1.7 a) single-stage, b) two-stage with an intermediate dc grid and c) three-stage and two intermediate dc grid ac-ac interconnection illustrations from [11]. . . . 10
1.8 a) Two-stage IC, b) two single-stage ICs. 10
1.9 Foreseen HVDC undersea interconnection between Spain and France by INELFE1213[12] 11
1.10 Illustration of *Combined Grid Solution* project1414[14] 12
1.11 Illustration of *Network Equilibrium* project area1515[15]. 13
1.12 ABB's Flexible Power Link (IC) installed at the Network Equilibrium project1616[16]. 14
1.13 Structure of the thesis and its relation with specified objectives, contributions and topic of each chapter. 18

2.1 Power flow equation-based power system simulation methods classified according to the capability to represent the system dynamics. 23
2.2 Description of the DFPF algorithm for an ac power system. 27
2.3 Flow chart of the power flow solver with the NR algorithm. 30
2.4 Conceptual interconnection diagram of a hybrid ac/dc link in the DFPF tool: a) dc system, b) IC and c) ac system. 31
2.5 Different ac grid-connected device configuration schemes at the DFPF tool. . . . 32
2.6 Different dc grid-connected device configuration schemes at the DFPF tool. . . . 33

2.7 WSCC 9 node system benchmark illustration. 36
2.8 SG model of the Slack node implemented in Simulink. 37
2.9 DFPF, Phasor and EMT simulation result comparison of three SGs' frequency for a 1 p.u. active load step in the nine node scenario. 38
2.10 a) WP generation profile, b) PV generation profile, c) active power load profile and d) first SG's frequency for DFPF, Phasor and EMT simulations. 40
2.11 a) Mean value of the difference with the EMT simulation of DFPF and Phasor methods and b), required simulation time of each simulation method. Both depending on the simulation step size T_s. 41
2.12 a) Variation of the inertia of the first SG (H_1) and b) variation of the prime mover's delay (T_{D1}) with six times less system inertia, both for a 1 p.u. active load step at node 8. 43
2.13 Simplified diagram of the hybrid ac/dc benchmark scenario. 44
2.14 WP plant ac grid topology. 44
2.15 Test 1: a) Nordic and Continental grid frequencies (at the IC connection node), b) MTDC slack node voltage and c) Load step-shaped profiles. 46
2.16 Test 2: a) Dynamic generation profiles, b) Dynamic load profiles, c) Nordic and Continental grid frequencies (at the IC connection node), d) WP plant frequencies, and e) MTDC slack node voltage. 47

3.1 Participation of inherent inertia, low-level control and the hierarchical control layers in the regulation of frequency at a converter dominated grid. 52
3.2 Possible contribution of ICs to the different control layers of interconnected subgrids. 53
3.3 Dynamic models and equations describing the power exchange for grid connected devices providing inertial behaviour in ac and dc systems, described in [46]. (a) synchronous machine, (b) dc machine, and (c) resistor-capacitor (RC) circuit. 59
3.4 Dynamic (primary and inertial) response decoupling of power electronic converters. 60
3.5 Illustration of the IC unified framework using p.u. grid measurements. 63
3.6 Literature review classification diagram. 64
3.7 Illustration of the single grid-supporting IC control. 64
3.8 Illustration of the dual grid-supporting IC control. 65
3.9 Illustration of the single grid-forming IC control. 68
3.10 Illustration of the dual grid-forming IC control. 70
3.11 Illustration of the single grid-forming and dual grid-supporting IC control. . . . 71

4.1 Representation of the IC with the proposed dual inertia-emulation technique and classical control approach. 77

4.2 Detailed Dual Inertia-Emulation control loop for ICs. 78
4.3 Proposed simulation scenario for testing the DIE technique on an IC tying two electric grids. 81
4.4 DIE operation concept test: a) Frequency of System 1, b) Frequency of System 2, c) Power references of the DIE control branches, and d) Power transferred by the IC 83
4.5 Case 1: a) Frequency of System 1, b) Frequency of System 2, and c) Power transferred by the DIE-controlled IC. 85
4.6 Case 2: a) Frequency of System 1, b) Frequency of System 2, and c) Power transferred by the interlinking device (transformer or DIE-controlled IC). 86
4.7 Case 3: a) Frequency of System 1, b) Frequency of System 2, and c) Power transferred by the interlinking device (transformer or DIE-DD-controlled IC). . . 88
4.8 Test case 4: a) Wind Power generation at System 2, b) PV generation at System 2, c) Power load profile at system 1, d) Power load profile at System 2, e) Frequency of system 1, and f) Frequency of System 2. 89

5.1 Two power systems tied by a power transmission line. 93
5.2 Representation example of a IC with the DGS-VPL control tying two power systems. 96
5.3 Detailed SGF-VPL control scheme a) to form dc grids and b) to form ac grids. . . 97
5.4 VPL operation concept test: a) frequency of System 1 and voltage of system 2 (both in p.u.) b) virtual angle δ_v c) active power profiles at system 1 and 2, d) frequency of the slack node at system 1 for different Z_{VPL} parameters and e) voltage of the slack node at system 2 for different Z_{VPL} 100
5.5 VPL operation compared to DIE-DD IC control: a) frequency of Systems 1 and 2 for both IC control approaches b) active power transfer for each control strategy. 102
5.6 AC wind power plant topology example with ac/dc IC link. 103
5.7 Disconnection of the main grid-forming unit from the WP plant with a) DGS-VPL control and b) SGF-VPL control. 103
5.8 Simplified diagram of the hybrid ac/dc benchmark scenario with representation of grid-forming ICs implementing the SGF-VPL. 104
5.9 a) Frequency of the WP ac systems, b) voltage of the MTDC grid, c) Frequency of the Nordic grid, d) Frequency of the Continental grid, e) Aggregated active power generation of the WP plants, f) Aggregated active power loading of Nordic and Continental systems. 105
5.10 SGF-VPL controlled IC power of a) WP-MTDC links, b) Nordic-MTDC link and c) Continental-MTDC link. 106

List of Tables

2.1 Classification of different simulation methods for ac power systems that employ power flow algorithms and represent frequency dynamics 25
2.2 Different node types on an ac static load flow problem 27
2.3 Different node types on a dc static load flow problem 28
2.4 Generator parameters for the WSCC 9 node system from [34] 37
2.5 Simulation settings and required time for Test A 39
2.6 Simulation settings for EMT, Phasor and DFPF simulations in Test B 41
2.7 Inertia constants of the grid-forming units in the test scenario 45

3.1 Variable analogy for grid-connected ac and dc elements 59
3.2 Summary of IC grid-supporting control techniques for the provision of transient support on interconnected grids. 72
3.3 Summary of IC grid-forming control techniques for the provision of transient support on interconnected grids. 73

4.1 System and IC parameter values for the simplified simulation scenario. 82
4.2 System and IC parameter values for the test cases. 84

5.1 System and IC parameter values for the simplified hybrid simulation scenario. . 99
5.2 System and IC parameter values for IC control comparison. 101

List of References

[1] P. Kundur, *Power System Stability And Control*, ser. EPRI power system engineering series. McGraw-Hill Education (India) Pvt Limited, 1994.

[2] F. Milano, F. Dorfler, G. Hug, D. J. Hill, and G. Verbic, "Foundations and Challenges of Low-Inertia Systems," in *2018 Power Systems Computation Conference (PSCC)*. IEEE, jun 2018, pp. 1–25.

[3] A. Ulbig, T. Rinke, S. Chatzivasileiadis, and G. Andersson, "Predictive control for real-time frequency regulation and rotational inertia provision in power systems," *Proceedings of the IEEE Conference on Decision and Control*, pp. 2946–2953, 2013.

[4] Q. Peng, Q. Jiang, Y. Yang, T. Liu, H. Wang, and F. Blaabjerg, "On the Stability of Power Electronics-Dominated Systems: Challenges and Potential Solutions," *IEEE Transactions on Industry Applications*, vol. 55, no. 6, pp. 7657–7670, 2019.

[5] H. Farhangi, "The path of the smart grid," *IEEE Power and Energy Magazine*, vol. 8, no. 1, pp. 18–28, jan 2010.

[6] T. L. Vandoorn, J. D. De Kooning, B. Meersman, and L. Vandevelde, "Review of primary control strategies for islanded microgrids with power-electronic interfaces," *Renewable and Sustainable Energy Reviews*, vol. 19, pp. 613–628, 2013.

[7] A. Abdali, R. Noroozian, and K. Mazlumi, "Simultaneous control and protection schemes for DC multi microgrids systems," *International Journal of Electrical Power and Energy Systems*, vol. 104, no. July 2018, pp. 230–245, 2019.

[8] O. Gomis-Bellmunt, E. Sánchez-Sánchez, J. Arevalo-Soler, and E. Prieto-Araujo, "Principles of operation of grids of DC and AC subgrids interconnected by power converters," *IEEE Transactions on Power Delivery*, vol. 8977, no. c, pp. 1–11, 2020.

[9] E. Bullich-Massagué, F. Díaz-González, M. Aragüés-Peñalba, F. Girbau-Llistuella, P. Olivella-Rosell, and A. Sumper, "Microgrid clustering architectures," *Applied Energy*, vol. 212, pp. 340–361, feb 2018.

[10] M. Najafzadeh, R. Ahmadiahangar, O. Husev, I. Roasto, T. Jalakas, and A. Blinov, "Recent Contributions, Future Prospects and Limitations of Interlinking Converter Control in Hybrid AC/DC Microgrids," *IEEE Access*, vol. 9, 2021.

[11] A. Ordono, E. Unamuno, J. A. Barrena, and J. Paniagua, "Interlinking converters and their contribution to primary regulation: a review," *International Journal of Electrical Power & Energy Systems*, vol. 111, no. March, pp. 44–57, 2019.

[12] M. Liserre, G. Buticchi, M. Andresen, G. De Carne, L. F. Costa, and Z. X. Zou, "The Smart Transformer: Impact on the Electric Grid and Technology Challenges," *IEEE Industrial Electronics Magazine*, vol. 10, no. 2, pp. 46–58, 2016.

[13] A. Gupta, S. Doolla, and K. Chatterjee, "Hybrid AC–DC Microgrid: Systematic Evaluation of Control Strategies," *IEEE Transactions on Smart Grid*, vol. 9, no. 4, pp. 3830–3843, jul 2018.

[14] J. W. Kolar and G. Ortiz, "Solid-State-Transformers : Key Components of Future Traction and Smart Grid Systems," in *Proceedings of the International Power Electronics Conference - ECCE Asia (IPEC)*, no. Ipec, 2014, p. 14.

[15] Q. Shafiee, T. Dragicevic, J. C. Vasquez, and J. M. Guerrero, "Hierarchical Control for Multiple DC-Microgrids Clusters," in *IEEE Transactions on Energy Conversion*, vol. 29, no. 4. IEEE, feb 2014, pp. 1–6.

[16] ENTSO-E, "System dynamic and operational challenges," *Ten Year Network Development Plan*, no. November, 2021.

[17] W. F. Tinney, S. Member, and C. E. Hart, "Power Flow Solution by Newton's Method," *IEEE Transactions on Power Apparatus and Systems*, vol. PAS-86, no. 11, pp. 1449–1460, 1967.

[18] J. J. Grainger and W. D. Stevenson, *Power System Analysis*, A. Brown Akay and E. Castellano, Eds. McGraw-Hill, 1994.

[19] M. A. Pai and D. Chatterjee, *Computer Techniques in Power System Analysis*. McGraw Hill Education, 2006.

[20] D. J. Glover, M. S. Sarma, and T. J. Overbye, *Power System: Analysis & Design*. Global Engineering, 2012.

[21] J. Paniagua, H. Gezala, E. Unamuno, M. Zubiaga, and J. Andoni Barrena, "A Dynamic Frequency-and-Voltage Power Flow Simulation Tool for Hybrid AC/DC Power Systems based on Simulink," in *IECON 2022 – 48th Annual Conference of the IEEE Industrial Electronics Society*. IEEE, oct 2022, pp. 1–6.

[22] EPRI, *Long term power system dynamics Volume I*. Electric Power Research Institute, 1974.

[23] T. Haines, "Long-Term Dynamic Simulation of Power Systems Using Python, Agent Based Modeling, and Time-Sequenced Power Flows," Ph.D. dissertation, Montana Tech, 2020.

[24] C. Fan, Z. Chen, X. Wang, Y. Teng, G. Chen, and H. Zhang, "Solution of dynamic power flow technique considering governor nonlinearity," *International Transactions on Electrical Energy Systems*, vol. 30, no. 2, pp. 1–13, 2020.

[25] A. Pawellek and L. Hofmann, "Comparison of Methods for the Simulation of Dynamic Power Flows in the International Grid Control Cooperation," *Conference Record of the 3rd IEEE International Workshop on Electronic Power Grid, eGrid 2018*, pp. 1–6, 2018.

[26] C. Li, Y. Liu, and H. Zhang, "Fast analysis of active power-frequency dynamics considering network influence," *IEEE Power and Energy Society General Meeting*, pp. 1–6, 2012.

[27] I. Abdulrahman, "MATLAB-Based Programs for Power System Dynamic Analysis," *IEEE Open Access Journal of Power and Energy*, vol. 7, pp. 59–69, 2020.

[28] I. Abdulrahman and G. Radman, "Simulink-based programs for power system dynamic analysis," *Electrical Engineering*, vol. 101, no. 2, pp. 345–356, 2019.

[29] G. Lammert, K. Yamashita, L. David, and P. Ospina, "International industry practice on modelling and dynamic performance of inverter based generation in power system studies," *CIGRE C4/C6.35/CIRED*, no. June, 2017.

[30] G. S. Misyris, S. Chatzivasileiadis, and T. Weckesser, "Grid-forming converters: Sufficient conditions for RMS modeling," *Electric Power Systems Research*, vol. 197, no. May, p. 107324, 2021.

[31] M. Laughton and M. Humphrey Davies, "Numerical techniques in solution of power-system load-flow problems," *Proceedings of the Institution of Electrical Engineers*, vol. 111, no. 9, p. 1575, 1964.

[32] B. Stott and O. Alsac, "Fast decoupled load flow," *IEEE Transactions on Power Apparatus and Systems*, vol. PAS-93, no. 3, pp. 859–869, 1974.

[33] F. Milano, *Power system modelling and scripting*. Springer Berlin Heidelberg, 2010, vol. 54.

[34] B. Dembart, A. M. Erisman, E. G. Cate, M. A. Epton, and H. Dommel, "Power system dynamic analysis: Phase I. Final report," U.S. Department of Energy, U.S. Department of Energy, Tech. Rep., jul 1977.

[35] J. Paniagua, E. Unamuno, and J. A. Barrena, "Dual Inertia-Emulation Control for Interlinking Converters in Grid-Tying Applications," *IEEE Transactions on Smart Grid*, vol. 12, no. 5, pp. 3868–3876, sep 2021.

[36] K. Walve, "Nordic32A - A Cigré test system for simulation of transient stability and long term dynamics," Svenska Kraftnät, Vällingy, Tech. Rep., 1993.

[37] K. Strunz, E. Abbasi, C. Abbey, C. Andrieu, U. Annakkage, S. Barsali, R. C. Campbell, R. Fletcher, F. Gao, T. Gaunt, A. Gole, N. Hatziargyriou, R. Iravani, G. Joos, H. Konishi, M. Kuschke, E. Lakervi, C.-C. Liu, J. Mahseredjian, F. Mosallat, D. Muthumuni, A. Orths, S. Papathanassiou, K. Rudion, Z. Styczynski, and S. C. Verma, "Benchmark Systems for Network Integration of Renewable and Distributed Energy Resources," CIGRE, Tech. Rep. April, 2014.

[38] J. Wang, X. Wang, and Y. Wu, "Operating reserve model in the power market," *IEEE Transactions on Power Systems*, vol. 20, no. 1, pp. 223–229, 2005.

[39] C. D. Parker, "Applications - Stationary | Energy Storage Systems: Batteries," *Encyclopedia of Electrochemical Power Sources*, pp. 53–64, 2009.

[40] European Union, "Commission Regulation (Eu) 2016/631," *Official Journal of the European Union*, no. 14 April 2016, p. 68, 2016.

[41] Y. Rebours and D. Kirschen, "What is spinning reserve?" *The university of Manchester*, pp. 1–11, 2005.

[42] X. Shen, D. Tan, Z. Shuai, and A. Luo, "Control Techniques for Bidirectional Interlinking Converters in Hybrid Microgrids: Leveraging the advantages of both ac and dc," *IEEE Power Electronics Magazine*, vol. 6, no. 3, pp. 39–47, 2019.

[43] J. Rocabert, A. Luna, F. Blaabjerg, and P. Rodríguez, "Control of Power Converters in AC Microgrids," *IEEE Transactions on Power Electronics*, vol. 27, no. 11, pp. 4734–4749, nov 2012.

[44] A. M. Bouzid, J. M. Guerrero, A. Cheriti, M. Bouhamida, P. Sicard, and M. Benghanem, "A survey on control of electric power distributed generation systems for microgrid applications," *Renewable and Sustainable Energy Reviews*, vol. 44, pp. 751–766, 2015.

[45] E. Unamuno, "Control and Stability of AC/DC Microgrids," PhD Thesis, Mondragon Unibertsitatea - Goi Eskola Politeknikoa, 2017.

[46] E. Unamuno, J. Paniagua, and J. A. Barrena, "Unified Virtual Inertia for ac and dc Microgrids: And the Role of Interlinking Converters," *IEEE Electrification Magazine*, vol. 7, no. 4, pp. 56–68, 2019.

[47] A. Navarro-Rodriguez, P. Garcia, R. Georgious, and J. Garcia, "Adaptive active power sharing techniques for DC and AC voltage control in a hybrid DC/AC microgrid," *IEEE Transactions on Industry Applications*, vol. 55, no. 2, pp. 1106–1116, 2019.

[48] E. Unamuno, J. A. Suul, M. Molinas, and J. A. Barrena, "Comparative Eigenvalue Analysis of Synchronous Machine Emulations and Synchronous Machines," *IECON Proceedings (Industrial Electronics Conference)*, vol. 2019-Octob, pp. 3863–3870, 2019.

[49] K. R. Vasudevan, V. K. Ramachandaramurthy, T. S. Babu, and A. Pouryekta, "Synchronverter: A Comprehensive Review of Modifications, Stability Assessment, Applications and Future Perspectives," *IEEE Access*, vol. 8, pp. 131 565–131 589, 2020.

[50] O. Mo, S. Darco, and J. A. Suul, "Evaluation of Virtual Synchronous Machines with Dynamic or Quasi-Stationary Machine Models," *IEEE Transactions on Industrial Electronics*, vol. 64, no. 7, pp. 5952–5962, 2017.

[51] S. D'Arco, J. A. Suul, and O. B. Fosso, "Control system tuning and stability analysis of Virtual Synchronous Machines," in *2013 IEEE Energy Conversion Congress and Exposition*. IEEE, sep 2013, pp. 2664–2671.

[52] Q. C. Zhong and G. Weiss, "Synchronverters: Inverters that mimic synchronous generators," *IEEE Transactions on Industrial Electronics*, vol. 58, no. 4, pp. 1259–1267, 2011.

[53] D. Chen, Y. Xu, and A. Q. Huang, "Integration of DC Microgrids as Virtual Synchronous Machines into the AC Grid," *IEEE Transactions on Industrial Electronics*, vol. 0046, no. c, pp. 1–1, 2017.

[54] Z. Shuai, Y. Hu, Y. Peng, C. Tu, and Z. J. Shen, "Dynamic Stability Analysis of Synchronverter-dominated Microgrid Based on Bifurcation Theory," *IEEE Trans. Ind. Electron.*, vol. 0046, no. c, pp. 1–1, 2017.

[55] S. Peyghami, P. Davari, H. Mokhtari, P. C. Loh, and F. Blaabjerg, "Synchronverter-based Power Sharing Approach for LVDC Microgrids," *IEEE Trans. Power Electron.*, vol. 8993, no. c, pp. 1–1, 2016.

[56] S. D'Arco, J. A. Suul, and O. B. Fosso, "A Virtual Synchronous Machine implementation for distributed control of power converters in SmartGrids," *Electr. Power Syst. Res.*, vol. 122, pp. 180–197, 2015.

[57] P. F. Frack, P. E. Mercado, M. G. Molina, E. H. Watanabe, R. W. De Doncker, and H. Stagge, "Control Strategy for Frequency Control in Autonomous Microgrids," *IEEE J. Emerg. Sel. Top. Power Electron.*, vol. 3, no. 4, pp. 1046–1055, dec 2015.

[58] W. Zhang, A. Tarraso, J. Rocabert, A. Luna, J. I. Candela, and P. Rodriguez, "Frequency Support Properties of the Synchronous Power Control for Grid-Connected Converters," *IEEE Transactions on Industry Applications*, vol. 55, no. 5, pp. 5178–5189, sep 2019.

[59] D. Pullaguram, S. Achary Buragappu, S. Mishra, and D. Ramasubramanian, "Single-phase synchronverter for a grid-connected roof top photovoltaic system," *IET Renew. Power Gener.*, vol. 10, no. 8, pp. 1187–1194, sep 2016.

[60] H. Alatrash, A. Mensah, E. Mark, G. Haddad, and J. Enslin, "Generator emulation controls for photovoltaic inverters," *IEEE Trans. Smart Grid*, vol. 3, no. 2, pp. 996–1011, 2012.

[61] H. Dharmawardena, K. Uhlen, and S. S. Gjerde, "Modelling wind farm with synthetic inertia for power system dynamic studies," in *2016 IEEE Int. Energy Conf.*, no. 2. IEEE, apr 2016, pp. 1–6.

[62] Q.-C. Zhong, Z. Ma, W.-L. Ming, and G. C. Konstantopoulos, "Grid-friendly wind power systems based on the synchronverter technology," *Energy Conversion and Management*, vol. 89, pp. 719–726, jan 2015.

[63] J. C. Martinez, S. A. Gomez, J. L. Rodriguez Amenedo, and J. Alonso-Martinez, "Analysis of the Frequency Response of Wind Turbines with Virtual Inertia Control," in *2020 IEEE International Conference on Environment and Electrical Engineering and 2020 IEEE Industrial and Commercial Power Systems Europe (EEEIC / I&CPS Europe)*. IEEE, jun 2020, pp. 1–6.

[64] J. Castro Martinez, S. Arnaltes, J. Alonso-Martinez, and J. L. Rodriguez Amenedo, "Contribution of Wind Farms to the Stability of Power Systems with High Penetration of Renewables," *Energies*, vol. 14, no. 8, p. 2207, apr 2021.

[65] A. Peña Asensio, F. Gonzalez-Longatt, S. Arnaltes, and J. L. Rodríguez-Amenedo, "Analysis of the Converter Synchronizing Method for the Contribution of Battery Energy Storage Systems to Inertia Emulation," *Energies*, vol. 13, no. 6, p. 1478, mar 2020.

[66] S. Mahajan and Y. P. Verma, "Performance of fast responding ultracapacitor energy storage for virtual inertia emulation control," *Energy Storage*, vol. 4, 10 2022.

[67] E. Rakhshani, D. Remon, A. Mir Cantarellas, and P. Rodriguez, "Analysis of derivative control based virtual inertia in multi-area high-voltage direct current interconnected power systems," *IET Generation, Transmission and Distribution*, vol. 10, no. 6, pp. 1458–1469, 2016.

[68] C. D. Booth, W. Hung, J. M. Guerrero, J. Zhu, and G. P. Adam, "Generic inertia emulation controller for multi-terminal voltage-source-converter high voltage direct current systems," *IET Renew. Power Gener.*, vol. 8, no. 7, pp. 740–748, sep 2014.

[69] J. Zhu, C. D. Booth, G. P. Adam, A. J. Roscoe, and C. G. Bright, "Inertia emulation control strategy for VSC-HVDC transmission systems," *IEEE Trans. Power Syst.*, vol. 28, no. 2, pp. 1277–1287, 2013.

[70] M. Amin, A. Ardal, and M. Molinas, "Self-synchronisation of Wind Farm in MMC-based HVDC System: A Stability Investigation," *IEEE Trans. Energy Convers.*, vol. 8969, no. c, pp. 1–1, 2017.

[71] J. A. Suul, S. DArco, and G. Guidi, "Virtual Synchronous Machine-Based Control of a Single-Phase Bi-Directional Battery Charger for Providing Vehicle-to-Grid Services," *IEEE Trans. Ind. Appl.*, vol. 52, no. 4, pp. 3234–3244, jul 2016.

[72] A. Saxena, R. Shankar, and S. Parida, "Vehicle-to-grid technology with virtual inertia control for enhanced frequency regulation in smart grid," *2022 IEEE Global Conference on Computing, Power and Communication Technologies, GlobConPT 2022*, 2022.

[73] C. Liu and J. Fang, "Analysis and design of inertia for grid-tied electric vehicle chargers operating as virtual synchronous machines," *Applied Sciences*, 2022.

[74] Z. Xinchen, W. Hui, and W. Ke, "Research on virtual synchronous generator control for vehicle-to-grid system," *IOP Conference Series: Materials Science and Engineering*, 2019.

[75] P. Magne, B. Nahid-Mobarakeh, and S. Pierfederici, "Dc-link voltage large signal stabilization and transient control using a virtual capacitor," *2010 IEEE Industry Applications Society Annual Meeting*, 2010.

[76] E. Unamuno and J. Andoni Barrena, "Design and small-signal stability analysis of a virtual-capacitor control for dc microgrids," *2017 19th European Conference on Power Electronics and Applications (EPE'17 ECCE Europe)*, 2017.

[77] M. Song, J. Meng, Y. Wang, and J. Peng, "Research on multiple constraints of flexible virtual capacitor control for vsc," *2019 IEEE Innovative Smart Grid Technologies - Asia (ISGT Asia)*, 2019.

[78] Z. Yi, X. Zhao, D. Shi, J. Duan, Y. Xiang, and Z. Wang, "Accurate Power Sharing and Synthetic Inertia Control for DC Building Microgrids With Guaranteed Performance," *IEEE Access*, vol. 7, pp. 63 698–63 708, 2019.

[79] X. Zhu, F. Meng, Z. Xie, and Y. Yue, "An Inertia and Damping Control Method of DC-DC Converter in DC Microgrids," *IEEE Transactions on Energy Conversion*, vol. 35, no. 2, pp. 799–807, 2020.

[80] W. Hao and Z. Chen, "An improved virtual capacitor control strategy for dc electric railway system," *2021 IEEE Southern Power Electronics Conference (SPEC)*, 2021.

[81] K. Shinoda, A. Benchaib, J. Dai, and X. Guillaud, "Dc voltage control of mmc-based hvdc grid with virtual capacitor control," *2017 19th European Conference on Power Electronics and Applications (EPE'17 ECCE Europe)*, 2017.

[82] ——, "Virtual capacitor control: Mitigation of dc voltage fluctuations in mmc-based hvdc systems," *IEEE Transactions on Power Delivery*, vol. 33, no. 1, pp. 455 – 65, 2018.

[83] ——, "Virtual capacitor control for stability improvement of hvdc system comprising dc reactors," *15th IET International Conference on AC and DC Power Transmission (ACDC 2019)*, 2019.

[84] L. Yu, Y. Wang, W. Zhang, X. Yan, R. Si, and Y. Wen, "A virtual capacitor control method for depression dc voltage fluctuation in mmc-hvdc system," *2021 International Conference on Power System Technology (POWERCON)*, 2021.

[85] N. Zhi, X. Ming, Y. Ding, L. Du, and H. Zhang, "Power-loop-free virtual dc machine control with differential compensation," *IEEE Transactions on Industry Applications*, vol. 58, no. 1, pp. 413 – 22, 2022.

[86] S. Samanta, J. Mishra, and B. Roy, "Virtual dc machine: an inertia emulation and control technique for a bidirectional dcdc converter in a dc microgrid," *IET Electric Power Applications*, vol. 12, no. 6, pp. 874 – 84, 2018.

[87] M. Neves, F. Alves, M. Aredes, J. Costa, and M. Aredes, "A virtual dc machine control strategy with nonlinear behavior to enhance power sharing and voltage regulation in dc microgrids," *2021 IEEE Fourth International Conference on DC Microgrids (ICDCM)*, 2021.

[88] J. Chen, Z. Meng, and H. Xu, "Parameter adaptive control of virtual dc machine based dc microgrid," *IET Conference Proceedings*, no. 5, pp. 461 – 7, 2022.

[89] Z. Liu and Y. Liu, "Virtual dc machine control strategy for stability improvement in dc microgrid with constant power loads," *Proceedings of 2022 IEEE 5th International Electrical and Energy Conference, CIEEC 2022*, pp. 2893 – 2899, 2022.

[90] H. Hu, M. Zhu, J. Zhang, M. Liu, and X. Cai, "Virtual dc machine control for pv converters in dc distribution system," *2021 IEEE 12th Energy Conversion Congress and Exposition - Asia (ECCE-Asia)*, pp. 1481 – 6, 2021.

[91] J. Zhu, J. Guerrero, C. Booth, H. Zhang, and G. Adam, "A generic inertia emulation controller for multi-terminal vsc-hvdc systems," *2nd IET Renewable Power Generation Conference (RPG 2013)*, 2013.

[92] J. A. Suul and S. Darco, "Comparative analysis of small-signal dynamics in virtual synchronous machines and frequency-derivative-based inertia emulation," *2018 IEEE 18th International Power Electronics and Motion Control Conference (PEMC). Proceedings*, pp. 344 – 51, 2018.

[93] J. Fang, R. Zhang, H. Li, and Y. Tang, "Frequency derivative-based inertia enhancement by grid-connected power converters with a frequency-locked-loop," *IEEE Transactions on Smart Grid*, vol. 10, no. 5, pp. 4918 – 27, 2019.

[94] T. Kerdphol, F. Rahman, M. Watanabe, Y. Mitani, D. Turschner, and H.-P. Beck, "Enhanced virtual inertia control based on derivative technique to emulate simultaneous inertia and damping properties for microgrid frequency regulation," *IEEE Access*, vol. 7, pp. 14 422 – 33, 2019.

[95] P. Saxena, N. Singh, and A. K. Pandey, "Enhancing the dynamic performance of microgrid using derivative controlled solar and energy storage based virtual inertia system," *Journal of Energy Storage*, vol. 31, no. June, p. 101613, 2020.

[96] C. Blanco, D. Reigosa, F. Briz, J. M. Guerrero, and P. Garcia, "Grid synchronization of three-phase converters using cascaded complex vector filter PLL," in *2012 IEEE Energy Conversion Congress and Exposition (ECCE)*. IEEE, sep 2012, pp. 196–203.

[97] P. Arboleya, D. Diaz, J. Guerrero, P. Garcia, F. Briz, C. Gonzalez-Moran, and J. Gomez Aleixandre, "An improved control scheme based in droop characteristic for microgrid converters," *Electric Power Systems Research*, vol. 80, no. 10, pp. 1215–1221, oct 2010.

[98] P. C. Loh, D. Li, Y. K. Chai, and F. Blaabjerg, "Autonomous Control of Interlinking Converter With Energy Storage in Hybrid AC-DC Microgrid," *IEEE Transactions on Industry Applications*, vol. 49, no. 3, pp. 1374–1382, may 2013.

[99] A. A. Eajal, M. A. Abdelwahed, E. F. El-Saadany, and K. Ponnambalam, "A Unified Approach to the Power Flow Analysis of AC/DC Hybrid Microgrids," *IEEE Transactions on Sustainable Energy*, vol. 7, no. 3, pp. 1145–1158, jul 2016.

[100] ENTSO-E, "High Penetration of Power Electronic Interfaced Power Sources and the Potential Contribution of Grid Forming Converters Technical Report," ENTSO-E, Tech. Rep., 2020.

[101] K. Oureilidis, K.-n. Malamaki, K. Gallos, A. Tsitsimelis, C. Dikaiakos, S. Gkavanoudis, M. Cvetkovic, J. M. Mauricio, J. M. Maza Ortega, J. L. M. Ramos, G. Papaioannou, and C. Demoulias, "Ancillary Services Market Design in Distribution Networks: Review and Identification of Barriers," *Energies*, 2020.

[102] P. Bucko, M. Jaskolski, Z. Lubosny, J. Klucznik, and K. Dobrzynski, "Delivery of ancillary services in distribution power systems," *International Conference on the European Energy Market, EEM*, vol. 2018-June, 2018.

[103] Y. Liu, X. Hou, X. Wang, C. Lin, and J. M. Guerrero, "A coordinated control for photovoltaic generators and energy storages in low-voltage AC/DC hybrid microgrids under islanded mode," *Energies*, vol. 9, no. 8, 2016.

[104] I. U. Nutkani, P. C. Loh, P. Wang, T. K. Jet, and F. Blaabjerg, "Intertied ac-ac microgrids with autonomous power import and export," *International Journal of Electrical Power and Energy Systems*, vol. 65, pp. 385–393, 2015.

[105] Y. D. Lee and S. Y. Park, "Reactive power support capabilities of nonsynchronous interconnection systems in microgrid applications," in *Conference Proceedings - IEEE Applied Power Electronics Conference and Exposition - APEC*, vol. 2016-May. IEEE, mar 2016, pp. 125–131.

[106] C. Hunziker and N. Schulz, "Potential of solid-state transformers for grid optimization in existing low-voltage grid environments," *Electric Power Systems Research*, vol. 146, pp. 124–131, may 2017.

[107] D.-M. Phan and H.-H. Lee, "Interlinking Converter to Improve Power Quality in Hybrid AC DC Microgrids With Nonlinear Loads," *IEEE Journal of Emerging and Selected Topics in Power Electronics*, vol. 7, no. 3, pp. 1959–1968, sep 2019.

[108] R. V. Shravan and C. Vyjayanthi, "Active power filtering using interlinking converter in droop controlled islanded hybrid AC-DC microgrid," *International Transactions on Electrical Energy Systems*, no. January, pp. 1–27, 2020.

[109] L. Wang, X. Fu, and M.-C. W. Wong, "Operation and Control of a Hybrid Coupled Interlinking Converter for Hybrid AC/LVDC Microgrids," *IEEE Transactions on Industrial Electronics*, vol. 0046, no. c, pp. 1–1, 2020.

[110] S. Hosseini and S. M. Barakati, "Interlinking Converter of Hybrid AC/DC Microgrid as an Active Power Filter," *2019 IEEE 2nd International Conference on Renewable Energy and Power Engineering, REPE 2019*, pp. 95–99, 2019.

[111] M. H. Albadi, A. S. Al Hinai, A. H. Al-Badi, M. S. Al Riyami, S. M. Al Hinai, and R. S. Al Abri, "Unbalance in power systems: Case study," in *2015 IEEE International Conference on Industrial Technology (ICIT)*. IEEE, mar 2015, pp. 1407–1411.

[112] K. Sun, X. Wang, Y. W. Li, F. Nejabatkhah, Y. Mei, and X. Lu, "Parallel Operation of Bidirectional Interfacing Converters in a Hybrid AC/DC Microgrid Under Unbalanced Grid Voltage Conditions," *IEEE Transactions on Power Electronics*, vol. 32, no. 3, pp. 1872–1884, mar 2017.

[113] X. Wang, K. Sun, Y. Li, F. Nejabatkhah, and Y. Mei, "Parallel operation of bi-directional interfacing converters in a hybrid AC/DC microgrid under unbalanced grid conditions," in *2015 IEEE Energy Conversion Congress and Exposition (ECCE)*, vol. 32, no. 3. IEEE, sep 2015, pp. 4574–4581.

[114] M. A. Allam, A. A. Hamad, M. Kazerani, and E. F. El-Saadany, "A Novel Dynamic Power Routing Scheme to Maximize Loadability of Islanded Hybrid AC/DC Microgrids Under Unbalanced AC Loading," *IEEE Transactions on Smart Grid*, vol. 9, no. 6, pp. 5798–5809, nov 2018.

[115] A. Eisapour-Moarref, M. Kalantar, and M. Esmaili, "Control strategy resilient to unbalanced faults for interlinking converters in hybrid microgrids," *International Journal of Electrical Power & Energy Systems*, vol. 119, no. February, p. 105927, jul 2020.

[116] A. Clerici, S. Negri, and E. Tironi, "Inertia Emulation in Multiterminal HVDC Networks," *Proceedings of 2019 IEEE PES Innovative Smart Grid Technologies Europe, ISGT-Europe 2019*, pp. 1–5, 2019.

[117] P. Ding, Z. Liu, J. Cai, and X. Lv, "Virtual capacitance based control for MMC-HVDC systems connected with weak AC grids," *Energy Reports*, vol. 8, pp. 259–266, 2022.

[118] G. Melath, S. Rangarajan, and V. Agarwal, "A Novel Control Scheme for Enhancing the Transient Performance of an Islanded Hybrid AC-DC Microgrid," *IEEE Transactions on Power Electronics*, vol. 34, no. 10, pp. 9644–9654, 2019.

[119] Z. Shen, J. Zhu, L. Ge, S. Bu, J. Zhao, C. Y. Chung, X. Li, and C. Wang, "Variable-Inertia Emulation Control Scheme for VSC-HVDC Transmission Systems," *IEEE Transactions on Power Systems*, vol. 37, no. 1, pp. 629–639, 2022.

[120] E. Rakhshani and P. Rodriguez, "Inertia Emulation in AC/DC Interconnected Power Systems Using Derivative Technique Considering Frequency Measurement Effects," *IEEE Transactions on Power Systems*, vol. 32, no. 5, pp. 3338–3351, 2017.

[121] L. He, Y. Li, Z. Shuai, J. M. Guerrero, Y. Cao, M. Wen, W. Wang, and J. Shi, "A flexible power control strategy for hybrid AC/DC zones of shipboard power system with distributed energy storages," *IEEE Transactions on Industrial Informatics*, vol. 14, no. 12, pp. 5496–5508, 2018.

[122] L. He, Y. Li, J. M. Guerrero, and Y. Cao, "A Comprehensive Inertial Control Strategy for Hybrid AC/DC Microgrid with Distributed Generations," *IEEE Transactions on Smart Grid*, vol. 11, no. 2, pp. 1737–1747, 2020.

[123] Z. Liu, S. Miao, Z. Fan, J. Liu, and Q. Tu, "Improved power flow control strategy of the hybrid AC/DC microgrid based on VSM," *IET Generation, Transmission and Distribution*, vol. 13, no. 1, pp. 81–91, 2019.

[124] Z. Ma, L. E, H. Deng, Z. Wang, and Y. Zhu, "Bidirectional Virtual Inertia Control Strategy for Interlinking Converter in Hybrid AC/DC Microgrid," *Journal of Physics: Conference Series*, vol. 1887, no. 1, p. 012040, 2021.

[125] D. Liu, C. Ye, Y. Wu, X. Ji, Y. Xia, Y. Kang, and Z. Liu, "Bidirectional Virtual Inertia Control Strategy for Hybrid Distributed Generations Integrated Distribution Systems," *Mathematical Problems in Engineering*, vol. 2022, pp. 1–10, nov 2022.

[126] J. Zhu, X. Wang, J. Zhao, L. Yu, S. Li, Y. Li, J. M. Guerrero, and C. Wang, "Inertia Emulation and Fast Frequency-Droop Control Strategy of a Point-to-Point VSC-HVdc Transmission System for Asynchronous Grid Interconnection," *IEEE Transactions on Power Electronics*, vol. 37, no. 6, pp. 6530–6543, jun 2022.

[127] J. Zhu, Z. Shen, L. Yu, S. Bu, X. Li, C. Y. Chung, C. D. Booth, H. Jia, and C. Wang, "Bilateral Inertia and Damping Emulation Control Scheme of VSC-HVDC Transmission Systems for Asynchronous Grid Interconnections," *IEEE Transactions on Power Systems*, vol. 47, no. 10, pp. 1–12, 2022.

[128] Z. Zhang, J. Fang, and Y. Tang, "A Hybrid AC/DC Microgrid with Bidirectional Virtual Inertia Support," *2019 IEEE 4th International Future Energy Electronics Conference, IFEEC 2019*, pp. 1–6, 2019.

[129] Z. Zhang, J. Fang, C. Dong, C. Jin, and Y. Tang, "Enhanced Grid Frequency and DC-link Voltage Regulation in Hybrid AC/DC Microgrids through Bidirectional Virtual Inertia Support," *IEEE Transactions on Industrial Electronics*, pp. 1–10, 2022.

[130] A. S. Morais and L. A. Lopes, "Interlink Converters in DC nanogrids and its effect in power sharing using distributed control," in *2016 IEEE 7th International Symposium on Power Electronics for Distributed Generation Systems (PEDG)*. IEEE, jun 2016, pp. 1–7.

[131] H.-J. Yoo, T.-T. Nguyen, and H.-M. Kim, "Multi-Frequency Control in a Stand-Alone Multi-Microgrid System Using a Back-To-Back Converter," *Energies*, vol. 10, no. 6, p. 822, jun 2017.

[132] X. Jianfang, W. Peng, L. Setyawan, J. Chi, and C. F. Hoong, "Energy management system for control of hybrid AC/DC microgrids," *2015 IEEE 10th Conference on Industrial Electronics and Applications (ICIEA)*, pp. 778–783, 2015.

[133] H. Shi, K. Sun, Y. Li, and H. Wu, "Virtual transformer control for DC-DC interlinking converters in DC microgrids," *2019 IEEE Energy Conversion Congress and Exposition, ECCE 2019*, vol. 1, pp. 4268–4273, 2019.

[134] M. Baharizadeh, H. R. Karshenas, and J. M. Guerrero, "An improved power control strategy for hybrid AC-DC microgrids," *International Journal of Electrical Power and Energy Systems*, vol. 95, pp. 364–373, 2018.

[135] H. A. Alsiraji, R. Elshatshat, and A. A. Radwan, "A novel control strategy for the interlinking converter in hybrid microgrid," *IEEE Power and Energy Society General Meeting*, vol. 2018-Janua, pp. 1–5, 2018.

[136] X. Li, L. Guo, Y. Li, Z. Guo, C. Hong, Y. Zhang, and C. Wang, "A unified control for the DC-AC interlinking converters in hybrid AC/DC Microgrids," *IEEE Transactions on Smart Grid*, vol. 9, no. 6, pp. 6540–6553, 2018.

[137] H. Alrajhi Alsiraji and R. El-Shatshat, "Virtual Synchronous Machine/Dual-Droop Controller for Parallel Interlinking Converters in Hybrid AC DC Microgrids," *Arabian Journal for Science and Engineering*, 2020.

[138] K. C. Bandla, M. V. Gururaj, and N. P. Padhy, "Decentralized and Coordinated Virtual Synchronous Generator control for Hybrid AC-DC Microgrids," *2020 IEEE International Conference on Power Electronics, Smart Grid and Renewable Energy, PESGRE 2020*, pp. 1–6, 2020.

[139] J. Fang, Y. Tang, H. Li, and F. Blaabjerg, "The Role of Power Electronics in Future Low Inertia Power Systems," *Proceedings - 2018 IEEE International Power Electronics and Application Conference and Exposition, PEAC 2018*, pp. 1–6, 2018.

[140] Z. Zheng, S. Liu, Q. Wang, and P. Chen, "Virtual Synchronous Generator Control Strategy with Adaptive Damping Coefficient for Interlinking Converter of the AC/DC

Hybrid Microgrid," *2020 5th International Conference on Power and Renewable Energy, ICPRE 2020*, pp. 648–652, 2020.

[141] W. Zhang, K. Rouzbehi, A. Luna, G. B. Gharehpetian, and P. Rodriguez, "Multi-terminal HVDC grids with inertia mimicry capability," *IET Renewable Power Generation*, vol. 10, no. 6, pp. 752–760, 2016.

[142] J. Xiao, A. Chen, Z. Lin, and H. Xue, "A Virtual Inertia Control Strategy of Interlinking Converters in Islanded Hybrid AC/DC Microgrid," *2019 IEEE Energy Conversion Congress and Exposition, ECCE 2019*, pp. 6301–6308, 2019.

[143] Z. Lv, Y. Zhang, Y. Xia, and W. Wei, "Adjustable inertia implemented by bidirectional power converter in hybrid AC/DC microgrid," *IET Generation, Transmission & Distribution*, vol. 14, no. 17, pp. 3594–3603, 2020.

[144] Y. Zhang, Q. Sun, J. Zhou, L. Li, P. Wang, and J. M. Guerrero, "Coordinated Control of Networked AC/DC Microgrids with Adaptive Virtual Inertia and Governor-Gain for Stability Enhancement," *IEEE Transactions on Energy Conversion*, vol. 36, no. 1, pp. 95–110, 2021.

[145] A. Navarro-Rodriguez, P. Garcia, C. Gomez-Aleixandre, and C. Blanco, "Cooperative Primary Control of a Hybrid AC/DC Microgrid based on AC/DC Virtual Generators," *IEEE Transactions on Energy Conversion*, pp. 1–14, 2022.

[146] K. C. Bandla and N. Prasad Padhy, "An Improved Virtual Synchronous Generator Control for Decentralized and Coordinated Sharing of Transient Response in Hybrid AC-DC Microgrids," *2022 IEEE IAS Global Conference on Emerging Technologies, GlobConET 2022*, pp. 769–774, 2022.

[147] D. Gross, E. Sanchez-Sanchez, E. Prieto-Araujo, and O. Gomis-Bellmunt, "Dual-port grid-forming control of MMCs and its applications to grids of grids," *IEEE Transactions on Power Delivery*, pp. 1–1, 2022.

[148] V. Karapanos, S. W. H. De Haan, and K. H. Zwetsloot, "Testing a Virtual Synchronous Generator in a Real Time Simulated Power System," *International Conference on Power Systems Transients*, vol. 31, no. 0, 2011.

[149] A. A. F. Vijay Vittal, James D. McCalley, Paul M. Anderson, *Power System Control and Stability*, 3rd ed. New Delhi, India: Wiley, 2002.